To the Graduate Council:

I am submitting herewith a dissertation written by Thomas Christopher Widner entitled "Analysis of a Transmission-Based Robotic Servoactuator Concept". I have examined the final copy of this dissertation for form and content and recommend that it be accepted in partial fulfillment of the requirements for the degree of Doctor of Philosophy, with a major in Mechanical Engineering.

William R. Hamel, Major Professor

We have read this dissertation
and recommend its acceptance:

Jay I. Frankel
(Mechanical Engineering)

John F. Jansen
(Oak Ridge National Laboratory)

Frank H. Speckhart
(Mechanical Engineering)

Accepted for the council:

Associate Vice Chancellor
and Dean of the Graduate School

Analysis of a Transmission-Based Robotic Servoactuator Concept

A Dissertation
Presented for the
Doctor of Philosophy
Degree
The University of Tennessee, Knoxville

Thomas Christopher Widner
May 1999

Copyright © Thomas Christopher Widner, 1999.

All rights reserved.

For my wonderful wife, Josie.

(we made it, Tayley!)

Acknowledgements

There are so many people that I should thank for helping me reach this goal that I have no way of listing them all. Over the course of the past five years while I worked like crazy to get those elusive three little letters to append my professional title, I've tried to continually thank my colleagues as their help and encouragement happened. It has been a very long journey—and a difficult one. One of my close friends (and fellow doctoral candidates) even conjectured that it would be easier to legally change the last three letters of a name to "Ph.D.". Humor in the face of despair provided the most assistance in my finally finishing this degree, and I thank each and every person that helped me laugh every day. Sometimes research just doesn't go smoothly, and laughter is a great healer.

Foremost, I must thank my wife Josie for standing by me throughout the pursuit of this degree. More times than not, the majority of my time was spent doing something academic related instead of doing something with her. Even though she has a time-consuming job of her own—and has been frustrated on numerous occasions with how much time she spent at the office—in a way I'm thankful that she has often been too busy to realize how little time I've been able to put aside for us. It is my promise to her, and my family in general, that my priorities will be more family-focused from here on.

I am truly grateful to have met my major professor, Dr. Bill Hamel, at the time in my life when I did. I had been in the Ph.D. program for almost a year when we met, and his influence and guidance were paramount in minimizing the pain-versus-time curve and making progress on a continuous basis. My dissertation topic was an idea of his, and I'm very grateful that he had enough faith in me to perform the work. I hope that he can look back at his first Ph.D. graduate with some pride. At the very least we've done some fascinating research. I'm forever grateful to him for everything, and I'll claim a lot of his insight as my own when I have graduate students someday. In our research meetings, Dr. Hamel would sometimes jokingly tell me that I should be writing all of his comments down—just in case he had a flash of brilliance. After all, we all have our moments. They're all written down, Dr. Hamel, and I'm taking them with me.

I thank my entire dissertation committee for all of their help. Dr. Frank Speckhart played a very special role in the majority of my education, and I can never thank him enough for his help. He has taught me more than any other single person at the university. But, then again, he's had the most time to get things into my sometimes thick skull—I've known him for over ten years. Dr. Jay Frankel provided an incredible amount of help over the past few years and I specifically thank him for instilling in me what I like to call "analytical fearlessness". Some of the work he does is so innovative it can seem like something out of the *Twilight Zone*, and I'm convinced he's from another planet. Even if he *is* human, I'm sure that the "Math Police" are eventually going to track him down. Dr. Rajiv Dubey and Dr. John Jansen also deserve thanks, and I humbly offer it for their help and encouragement.

My colleagues provided countless hours of help, encouragement, laughter, and

venting. I could not have possibly made it without my partners in crime, Scott Hale and Dean Edwards. They will both make terrific professors and researchers; I'm just glad that I'll never be one of their students (they're both dangerously sharp). I thank all of my co-researchers in the Robotics and Electromechanical Systems Laboratory. Steve Everett and Scott Marland have been in hot pursuit of the same degree as myself, and I'm grateful that they took time out on numerous occasions to help me complete my research while, in essence, they were neglecting their own. The list of others in the lab is long, but I must give thanks to Jeff Buck, James Franks, Quentin Fu, Yas Isoda, David Lennon, Stacey Mitchell, and Sam Richardson. What a crew! I'm so proud to say that the majority of the researchers in the lab—upon my recommendation—have used the LaTeX typesetting system for their theses/dissertations. Because of this, we've all learned a lot about typesetting (myself included). Thanks, guys!

Josie and I both would like to say a huge thanks to our best friends, Mark and Julia Madgett. They were constant supporters of my finishing this degree and finding a local job. They never once expressed doubt that either would happen and both did. Thanks, guys, you're the greatest! We truly love you.

Sincere thanks go to the "Brightest Beacon at the University of Tennessee"—the thesis/dissertation consultant—Ann Lacava. She is truly the lady of eternal smiles. You are wonderful, Ann.

I humbly thank the entire congregation at West Knoxville Free Will Baptist Church. The pastor, Gerald Fender, has helped me so much in pushing this degree over the top. His prayers, along with those of the congregation, have not only allowed me to complete this degree but to find a wonderful job here in Knoxville.

Josie and I are truly blessed, and we humbly thank God for all of the wonderful blessings He provides.

Finally, I must thank my entire family for always standing behind me. They couldn't always (if ever) understand how in the world it could take so long for me to get out of school. They are almost as happy as I am that I'm finally graduating, and I love each and every one of them for their support and love. My parents faithfully stood behind me throughout all of this. My father always said that one never quits learning, but I'm almost positive that over the past several years he thought I had misunderstood his point. I didn't. Thanks Mom and Dad. I finally made it.

Abstract

This research was a pioneering effort toward the investigation of incorporating multi-speed transmissions into electric actuation devices for robotic and industrial applications. This new idea has been conceptually developed from first principles using an application-based approach to parametric study. First, the full gamut of literature, both from the academic and research domains, was exhaustively surveyed. The design space criteria of an existing robot manipulator design was revisited for the purpose of studying feasibility for the transmission-based actuator (TBA) concept. This initial study verified that with conservative assumptions concerning gross transmission parameters, size, and weight, distributed actuation is possible for a much wider class of manipulator mechanisms than is currently available. Multi-speed transmissions inherently allow smaller, high power motors to also deliver high torque at low speeds, effectively allowing the overall actuator power density to be increased to a level more on par with electrohydraulics.

This work also emphasized a methodology for developing logical, optimized, shifting algorithms for both continuously variable transmission (CVT) and discrete speed transmission (DST) concepts. The resulting algorithms were fully defined and presented in closed form. When optimized with respect to the acceleration delivered to a load, all motor-transmission combinations (both CVT and DST) required shifting

profiles that were definitively related to the maximum power operating point of the driver motor. It was found that, for maximum acceleration, the transmission should manipulate mechanical advantage in terms of torque and speed capacity such that the motor can achieve and maintain an operating point within a close vicinity of maximum power. During shifting, the *CVT*-based actuators proved to be capable of placing the motor at exactly the maximum power point in minimum time; the *DST*-based actuators, having only a finite number of gear ratios available, operate within a "speed bandwidth" around the maximum power point defined by the discrete shifting points.

The optimal shifting profiles (for either *CVT*'s or *DST*'s) proved to form a logical basis for evaluating motor potential for a given application in that the associated algorithms clearly define an upper bound on the performance potential for a given motor with *any* transmission system. The optimization results are shown to provide concise and logical methods for selecting motor-transmission combinations and designing transmission parameters to meet a required actuator payload/response requirement.

Fundamental mechanical design concepts for multi-speed transmissions are discussed and expanded upon in detail. The next steps must address the feasibility of mechanical implementation and effective servo-control of *TBA*'s. These investigations should include a prototype testbed, further examination into low-level actuator control, quantitative parametric studies, and further development and verification of the transmission shifting algorithms.

Contents

1 Background **1**
- 1.1 Robotic Actuator Technologies . . . 1
  - 1.1.1 DC Electric Motors . . . 2
  - 1.1.2 Geared Electric Actuators . . . 6
  - 1.1.3 Hydraulic Actuation . . . 8
  - 1.1.4 Power and Torque Density . . . 9
- 1.2 Distributed vs. Centralized Actuation . . . 13
- 1.3 Bottom Line: Moving the Payload . . . 16

2 The Transmission-Based Actuator Concept **20**
- 2.1 Overview . . . 20
- 2.2 The Concept . . . 21

3 Feasibility Analysis **26**
- 3.1 Background: Modeling of an Electric Fixed Reduction Actuator . . . 26
- 3.2 Development of a Discrete-Speed Transmission Model . . . 30
  - 3.2.1 General Transmission-Based Actuator Model . . . 30
  - 3.2.2 Performance Comparison . . . 36
- 3.3 Feasibility Study for Distributed Actuation . . . 37
  - 3.3.1 A Brief Introduction to *ORNL*'s Advanced Servomanipulator . 37
  - 3.3.2 *ASM* Baseline Design and Model . . . 37
  - 3.3.3 Modified *ASM* Model: Distributed *TBA* Design with Discrete Shifting . . . 40
  - 3.3.4 Feasibility Results . . . 41
  - 3.3.5 Feasibility Conclusions . . . 45

4 Low Level Joint Control **46**
- 4.1 Overview . . . 46
- 4.2 Overall Control Scenarios . . . 47
  - 4.2.1 Introduction . . . 47

4.2.2 Characteristics of Robot Control 47
4.2.3 General Control Objectives 49
4.2.4 Generalization 50
4.3 Optimal Control Analyses 51
4.3.1 Time Optimal Continuous Shifting Strategy 51
4.3.2 Optimal Control Preliminaries 52
4.3.3 Calculus of Variations Preliminaries 54
4.3.4 Problem Statement 55
4.3.5 Optimal Analyses 56
4.3.6 Correlation to a Maximum Acceleration Maneuver 59
4.3.7 Demonstration of Results 60
4.3.8 Parametric Plots 65
4.3.9 Time Optimal Discrete Shifting Strategy 67
4.4 Modified Control Architecture 79
4.5 Conclusions: Control Considerations 80

5 Transmission Parameter Design **83**
5.1 Introduction 83
5.2 Selection of Maximum/Minimum Gear Ratios 86
5.2.1 Maximum Gear Ratio Selection 87
5.2.2 Minimum Gear Ratio Selection 90
5.3 Transmission Ratio Design 93
5.3.1 Continuously Variable Transmissions 93
5.3.2 Discrete-Speed Transmissions 94
5.4 *CVT* vs. *DST*: The Best Transmission for the Job 97
5.5 Summary 99

6 Transmission Hardware Conceptual Designs **102**
6.1 Planetary Gear Trains: Discrete Speed Transmissions 102
6.2 Continuously Variable Transmissions 105
6.2.1 Van Doorne Push-Belt *CVT* 105
6.2.2 Split Toroid Type *CVT* 108
6.2.3 Dual Motor Actuator 112
6.2.4 Planetary Cone *CVT* 116
6.2.5 Dual Motor Planetary *CVT* Actuator 118

7 Conclusions **120**
7.1 The Fundamental Idea of *TBA* 120
7.2 The Initial *TBA* Study 121
7.3 Transmission Shifting Strategies 122

7.4 Selection of Physical Transmission Parameters 124
7.5 Transmission Design Ideas 126
7.6 Future Work 128
7.7 The Challenges Ahead 130

A Discrete Shifting: Angular Momentum Considerations 139

B Joint-Level Model with Non-Linear Loading 142
B.1 Introduction 142
B.2 Problem Statement 143
B.3 Problem Formulation 145
B.4 Method of Solution 146
B.4.1 Elimination of Boundary Error 147
B.4.2 Explicit Expression for the Residual Function 149
B.4.3 Collocation Statement 150
B.5 Results 153

C *CVT* Shifting Strategy for a Desired Trajectory 157
C.1 Matching the *ASM* Baseline Performance 157
C.1.1 Calculation of the Gear Reduction as a Function of Time . . . 157
C.1.2 Sample Result for Calculation of Gear Reduction 158
C.2 The Transmission's Job: A Closer Look 159

D Selecting a Motor: A Power Constraint 161
D.1 Derivation of the Constraint 161
D.2 Interpretation of the Result 165

VITA 168

List of Figures

1.1 DC motor constant voltage torque-speed curve 4
1.2 Machinery comparison: Power and response time 11
1.3 Actuator comparison: torque density 12
1.4 Actuator comparison: power density 13
1.5 Distributed actuation: why it is generally not possible 15
1.6 Exploded view of a centralized actuator manipulator arm. (Figure courtesy of Oak Ridge National Laboratory). 17

2.1 Torque-speed tradeoff 22
2.2 Increasing overall power density 25

3.1 Schematic of a fixed reduction actuator (*FRA*). 27
3.2 Motor speed response (5-speed transmission) 34
3.3 The Advanced Servomanipulator (*ASM*). (Photo courtesy of Oak Ridge National Laboratory) 38
3.4 Schematic of current *ASM* design and a Distributed Actuator System 39
3.5 Joint torque-speed curves: *ASM* curve is marked. 42
3.6 Motor speed comparison 43
3.7 Joint speed response for a 40° maneuver 43
3.8 Joint position response for a 40° maneuver 44

4.1 Joint Speed Task Trajectory 49
4.2 Gear reduction vs. speed. $N^*(\omega)$ is optimal. 62
4.3 Joint speed response. $\omega^*(t)$ is optimal. 62
4.4 Joint position response. $\theta^*(t)$ is optimal. 63
4.5 Motor Speed Response 64
4.6 N^* vs. speed ratio. ($\sigma \leq 200$, $\rho \leq 10^6$). 65
4.7 N_{max} vs. torque ratio, σ. ($\rho \leq 10^6$). 66
4.8 N_{max} vs. inertia ratio, ρ. ($\sigma \leq 1000$). 66
4.9 N^2_{max} vs. inertia ratio, ρ. ($\sigma \leq 1000$). 67
4.10 Optimal discrete shifting speeds for "hypothetical" case $\Gamma \approx 1$. . . . 73

4.11 Optimal shifting points for a hypothetical discrete transmission . . . 75
4.12 Discrete transmission optimal shifting curves. $\Gamma \in [0.5, 1)$, $\sigma_d = 0.001$. 76
4.13 Discrete transmission optimal shifting curves. $\Gamma \in [0.5, 1)$, $\sigma_d = 0.01$. 77
4.14 Discrete transmission optimal shifting curves. $\Gamma \in [0.5, 1)$, $\sigma_d = 0.1$. . 77
4.15 Discrete transmission optimal shifting curves. $\Gamma \in [0.5, 1)$, $\sigma_d = 0.25$. 78
4.16 Modified control architecture for variable gear reduction 79

5.1 Optimal shifting strategy vs. joint speed 91
5.2 Optimal shifting strategy vs. time 92

6.1 A basic planetary gear train 103
6.2 A compound planetary gear train 104
6.3 Van Doorne "push belt" *CVT* 106
6.4 Split toroid *CVT* 108
6.5 Input and output coupled transmission schematics 110
6.6 Dual motor actuator 113
6.7 Planetary cone *CVT* 117
6.8 Dual motor planetary *CVT* Actuator 118

B.1 Schematic of an electric actuator (repeated). 144
B.2 Plot of the first 5 trial functions, $\Psi_k(\xi)$, $k = 1, 2, \ldots, 5$. 148
B.3 Weighted residual and R-K solutions for $\theta^N(t)$. $t_{max} = 1$ second. . . 153
B.4 Weighted residual and R-K solutions for $\theta^N(t)$. $t_{max} = 3$ seconds. . 154
B.5 Weighted residual and R-K solutions for $\theta^N(t)$. $t_{max} = 10$ seconds. . 154
B.6 Plot of residual function, $R_N\left(\phi^N(\xi)\right)$, for $t_{max} = 1$ second. 155
B.7 Plot of residual function, $R_N\left(\phi^N(\xi)\right)$, for $t_{max} = 3$ seconds. 155
B.8 Plot of residual function, $R_N\left(\phi^N(\xi)\right)$, for $t_{max} = 10$ seconds. 156

C.1 *CVT* gear reduction vs. time needed for equivalent joint motion. . . 159

List of Tables

1.1 Shoulder pitch reduction ratios 8

3.1 Motor parameters 41

4.1 System parameters 61

5.1 Maneuver time comparison: *DST* vs. *CVT* 98

Nomenclature

Roman

a_m	Expansion coefficients (Appendix B)
A_g	Air gap area (Chapter 1)
B_g	Effective field distribution (Chapter 1)
C_k^N	Expansion coefficients (Appendix B)
D	Stator outer diameter (Chapter 1)
F	Calculus of variations integrand (Chapter 4)
H	Hamiltonian (Chapter 4)
$\bar{H}$	System angular momentum (Chapter A)
i	Motor current (Chapter 1)
i_g	Effective current per axial length (Chapter 1)
I_{eff}	Effective mass moment of inertia
I_{ext}	External mass moment of inertia
I_m	Motor rotor mass moment of inertia
j	Gear number
K_{motor}	Motor constant (Chapter 1)
K_T	Motor torque constant
l	Motor length (Chapter 1)
L	Motor inductance (Chapter 1)
L	Optimization integrand (Chapter 4)
m	Mass
n	Number of transmission speeds
N	Fixed gear reduction
$N+1$	Number of terms retained in series expansion (Appendix B)
N_j	Gear reduction for gear j
P_{mech}	Mechanical power (Chapter 1)
P_{loss}	Power loss (Chapter 1)
r	Motor radius (Chapter 1)
R	Winding resistance (Chapter 1)

R_{therm}	Motor thermal resistance (Chapter 1)
R_i	Gear radius, $i = 1, 2$.
$R_N\left(\phi^N(\xi)\right)$	Residual function (Appendix B)
t_j	Time of shift from gear "j" to "$j+1$"
t_j^*	Relative time of shift, $t - t_j$, (Chapter 3)
T_a	Ambient temperature (Chapter 1)
T_{cont}	Continuous motor torque (Chapter 1)
T_{eff}	Effective torque
T_{ext}	External torque
T_m	Motor torque
$T_n(\xi)$	Chebyshev polynomials of the first kind
T_o	Motor torque at stall (Chapter 1)
T_w	Winding temperature (Chapter 1)
$u(t)$	Control variable (Chapter 4)
$u(t - t_j)$	Heaviside unit step function triggered at $t = t_j$
V	Motor voltage (Chapter 1)
$w(\xi)$	Weight function for Weighted Residual Method (Appendix B)
$y(t)$	State variable (Chapter 4)

Greek

α	Angular acceleration
α_j	Angular acceleration, gear "j"
β	Torque ratio (Chapter 3)
γ	Speed ratio (Chapter 3)
γ_j	Speed ratio, gear j (Chapter 3)
Γ	Inertial parameter (Chapter 4)
$\delta(\xi - \xi_j)$	Dirac delta function triggered at $\xi = \xi_j$
ϵ	Small parameter (Appendix C)
θ	Angular position
Θ	Joint angular position (Chapter 3)
$\Theta_{i,j}$	Initial rotation, gear "j"
Θ_{load}	Angular position of the load
λ	$t_{max}/2$ (Appendix B)
$\lambda(t)$	Lagrange multiplier function (Chapter 4)
ξ	Mapped time variable, $\xi \in [-1, 1]$ (Chebyshev domain)
ρ	Mass density
ρ	Inertia ratio (Chapter 4)
σ	Torque ratio (Chapter 4)

σ_d	Torque ratio, discrete transmissions (Chapter 4)
τ	Motor time constant (Chapter 3)
ϕ	Angular position (Chebyshev domain)
ψ	Test function for Weighted Residual Method (Appendix B)
$\Psi_k(\xi)$	Trial functions $k = 1, 2, \ldots, N$ (Appendix B)
ω	Motor speed (Chapter 1)
ω_i	Initial motor speed
$\omega_{i,j}$	Initial motor speed, gear "j"
ω_j	Motor speed response, gear j
ω_{load}	Angular speed of the joint load (Chapter 3)
ω_m	Motor speed (Chapter 3)
$\omega_{motor,s}$	Motor speed at shift (Chapter 4)
ω_o	No-load (free) motor speed
ω_s	Joint speed at shift
Ω	Maximum motor speed (Chapter 3)

Superscripts

$-$	Before shift
$\sim$	Relative to last shift
$+$	After shift
$*$	Optimal
N	Denotes that infinite series has been truncated
$N+1$	Denotes number of terms retained in series expansion

Subscripts

ASM	Pertaining to the Advanced Servomanipulator
d	Discrete
eff	Effective
ext	External
g	Gap
i	Initial
j	Gear number
k	Counter
l	Length
m	Motor
m	Denotes Chebyshev polynomial and coefficient number (Appendix B)

o	Denotes limiting value of either speed or torque
s	shift
T	Torque

List of Acronyms

ASM	Advanced Servomanipulator
CVT	Continuously Variable Transmission
D&D	Deactivation and Decommissioning
DAS	Distributed Actuator Servomanipulator
DC	Direct Current
DST	Discrete-Speed Transmission
DOE	Department of Energy
DoF	Degree of Freedom
FRA	Fixed Reduction Actuator
IVT	Infinitely Variable Transmission
ORNL	Oak Ridge National Laboratory (Oak Ridge, TN)
QFT	Quantitative Feedback Theory
REMSL	Robotics and Electromechanical Systems Laboratory
R-K	Runge-Kutta
SSRMS	Space Station Remote Manipulator System
TBA	Transmission–Based Actuator

Chapter 1

Background

1.1 Robotic Actuator Technologies

The need to build machinery for the purpose of accomplishing automated or semi-automated tasks drives the development of what is sometimes termed application-driven technology [1]. In robotics, a fundamental machine limitation is often directly related to limitations in the actuator technology driving the system. Particularly in larger machines, issues concerned with power density (power-to-mass ratio) and torque density (torque-to-mass ratio) of the actuators can greatly restrict the overall machine payload and power range. In the introduction of his comprehensive review of robot actuator technologies, Hollerbach states in 1991 that [1]:

> There has been considerable progress in developing traditional actuator technologies for robotics in the past few years. Nevertheless, if we are to achieve the lightweight, high performance, and mobile robots envisioned for the future, new technologies may be required.

This dissertation is a first investigation toward the development of a new *variable gear transmission-based* actuator technology for robotics. This section briefly

compares existing robot actuator technologies with respect to areas such as cost, complexity, and maintenance, as well as the vital concerns with power density and torque density. The interested reader is referred to the article by Hollerbach [1] for a more extensive survey of actuator technology for robotic systems of all sizes. Particular attention in this dissertation is paid to electric and electro-hydraulic drives, with reference to the large-scale robotic applications.

It should be noted that the amount of available literature on transmission-based[1] robot actuators is all but non-existent. This work is a pioneering effort toward introducing this concept into electric actuation. With respect to the citations that are mentioned in this work, they are all related to the *component* technologies that are (as a minimum) required to produce a transmission-based actuator concept. The only references to literature that are solely based on transmission-based actuators as applicable to robotics are those of the author. Hopefully this work will ignite an interest in this exciting new area.

1.1.1 DC Electric Motors

To begin, the mechanical equations for a permanent magnet direct current (DC) motor are shown to start the discussion. The mechanical equation relates motor torque to current:

$$T_m(i) = K_T i, \tag{1.1}$$

[1] Multi-speed

where K_T is the motor torque constant. The electrical equation relates voltage to speed:

$$V(\omega) = K_T\omega + iR, \tag{1.2}$$

where R is the winding resistance and $K_T\omega$ is the back electro-motive force (emf)[2]. For a constant voltage V, the torque speed relation is obtained by solving (1.2) for current and using the result in (1.1):

$$T_m(\omega) = \frac{K_T\left(V - K_T\omega\right)}{R} = \frac{K_T V}{R} - \frac{K_T^2\omega}{R}. \tag{1.3}$$

Note that torque is a *linear* function of speed. The constant term defines the *stall torque*, or the holding torque at zero speed, for the motor at that voltage:

$$T_o = \frac{K_T V}{R}. \tag{1.4}$$

The coefficient of the speed term is related to what is sometimes referred to as the *motor constant*:

$$K_{motor} \equiv \frac{K_T}{\sqrt{R}}.$$

Numerically, the square of K_{motor} represents the slope of the torque-speed curve. Finally, the theoretical "no-load" speed is found to be:

$$\omega_o \equiv \frac{V}{K_T}. \tag{1.5}$$

Using (1.4) and (1.5), (1.3) can be written as:

$$T_m(\omega) = T_o\left(1 - \frac{\omega}{\omega_o}\right). \tag{1.6}$$

This torque-speed relation is used several times in this work. The relation is shown graphically in Figure 1.1. By conservation of energy, the mechanical power output

[2]The motor inductance, L, is assumed small.

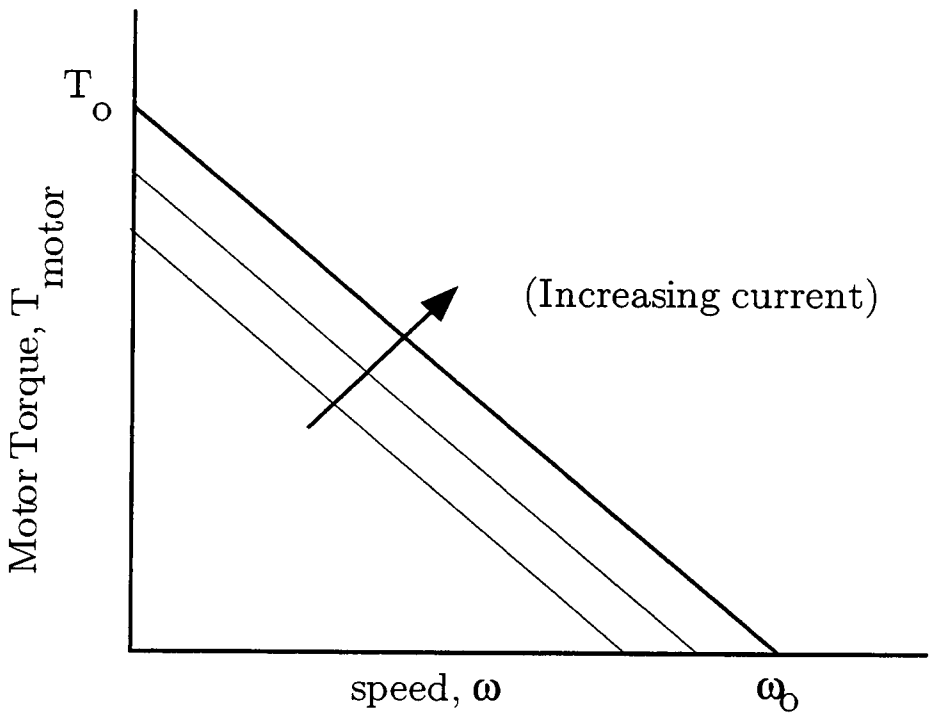

Figure 1.1: DC motor constant voltage torque-speed curve

of the motor is the difference in the input electrical energy (Vi) and the i^2R losses to heat. This mechanical power is a torque-speed product and has a parabolic form with a maximum power point at half of the free speed:

$$\begin{aligned} P_{mech} &= T(\omega)\omega, \\ (P_{mech})_{max} &= \frac{T_o}{2}\frac{\omega_o}{2} = \left(\frac{VK_{motor}}{2K_T}\right)^2. \end{aligned} \tag{1.7}$$

The achievable amount of torque that can be delivered by a motor depends on the time duration or "duty cycle" that is required. Much larger torques can be delivered for shorter duty cycle times than that for extended or continuous periods. The sustainable current that a motor can handle is fundamentally dependent on both the allowable winding temperatures and the thermal resistance of the motor [1]. An important motor specification is the continuous torque that the motor can provide at stall. It was shown in [1] that the continuous power loss is written as:

$$(P_{loss})_{cont} = \frac{T_w - T_a}{R_{therm}} = i_{cont}^2 R, \tag{1.8}$$

where T_w is the winding temperature, T_a is the ambient temperature, and R_{therm} is the thermal resistance of the motor expressed in °C/W. Solving for the current and multiplying by K_T gives the continuous torque available from the motor:

$$(T_m)_{cont} = K_T\frac{\sqrt{(P_{loss})_{cont}}}{R} = K_{motor}\sqrt{\frac{(P_{loss})_{cont}}{R}}. \tag{1.9}$$

This equation shows a fundamental fact: energy *must* be dissipated in the windings for the production of torque to happen. The resulting heat energy must be dissipated at a rate which avoids overheating of the windings. In many cases, accommodating the heat energy dissipation can be a limiting design factor. Also, heat dissipation sometimes becomes the limiting *performance* factor during motor operation. In other

words, the maximum performance of a motor may be limited by thermal as well as mechanical considerations.

1.1.2 Geared Electric Actuators

The available torque density and power density of currently available DC motors are many times limited physically by the magnets themselves. An excellent demonstration of this fact is given in [1] and is summarized here.

For a motor length l with a rotor radius r, the air gap area is given by:

$$A_g = 2\pi r l.$$

From the Lorentz relation [2], the maximum tangential force per unit air gap area is given by:

$$\frac{dF}{dA} = i_l B_g,$$

where i_l is the effective current per axial length (A/m), and B_g is the effective field distribution in the air gap (T). The total (continuous) torque is then given by

$$\begin{aligned} T_{cont} &= \left(\frac{dF}{dA}\right) r A_g, \\ &= 2\pi r^2 l i_l B_g. \end{aligned} \tag{1.10}$$

Hollerbach states that a survey of motor specifications indicates that the mass per unit volume for housed motors ranges from 3000-5000 kg/m^3; for purposes of comparison, the density of steel is 8000 kg/m^3. Assuming a mass/volume of ρ =3000 kg/m^3, an upper limit on the torque-to-mass ratio can be calculated as

$$\frac{T_{cont}}{m} = \frac{2\pi r^2 l i_l B_g}{\rho\,(\pi r^2 l)} = \frac{i_l B_g}{\rho} \leq 12 \frac{Nm}{kg}. \tag{1.11}$$

A maximum torque density of 12 Nm/kg (4 $ft-lb/lb$) is a very low number, especially for high payload systems, and is not subject to much improvement [3]. (For comparison, see the torque density calculation for a hydraulic actuator in Section 1.1.3). However, higher power density can be achieved with electromechanical motors by allowing the motors to run at higher speeds. As shown earlier, maximum power is achieved at half the free speed of the motor, i.e.

$$\omega_{\text{maximum power}} = \frac{\omega_o}{2} = \frac{V}{2K_T}.$$

This shows that mechanical power can be increased at the expense of torque capacity by choosing a lower torque constant K_T. For a selected motor, however, K_T is fixed and may not be used as a parameter for increasing performance. However, the statement— "*Higher power density can be achieved by running the motors at higher speeds.*"— is a true statement in general. Hence, gear reducers (sometimes referred to as speed reducers, torque multipliers, or transmissions[3]) are used to reduce the effective external torque on the motor to a level that allows smaller (hence faster) motors to achieve higher external torques.

Gearing introduces several undesirable characteristics into a robotic system which make accurate control more difficult. Among these, the most prominent are nonlinearities associated with friction (caused by the sliding interfaces between gear teeth), backlash (lost motion due to imperfectly mated gears), and compliance. Research in direct drive machines—those which directly couple motors to the actuated joints *without* gearing [4]—all but circumvents these problems by eliminating the gearing, but power density and torque density are limiting factors. Torques can be increased

[3]In all previous related robotics works known to the author, the word "transmission" refers to a single, fixed gear ratio.

Table 1.1: Shoulder pitch reduction ratios

Machine	Shoulder pitch gear reduction
Advanced Servomanipulator	45:1
PUMA 560	50:1
Spar SSRMS	1800:1

somewhat by making the physical size of the motors larger, but the increase comes at the expense of motor size, volume, and weight; hence, increasing motor size alone doesn't address problems with power density and torque density. The final result is that gearing is generally a necessity.

For reasons such as those outlined in this section, the vast majority of commercial electric robots use direct current motors with gear reducers. Further, it is highly unlikely that this situation will change soon. Table 1.1 shows examples of the shoulder pitch reduction ratios seen on a few existing robots[4].

1.1.3 Hydraulic Actuation

Hydraulic actuators convert energy supplied by pressurized hydraulic fluid into either linear or rotary motion. The hydraulic fluid flowing through the actuator is generally controlled by electromagnetically actuated servovalves and/or by variable displacement pumps. In comparison to an electric drive, hydraulic drives are mechanically complex and require specialized periodic maintenance to keep them in working order. However, hydraulic systems have two very positive attributes: high power density and high torque density. For example, a Rotac 26R-5 two vane hydraulic actuator

[4]In the table, SSRMS is an acronym for "Space station remote manipulator system".

weighing 29 kg produces 2790 N-m of torque at a supply pressure of 20 MPa (3000 psi), resulting in a torque density of 96 N-m/kg [1]. This is impressive in comparison to the calculated upper limit for electric actuators (i.e. $\leq$ 12 N-m/kg). High torque density and power density are indeed the most desirable trait inherent to hydraulic actuation. Torque and power can be increased by increasing the supply pressure, but this often leads to problems with leakage (among others).

The separation between electric and hydraulic actuation schemes concerning power density and torque density is considerable—a factor of eight in our example. Because of this, hydraulic actuators have been used in vast arrays of large machinery, including large-scale robotic systems. For robotics, however, there is an overall trend of replacing hydraulic robots with electrically actuated robots wherever possible to eliminate problems such as overall complexity and leakage. Nevertheless, electric drives with fixed gear reducers cannot compete with hydraulics in terms of generating both high torques *and* speeds; this is mainly due to the fundamental gap in power density and torque density. The next section illustrates the situation with the assistance of a few plots.

1.1.4 Power and Torque Density

The majority of this chapter has discussed two actuator characteristics that are common measures of an actuator's performance capability (in terms of torque, speed, and power) in comparison to its physical size. These characteristics, torque density and power density, are especially important to applications such as robotics where actuators may add to the overall payload of the system; in other words, in most cases

robot actuators are responsible for lifting the robot arm and external payload, *plus themselves* and any actuators "downstream". We continue the discussion of these ideas in this section.

First, a nice comparison of how various types of machinery compare is shown in Figure 1.2, which is a graphical representation of several types of machinery concerning their power capacity and response time[5] [5]. The figure quantitatively depicts the relative capacity of various actuators within various system applications. The vertical axis is associated with the amount of power that the actuator delivers to the mechanism that is being driven; obviously, the intercepts of the vertical axis represent the most powerful actuators in their category. Specifically, the electric actuator with the highest available power rating marks the intercept in the electric range. A similar statement holds for the horizontal axis concerning (the reciprocal of) response time. The actuators with the most speed capacity in their respective group mark the horizontal intercept. So, if the vertical axis is marked with the highest power value available from electric actuation, and the horizontal axis is marked with the fastest response time available from electric actuation, then these two points can be connected to form an absolute envelope for the capacity range of electric actuation devices in general. A similar procedure allows development of an absolute envelope for hydraulic devices. It should be noted that both of the envelopes contain the entire quadrant of the plot. Outside of the hydraulic envelope is considered to be beyond the current state-of-the-art. The fundamental reason that hydraulic actuation currently dominates electric actuation in heavy payload applications has everything to do with both power density and torque density.

[5]the horizontal axis actually depicts the reciprocal of response time.

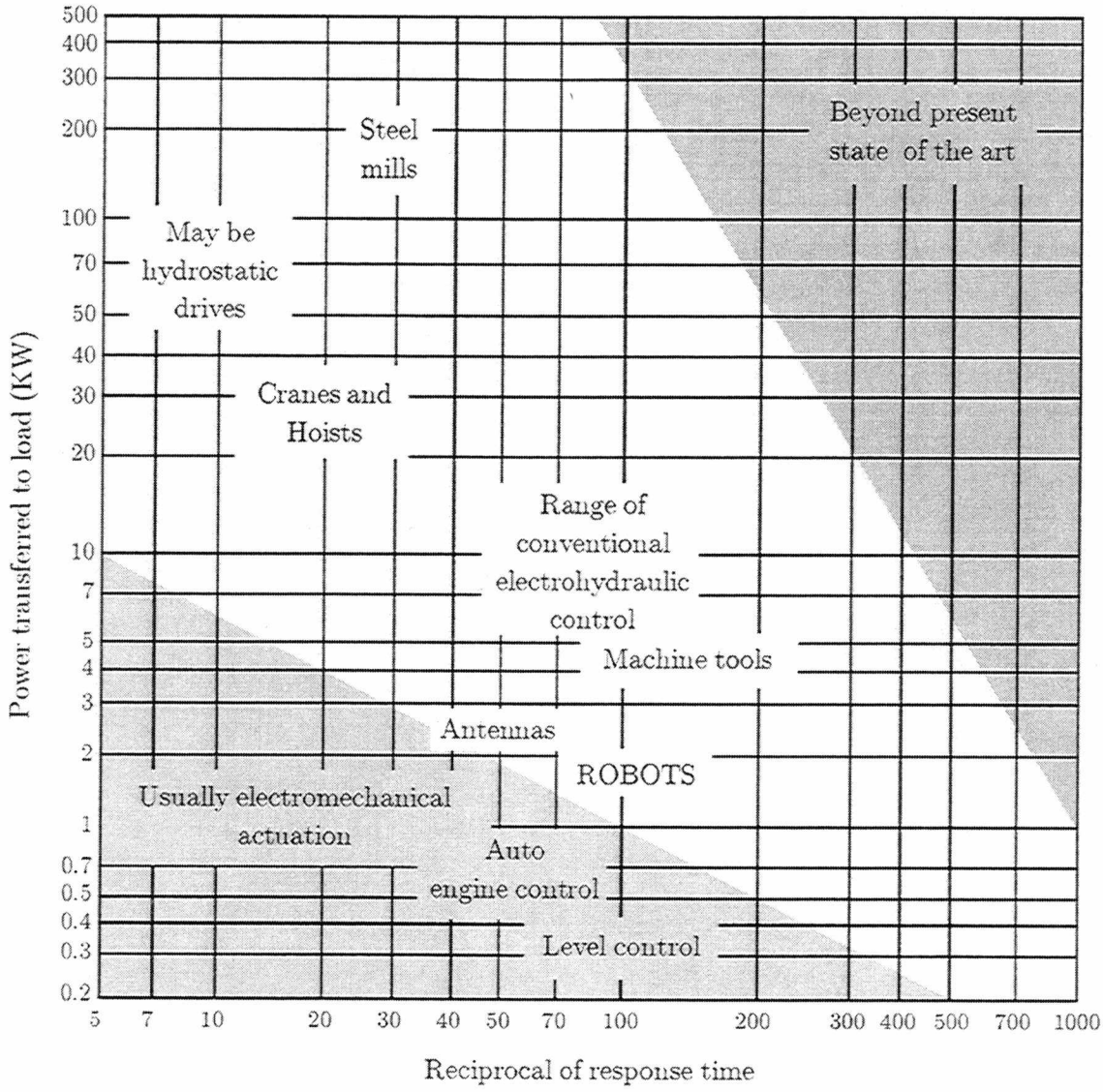

Figure 1.2: Machinery comparison: Power and response time

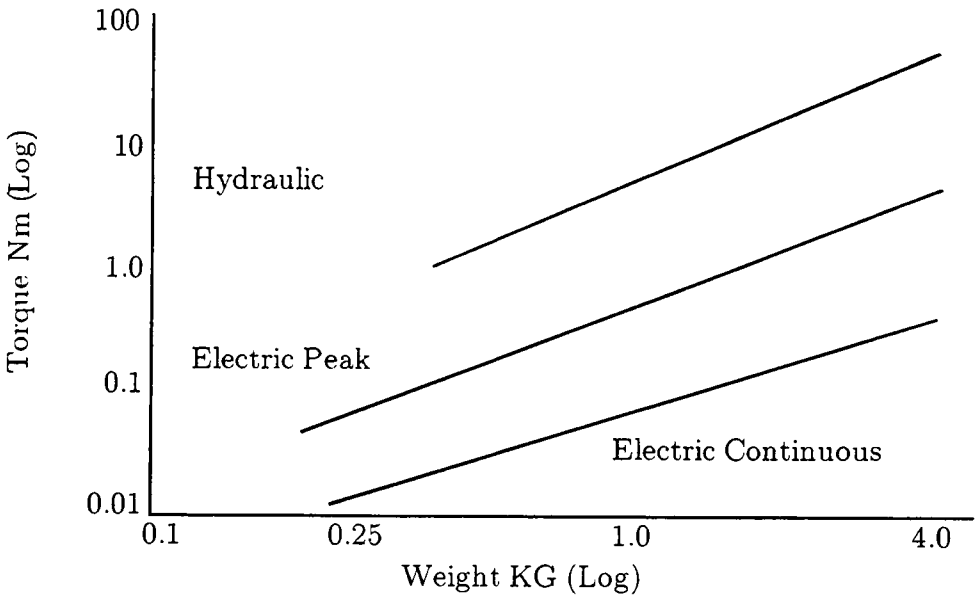

Figure 1.3: Actuator comparison: torque density

Figures 1.3 and 1.4 depict the differences between electric and hydraulic actuation concerning these parameters [6]. From the figures it can be seen that hydraulics have the upper hand concerning both power and torque versus weight. In fact, since even the peak outputs of power and torque available with electromechanical actuators cannot approach the "hydraulic range", the actuators aren't comparable for even short duty cycles. The fundamental gaps of torque density and power density are the primary "deficiencies" of electric actuators when compared to hydraulic actuators. Addressing this problem was a (if not *the*) major motivation for this dissertation work.

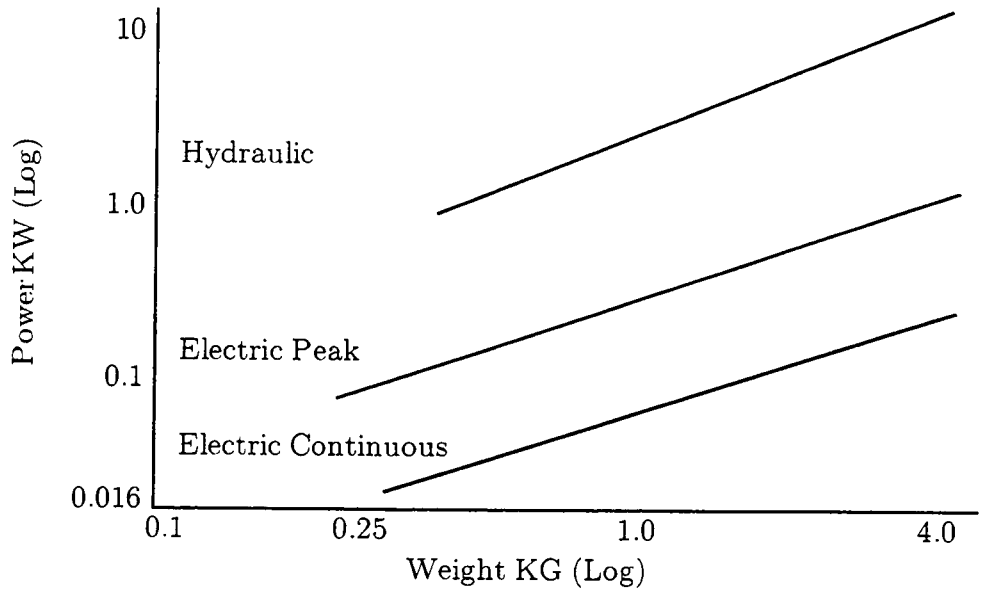

Figure 1.4: Actuator comparison: power density

1.2 Distributed vs. Centralized Actuation

As mentioned several times, robotic manipulators often require both high speed and high payload operation while minimizing friction and inertia [7]. If it is even possible to implement the system with electric drives, these combined requirements generally result in the use of comparatively high torque drives operating through relatively small gear reductions. That is, generally the motors are made as physically large as is feasible such that the amount of introduced gear reductions may be as "few" or "small" as possible. Clearly, there is a real tradeoff: larger motors require less gearing (hence less friction, etc.), but are physically larger. Therefore, in this example, reduced friction comes at the expense of overall actuator size. As we have seen, this greatly affects the important parameters of torque density and power density, and more times than not, these are limiting design and performance factors.

Ideally, for overall robot manipulator arm design simplicity, the joint actuators (including the associated gear-reducers) would be coupled directly to the respective joint in what is termed *distributed actuation.* Distributed actuators tend to minimize overall drivetrain complexity. This is not to be confused with a similar idea of direct drive actuators. Direct drive tacitly implies that gear reducers are absent, whereas distributed actuation is a general actuator term. All direct drive robots are distributed actuator systems, but the reverse is not necessarily true. When distributed actuation can be achieved (i.e., the actuators each can meet the necessary performance requirements with all actuators attached at the respective driven joints), the manipulator design does not involve mechanical transmission of torque through the arm joints. Avoiding the transmission of torque through joints greatly simplifies the design. However, for all manipulator classes, it is *not generally possible* to distribute the joint actuators in the arm extremities because the motors basically would have to lift themselves as well as the arm structure and the payload [4]. Further, if the actuators are direct-drive, the size and weight of the servomotors increases exponentially (actually faster than exponentially) for each upstream joint [8]. It is staggering how fast the payloads go up with distributed actuators. This is demonstrated in Figure 1.5. Starting at the most "downstream" joint in an articulated configuration, the wrist has only to lift itself, the end effector, and the payload. In other words, in general, a joint has to lift itself and everything downstream of it. As shown in Figure 1.5, moving upstream on the arm not only means a joint has *more* to lift, but it also means that the joint has *larger* things to lift also. Even in the static case this is daunting, but considering even moderate dynamic motions makes distributed actuation a lost cause. Motors with a fixed gear ratio (or no gear ratio at all) simply

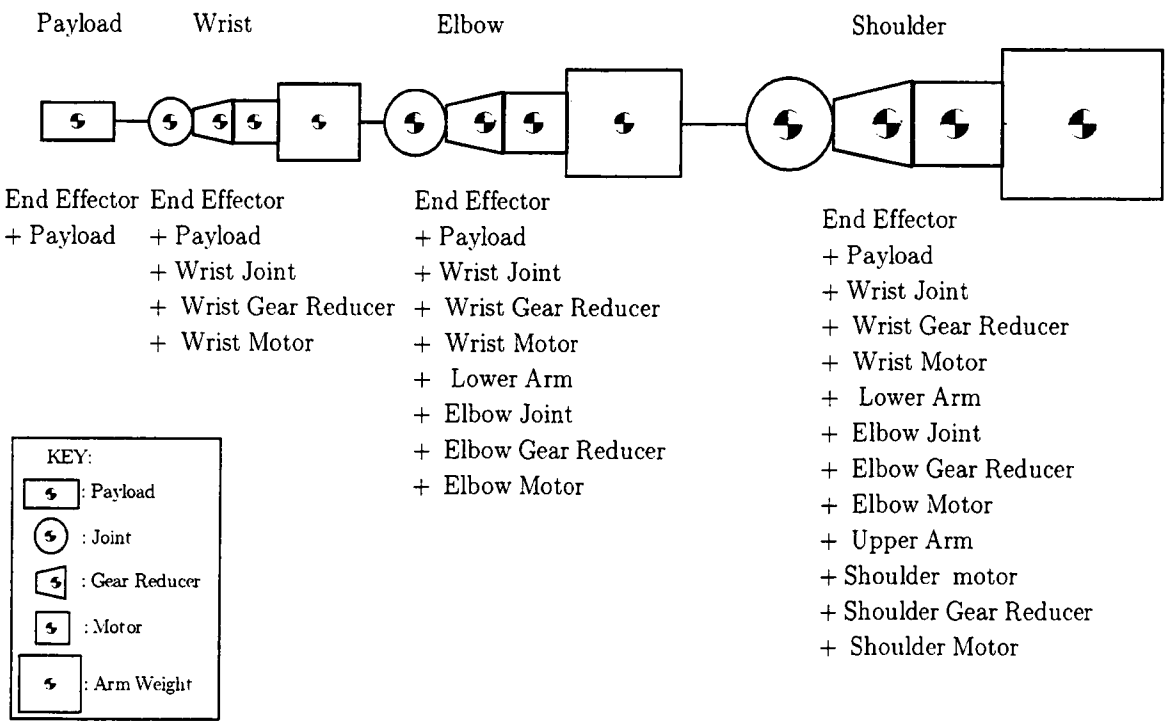

Figure 1.5: Distributed actuation: why it is generally not possible

can't be used in a distributed sense as a general rule. With current electric servoactuator technology, the only alternative is to resort to centralized actuators which, in essence, position the actuators such that their contribution to static weight and inertia are minimized [9]. Centralized actuation essentially places all or most of the joint actuators in one local (or "centralized"—hence the name) area that can be used to counterbalance and minimize the local actuator weight with respect to the overall arm design. However, this greatly complicates the specifics of the arm design in that extensive engineering design work is involved with the physical specifics of choosing actuators and gear reducers and integrating them into the overall manipulator topology. Figure 1.6 demonstrates just how complex centralized actuation can be. This figure shows an exploded view of the internal gearing required to implement a centralized design with 7 identical (state-of-the-art at the time) motors located on the shoulder [10]. All of that effort was for a back-driveable, low friction arm with a *maximum* end effector capacity of only 35 lbs. In high payload cases, even strategic placement and counterbalancing of the motors is not sufficient; in such instances, with currently available technology, electrohydraulic actuators are the only remaining choice.

1.3 Bottom Line: Moving the Payload

The major motivator for this dissertation was the "dead end" that can be reached when evaluating the possibilities of using electric actuation. Many times, the payload-power requirements needed for the design situation are beyond electric actuation feasibility and the *bottom line* is that electric actuators just cannot manipulate the

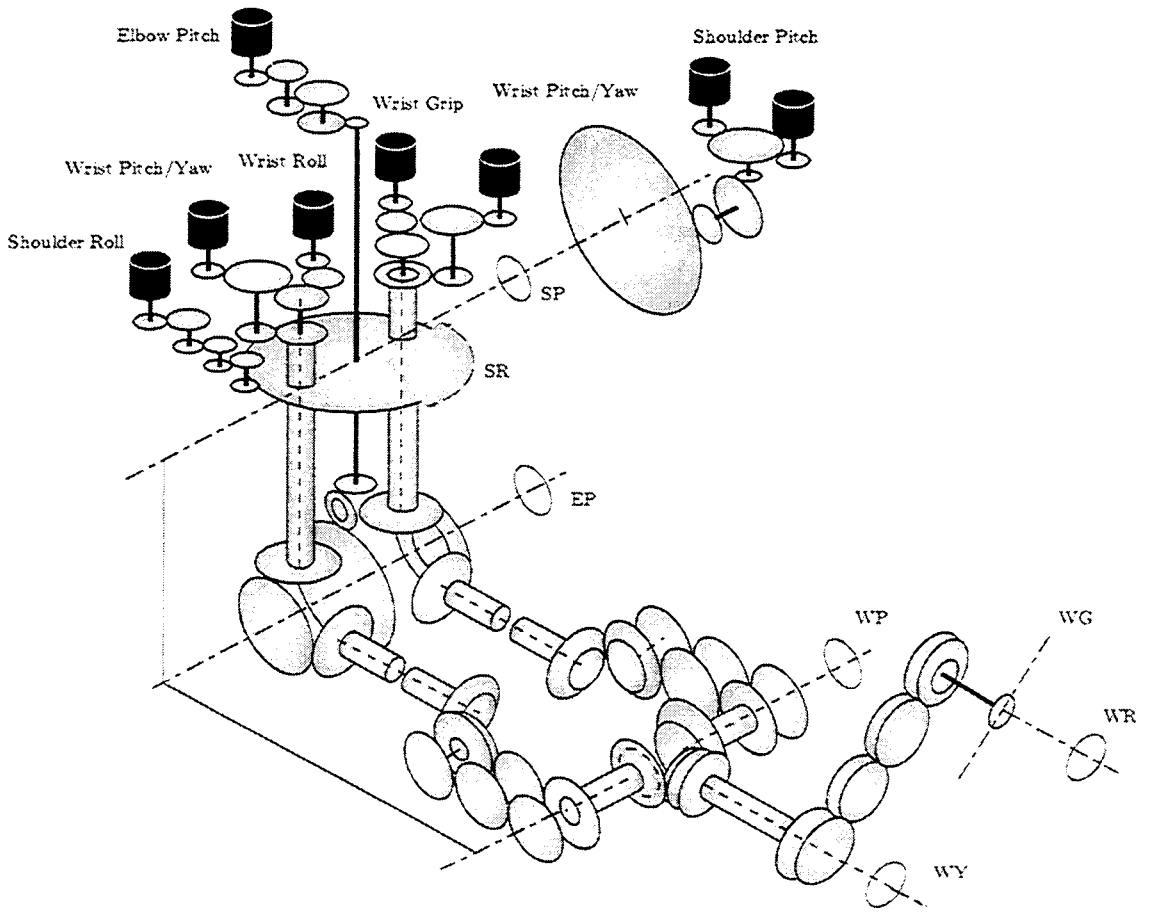

Figure 1.6: Exploded view of a centralized actuator manipulator arm. (Figure courtesy of Oak Ridge National Laboratory).

payload as defined in the design space with the speeds required. For instance, if high torque *and* high speed are required for the design, then fixed gear reducers can help one situtation only at the expense of the other. If a high torque range is required, a high gear ratio can help reach the torque requirement, but only at the cost of overall speed range. Obviously, the converse is also true. Centralized actuation is usually a necessity in which the designer physically arranges the actuators of a manipulator such that electric actuation with gear reducers can be used. Certainly, it is generally true that a distributed actuator design is completely out of the question if no centralized actuation arrangement can be implemented. As we have seen, the fundamental problem is with the electric actuator and its torque/power density. The question is, how do we circumvent this problem? The answer up until this point generally has been to use another type of actuation—typically hydraulics. But, as has been discussed, there may be unwanted characteristics associated with other forms of actuation. The motivation is to find a way to implement *electric* actuation in a much wider range of robotic applications. Ideally, many of the applications would also allow distributed actuation to be achieved.

The fundamental idea behind this work is to release the constraint that electric motors need be coupled to a fixed gear reducer. Instead, the design becomes more robust in that "several" gear reducers are physically available for each joint motor, allowing torque to be traded for speed and vice-versa as needed on-line.

This idea is *not* new, but it is pristinely new in the field of robotics. Just think of all of the machines in the world that use multi-speed (hence several gear ratio) transmissions. Further, think of how large and powerful a car engine would have to be if only *ONE* gear ratio was available. The engine would have to be massive in

order to have the torque/speed range necessary to both start from a stop and maintain an interstate level cruising speed. As another example, think of using a one-speed bicycle to go mountain biking. The thought seems ridiculous, and we argue that as much as a transmission[6] does for an automobile or bicycle, it can also do for an electric actuator. Just as an automatic transmission on an automobile shifts gears to exchange torque capacity for speed capacity as the car begins to move, *so can a multi-speed transmission for an electric motor*! The concept is introduced in detail in the next chapter.

[6]From this point on in this work, unless otherwise stated, transmission tacitly refers to *multi-speed*, or *variable ratio transmissions*.

Chapter 2

The Transmission-Based Actuator Concept

2.1 Overview

This chapter introduces the concept of a *variable reduction* or *transmission-based actuator* (*TBA*) for the purpose of increasing the torque and speed range of an electric actuator in such a way that the power and torque density of electric actuators are more on the order of hydraulics. Electric actuator systems based on multi-speed transmissions will inherently be operable over a wider load and speed range because of their capability of exchanging torque and speed. From a robotics point of view, this can allow electric actuation to be used on a much wider range of manipulators and payloads including larger applications that currently require hydraulic actuation.

The *TBA* concept uses multi-speed transmissions such that heavy, high-torque motors can be traded for high-speed, reduced mass motor-transmission combinations. Use of transmission-based actuators can eliminate the need to employ centralized actuators. Use of distributed actuators can substantially simplify fundamental manipulator design (hence cost) and also expand the feasible scope of electric drives to a

much broader range of applications.

2.2 The Concept

When a fixed ratio gearing system is designed for an actuator, the proper choice of the transmission ratio is centered around meeting the payload and speed requirement for the joint. In some cases, the transmission ratio is selected such that maximum acceleration is achieved for the nominal loading conditions. Systems often have varying loading conditions as well as varying geometry (i.e. arm orientation), and if the design space is limited to a single transmission ratio, the ratio is generally designed to meet torque and speed requirements at a position near the center of the workspace [11]. Conversely, expansion of the actuator design to include several transmission ratios effectively expands the overall portion of the robot workspace where performance is considered optimal in some sense.

Designing an actuator system that has multiple gear ratios available makes the system much more robust. Each ratio can be optimized with respect to a given payload-response requirement. And further, since several ratios are available, several "nominal" loading conditions may be accommodated. For example, an actuator with a range of loading conditions, as is almost always the case for robot actuators because of varying arm configurations, is no longer limited to one gear ratio. The compromises in fixed-ratio design are obviously reduced as the number of available gear ratios increases. This is also true if the transmission is never shifted during motion; each motor and reducer pair are literally another available system. An example would be optimizing gear sizes with respect to several "nominal" loading conditions. Ranges

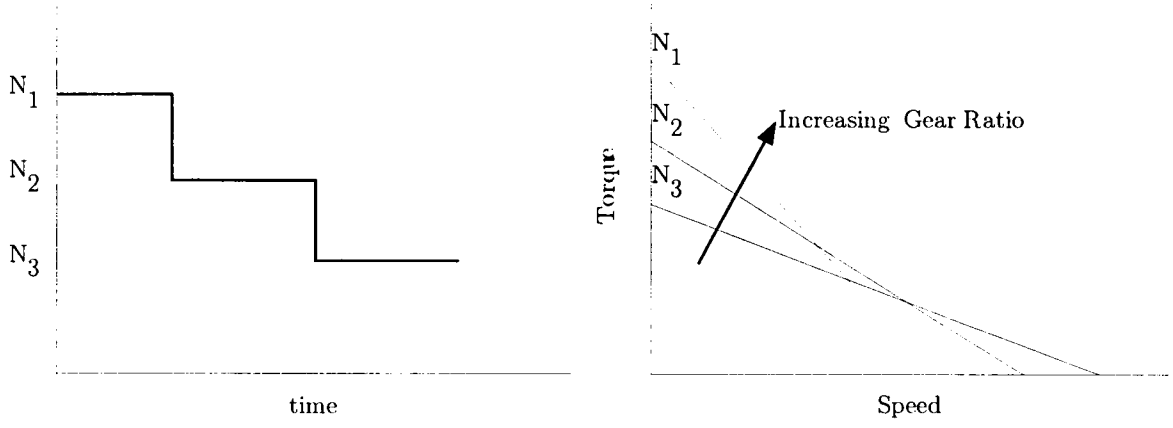

Figure 2.1: Torque-speed tradeoff

of loading and speed requirements could correspond to high payloads, various arm configurations for several "stations" within the overall workspace, travel between two tasks with low end-effector loads, etc. Single, optimized, gear selections can be chosen for each of these situations and coupled to the same electric motor; this in effect (as an absolute minimum) turns one actuator into several "fixed-reduction" actuators (*FRA*'s)[1].

The system is made even more robust when the transmission ratio is allowed to change *during* joint motions. This effectively expands both the torque and speed range of the actuator. When a loaded joint is accelerated from rest, the majority of the available actuator torque is needed to overcome load inertia. However, when the joint is set into motion, inertial effects diminish and less torque is needed. Ideally, the actuator power—recall power is a torque-speed product—can be manipulated such that torque capacity is exchanged for speed capacity when less torque is needed. This is exactly what a transmission does. The situation is illustrated in Figure 2.1. In

[1] "fixed" here refers to no transmission shift during joint motion

the figure, the first plot represents a multi-speed transmission having three available ratios; the plot schematically depicts the gear ratio changing over time with two distinct shifts. The second plot corresponds to the corresponding joint torque-speed curves[2] for each gear ratio. The first gear, N_1, offers the highest mechanical advantage (hence the lowest maximum speed) and is used to set the joint into motion. For the lower gear ratios N_2 and N_3, the torque capacity is traded for speed capacity and the result is an overall expansion of the actuator torque-speed capacity.

This torque-speed tradeoff makes the actuator much more robust in terms of both payload range and speed range. It will be seen in Chapters 4 and 5 that there are strategic ways of shifting the transmission ratios to get desirable results at the joint. Even without shifting, the availability of several gear ratios could allow for strategic selection of a single gear ratio that best meets some criteria for a joint maneuver. For example, for a given payload and nominal arm configuration, a single gear ratio can be selected which optimizes some performance criteria, such as speed, accuracy, or some combination. For any payload-response requirement, there are methods for selecting a single gear ratio to optimize the overall mechanism with respect to a local set of performance goals [11, 12, 13]; these algorithms can be used online, and the available motor-curve/gear-ratio that most closely matches the optimal result is used. This looks at a *TBA* simply as several actuators (several *FRA*'s to be specific) in one package. Multi-speed transmissions have been used in industrial applications in this manner where the transmission ratio is selected and engaged while the machine is offline [14, 15, 16]. The benefits of having several gear ratios available are greatly multiplied if the transmission uses some or all of the ratios while the machine is

[2]Linear joint torque speed curves associated with a direct current motor under constant voltage conditions.

online (i.e. the mechanism is in motion). Strategies for shifting will be discussed later in this work. Overall, the incorporation of a multi-speed transmission expands the capacity of the actuator in terms of both speed and torque simply because of the design modularity; a higher number of motor/transmission combinations along with very strategic ways using them can lead to greatly improved actuators in terms of both speed and torque.

It has been shown that one key aspect of an effective actuator is its power density. Introduction of a transmission into the actuator must not significantly lower the overall power density of the actuator. Clearly, incorporation of a multi-speed transmission to a given motor adds mass to the actuator—hence lowering power density—and cannot itself change the actuator power because power is simply a torque-speed product. The basis for this research and the overall promise of this idea relies on the fact that a multi-speed transmission can allow *smaller*, high power motors (sometimes referred to as "speeders") to also deliver high torque at low speeds. Historically for electric actuators, high torque requirement has demanded that large motors be used with relatively small, and fixed-ratio, gear reductions. The *TBA* concept suggests that these systems can be replaced with smaller motor-transmission[3] combinations. The desired result is an overall increase in the actuator power density. This is depicted in Figure 2.2.

[3]Multi-speed, of course.

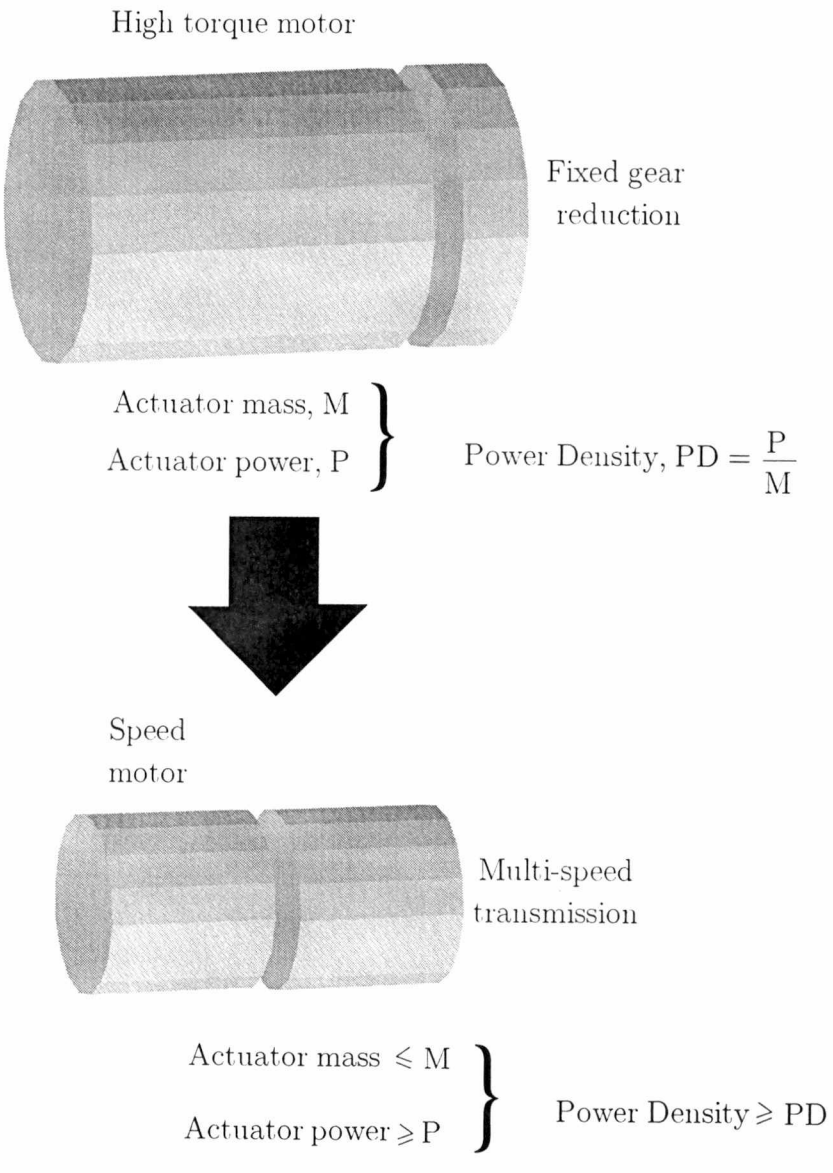

Figure 2.2: Increasing overall power density

Chapter 3

Feasibility Analysis

3.1 Background: Modeling of an Electric Fixed Reduction Actuator

A schematic of a fixed-reduction actuator is shown in Figure 3.1. The gear reduction, N, is fixed in value for this system. The terms T_{ext} and I_{ext} represent the total external torque and mass-moment of inertia about the joint axis. When reflected through the gear reduction, the *effective* mass moment of inertia about the motor axis can be obtained using energy methods[1]:

$$\omega_{load} = \frac{\omega_m}{N},$$
$$\frac{1}{2} I_m \omega_m^2 + \frac{1}{2} I_{ext} \omega_{load}^2, \stackrel{set}{=} \frac{1}{2} I_{eff} \omega_m^2.$$

Hence we have:

$$I_{eff} = \frac{I_{ext}}{N^2} + I_m. \tag{3.1}$$

Similarly, virtual work arguments give the effective torque about the motor axis:

$$\frac{\delta \theta_m}{\delta \Theta_{load}} = N,$$

[1]Here, the inertia of the transmission gears are neglected

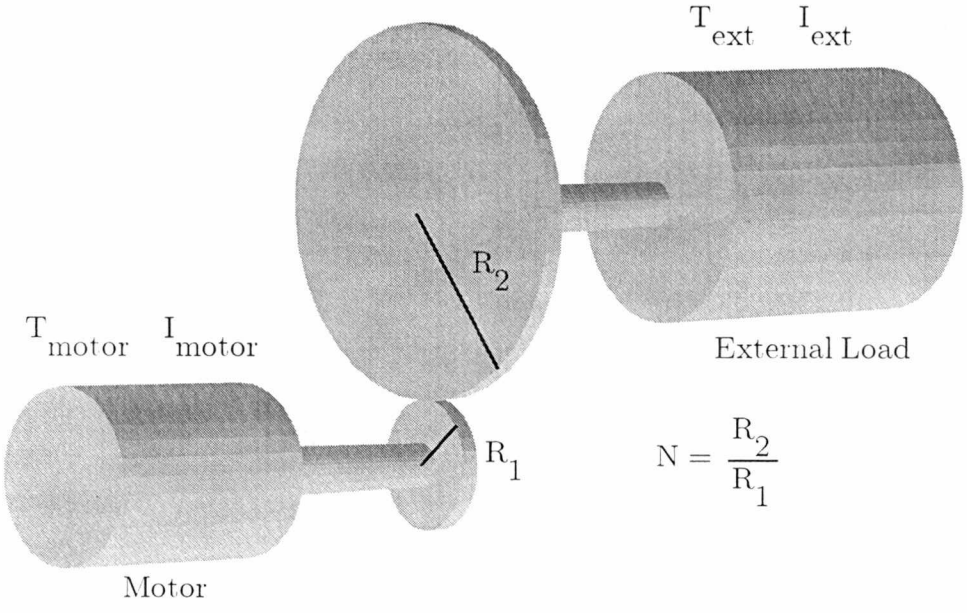

Figure 3.1: Schematic of a fixed reduction actuator (*FRA*).

$$T_{eff}\delta\theta_m = T_{ext}\delta\Theta_{load},$$
$$T_{eff} = \frac{T_{ext}}{N}. \tag{3.2}$$

Under constant voltage conditions, the motor has a linear torque-speed relation given by

$$T_m(\omega(t)) = T_o\left(1 - \frac{\omega_m(t)}{\omega_o}\right), \quad \omega_m(t) \in [0, \omega_o) \tag{3.3}$$

where T_o and ω_o are the stall torque and no-load (theoretical maximum) speed for the motor, respectively [2]. Making use of equations (3.1), (3.2), and (3.3) and *assuming the load is being accelerated*, a summation of moments about the motor axis gives:

$$T_m(\omega(t)) - T_{eff} = I_{eff}\frac{d\omega(t)}{dt},$$
$$T_o\left(1 - \frac{\omega_m(t)}{\omega_o}\right) - T_{eff} = I_{eff}\frac{d\omega(t)}{dt}. \tag{3.4}$$

Rearranging gives:

$$\frac{d\omega_m(t)}{dt} + \left(\frac{T_o}{I_{eff}\omega_o}\right)\omega_m(t) = \frac{T_o - T_{eff}}{I_{eff}}, \tag{3.5}$$

which is a first order, linear, ordinary differential equation for the motor speed, subject to the initial condition

$$\omega_m(0) = \omega_i. \tag{3.6}$$

For robotic applications, the effective inertia and torque may sweep across a wide range of values because of manipulator configuration changes. Consequently, for variable loading and inertia, (3.5) is non-linear and must be solved numerically. In the interest of working with closed-form solutions for the purpose of gaining insight into actuator performance, the remaining derivations in this section assume *constant* effective parameters (set to the most challenging values over the range of motion). As will be seen in a later section, the eventual use of these derivations will be actuator performance *comparisons*; hence, this assumption will not affect the *relative* performance of the actuators.

For the constant parameter case, the solution to (3.5) is given by

$$\omega_m(t) = \omega_i e^{-\frac{t}{\tau}} + (1-\beta)\omega_o\left(1 - e^{-\frac{t}{\tau}}\right), \quad t \geq 0, \tag{3.7}$$

where ω_i is the initial speed of the motor. The *time constant*, τ, and the *torque ratio*, β are defined by the relations

$$\tau \equiv \frac{I_{eff}\omega_o}{T_o} \tag{3.8}$$

$$\beta \equiv \frac{T_{eff}}{T_o}, \quad \beta \in (0,1). \tag{3.9}$$

The motor time constant, τ, provides an indication of the length of time the motor requires to reach its maximum speed for a given loading condition. Furthermore, the

torque ratio β is constrained as shown such that the motor is capable of accelerating the load. We may also note from (3.7) that the maximum speed at which the motor can possibly run under a given loading condition is given by

$$\Omega \equiv \omega_{max} = (1 - \beta)\omega_o. \tag{3.10}$$

Examination of (3.8), (3.9), and (3.10) offers some insight toward motor performance in a given situation. For example, a high torque, low speed motor (τ, β, and Ω are all small quantities) can, in general, reach maximum speed quickly (see (3.8)), but the maximum motor speed can still be quite slow (see (3.10)); keeping in mind that a slow motor speed results in an even slower joint speed via the gear reduction, N, high torque motors lead to relatively slow systems for low payload situations (as in travel between two tasks).

Finally, we conclude the background analysis by remarking that the position response at the joint is obtained by simply integrating (3.7) with respect to time, t, and dividing by the fixed gear-ratio, N:

$$\begin{aligned}
\Theta_{load}(t) &\equiv \frac{1}{N}\int_{\xi=0}^{t} \omega_m(\xi)d\xi + \Theta_i, \\
\Theta_{load}(t) &= \frac{1}{N}\left[\omega_i\tau\left(1 - e^{-\frac{t}{\tau}}\right) + \Omega\left[t - \tau\left(1 - e^{-\frac{t}{\tau}}\right)\right]\right] + \Theta_i,
\end{aligned} \tag{3.11}$$

where Θ_i is the initial angular position of the joint.

3.2 Development of a Discrete-Speed Transmission Model

3.2.1 General Transmission-Based Actuator Model

The simple model for a fixed reduction actuator can be modified to analyze a *discrete-speed* transmission by considering the effects of changing the gear ratio while the motor is in motion. First, it is evident that the effective torque and mass moment of inertia about the motor axis are functions of the gear reduction, being inversely proportional to N and N^2, respectively. However, if the gear reduction is changed in a stepwise or discrete manner, the motor speed equation (3.7) is fully valid[2] for each gear ratio provided that the "initial" motor speed for each gear is adjusted such that the angular speed at the joint remains continuous. For a transmission having n gears, the effective torque and inertia about the motor axis for the "j^{th}" gear are given by

$$T_{eff,j} = \frac{T_{ext}}{N_j}, \quad (j = 1, 2, \ldots, n), \tag{3.12}$$

$$I_{eff,j} = \frac{I_{ext}}{N_j^2} + I_m, \quad (j = 1, 2, \ldots, n). \tag{3.13}$$

Similarly, the definitions of motor time constant, torque ratio, and maximum speed can be defined for each gear:

$$\tau_j = \frac{I_{eff,j}\,\omega_o}{T_o}, \quad (j = 1, 2, \ldots, n), \tag{3.14}$$

$$\beta_j = \frac{T_{eff,j}}{T_o}, \quad (j = 1, 2, \ldots, n), \tag{3.15}$$

$$\Omega_j = (1 - \beta_j)\,\omega_o, \quad (j = 1, 2, \ldots, n). \tag{3.16}$$

As an initial assumption, we will use *motor speed* as a criterion for transmission shift; we can specify that a shift occur when the motor reaches a certain fraction of the

[2]This still assumes that external loading and inertia are constant.

maximum speed that the motor can achieve for the gear[3]. Hence we define the *speed ratio* for the "j^{th}" gear as the ratio of the actual motor speed to the maximum speed that the motor can achieve for gear j:

$$\gamma_j(t) \equiv \frac{\omega_j(t)}{\Omega_j}, \quad \gamma_j \in (0,1), \quad (j = 1, 2, \ldots, n). \tag{3.17}$$

For purposes of initial conditions for each gear, we demand that the angular velocity at the joint axis remain continuous. Assuming a specified initial motor speed for first gear (i.e. maximum gear reduction) and instantaneous shifting, this leads to an expression for the initial motor velocity for the $(j+1)^{th}$ gear[4]:

$$\omega_{i,j+1} = \left(\frac{N_{j+1}}{N_j}\right)\gamma_j\Omega_j, \quad (j = 1, 2, \ldots, n-1). \tag{3.18}$$

This equation is only approximate but is accurate for the system parameters under consideration in this dissertation[5]. The initial motor velocity for first gear is specified. For our purposes here, zero initial conditions for first gear are assumed. Equations (3.12) through (3.18) contain the elements needed to express the motor speed response for each gear ratio of the transmission. Again, it is assumed that the reduction N for each gear is consistent with the constraint that the torque ratio β remain within the range allowing the motor to accelerate the load; i.e. $\beta \in (0,1)$. Each equation for the motor response in a certain gear is of a form identical to that of (3.7) but is *only valid* while the transmission is in that gear. In order to fit the solutions together in a piecewise manner, an expression for the time interval over which each piecewise response is valid must first be obtained. Along these lines, we denote the *time of shift*

[3]It is shown in later chapters that there are more "strategic" ways to select when the transmission shifts!

[4]For compactness, the subscript "m" is omitted; all foregoing equations are understood to be valid around the motor axis.

[5]See Appendix A for a validation analysis using the conservation of angular momentum.

from "j^{th}" to "$(j+1)^{th}$" gear as

$$t_j \equiv \text{time of shift from gear "j" to "j+1"} \tag{3.19}$$
$$t_0 \equiv 0.$$

Furthermore, for simplicity of notation we define a new time coordinate relating the piecewise intervals to *absolute* time as

$$\tilde{t}_j = t - t_j. \tag{3.20}$$

Using (3.12) through (3.20) and denoting the Heaviside step function by $u(t)$, the piecewise motor response for each value of gear reduction is given by

$$\omega_j(\tilde{t}_j) = \left[\omega_{i,j}\exp\left(-\frac{\tilde{t}_{j-1}}{\tau_j}\right) + \Omega_j\left(1-\exp\left(-\frac{\tilde{t}_{j-1}}{\tau_j}\right)\right)\right]\cdot\left[u(\tilde{t}_{j-1}) - u(\tilde{t}_j)\right], \quad (j=1,2,\ldots,n). \tag{3.21}$$

Note that (3.21) is valid for all time $t \geq 0$, once an expression for the shift time, t_j, is known for each gear. To obtain an expression for the shift times, recall that the shift occurs when the motor reaches a specified fraction of the maximum speed for a gear as defined by (3.17). Thus, evaluation of (3.21) at the shift time t_j gives[6]

$$\omega_j(t=t_j) = \omega_{i,j}\exp\left(-\frac{\Delta t_j}{\tau_j}\right) + \Omega_j\left[1-\exp\left(-\frac{\Delta t_j}{\tau_j}\right)\right] \equiv \gamma_j\Omega_j, \quad (j=1,2,\ldots,n) \tag{3.22}$$

where Δt_j is defined as

$$\Delta t_j \equiv t_j - t_{j-1}, \quad (j=1,2,\ldots,n). \tag{3.23}$$

[6]The step functions are omitted during this process since this evaluation takes place strictly within the valid time interval for gear j.

With use of (3.23), (3.22) can be solved for the time of shift, t_j, from "j^{th}" to "$(j+1)^{th}$" gear. The result is

$$t_j = \sum_{k=j}^{0} \left[\tau_k \ln \left(\frac{1 - \frac{\omega_{i,k}}{\Omega_k}}{1 - \gamma_k} \right) \right], \quad (j = 1, 2, \ldots, n). \tag{3.24}$$

Note that the summation runs from j to 0 in descending order. A few points about this equation are in order. The time of shift, t_j as shown by (3.24) is *not* a time which is directly specified. In fact, (3.24) allows determination of, for a given situation, when the gear change *takes* place; in other words, the shift time is not a specification but a *result.* For a given actuator and payload, (3.24) determines the resulting absolute time at which the motor reaches a *given* percentage of its maximum speed for a gear. This information is necessary for both graphical interpretation of the motor speed response and construction of the composite solution from the piecewise relations (3.21). Another important note is that (3.24) is only valid within the bounds of a reasonable gear reduction scheme. Specifically, the strict constraint on the speed ratio range, $\gamma_j \in (0, 1)$, is quite clear here. Physically unrealizable results from (3.24) such as a negative or imaginary relative time of shift indicate a mismatch between the transmission gear ratios available and the load-response requirement.

Finally, using (3.20), (3.21), (3.23), and (3.24), the total speed response of the motor can be formed by a piecewise superposition of equations (3.21). The result is summarized as

$$\omega(t) = \sum_{j=1}^{n} \omega_j(t), \tag{3.25}$$

where n = the total number of gears in the transmission. Figure 3.2 shows a typical motor speed response for a 5-speed transmission. The total speed response *of the*

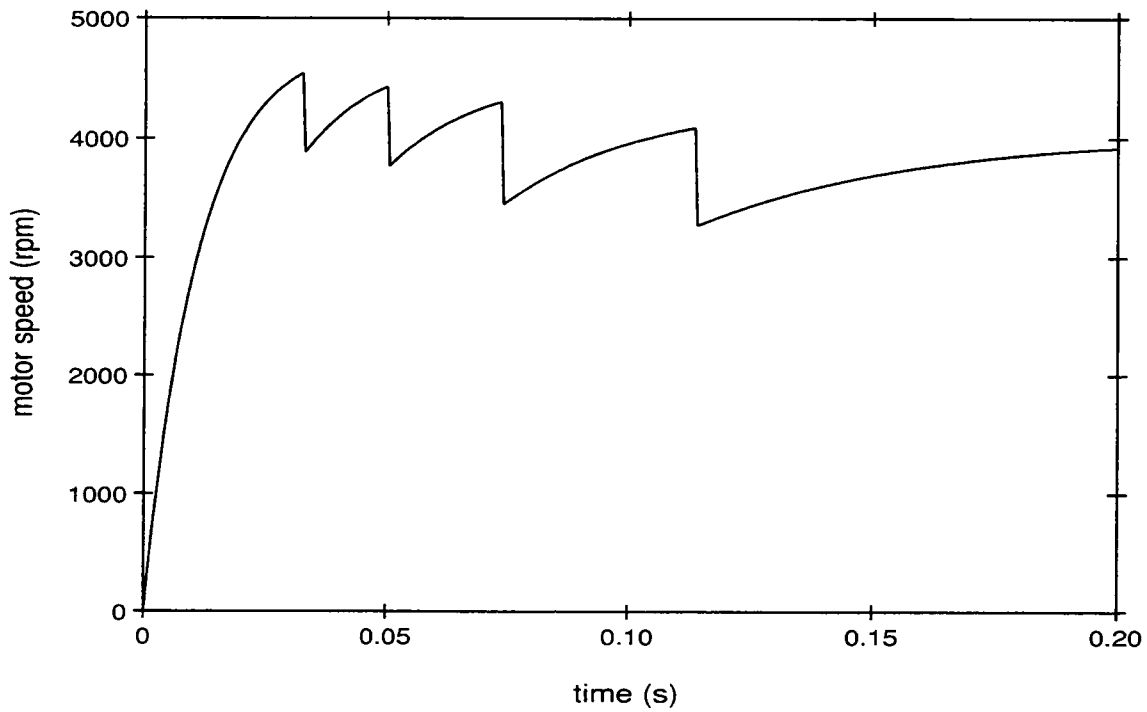

Figure 3.2: Motor speed response (5-speed transmission)

load (i.e. at the joint) is given by

$$\omega_{load}(t) = \sum_{j=1}^{n} \left(\frac{\omega_j(t)}{N_j} \right). \tag{3.26}$$

It is emphasized again that all of the foregoing equations are only valid for the acceleration portion of the response since that assumption was made for the moment summation equation, (3.5). In essence, the deceleration portion of the speed response is a mirror image of the acceleration portion of the speed response about the point at which half of the maneuver has been achieved; in other words, a plot of the speed response vs. time, t, ($t \in [0, t_{max}]$) is symmetrical about the line $t = \frac{t_{max}}{2}$.

With the speed response of the motor now known, an expression for the rotational response, or the position of the load vs. time, can be obtained. This is done by integrating the speed response (3.21) with respect to time. In a manner similar to

that for the speed response, care must be taken to assure that the rotation at the joint remain continuous throughout the superposition of the piecewise solutions. We first assume that the initial rotation of the load in first gear ($j = 1$) is specified. Again, for our purposes here, it is assumed that this initial rotation is zero. Once the rotational response of the arm in a given gear is known, the "initial" rotation of the joint in the following gear is given by

$$\Theta_{i,j} = \Theta_{j-1}\left(t = t_{j-1}\right), \quad (j = 2, 3, \ldots, n). \tag{3.27}$$

Equation (3.27) demands that the "initial" joint rotation in the "j^{th}" gear be mathematically identical to that of the "$(j-1)^{th}$" gear at the time of shift, t_{j-1}; this enforces the assumption of instantaneous shifting. The rotational response of the load during engagement of gear j is given by:

$$\Theta_j(\tilde{t}_j) = \left[\frac{1}{N_j}\left\{\omega_{i,j}\tau_j\varphi(\tilde{t}_{j-1}) + \Omega_j\left[\tilde{t}_{j-1} - \tau_j\varphi(\tilde{t}_{j-1})\right]\right\} + \Omega_{i,j}\right] \cdot \left[u(\tilde{t}_{j-1})) - u(\tilde{t}_j)\right], \quad (j = 1, 2, \ldots, n), \tag{3.28}$$

where

$$\varphi(\tilde{t}_{j-1}) = 1 - \exp\left(-\frac{\tilde{t}_{j-1}}{\tau_j}\right) \quad (j = 1, 2, \ldots, n). \tag{3.29}$$

Equations (3.28) are valid for all gears in their respective time interval, and represent the contribution of each gear to the total change in displacement. The total rotational response of the load during the acceleration portion of the maneuver is given by a superposition of equations (3.28):

$$\Theta_{load}(t) = \sum_{j=1}^{n} \Theta_j(t). \tag{3.30}$$

3.2.2 Performance Comparison

When analyzing the relative performance between the fixed-reduction actuators (FRA) and the transmission-based actuators (TBA), the focus here is the *required time* for a specified maneuver under specific loading conditions. In other words, for a specified loading condition and rotational maneuver, it is of interest to determine the time required for each type of actuator to achieve the motion. Concerning loading, it was decided to use a maximum load (and inertia) situation involving a shoulder pitch-up maneuver with a fully extended manipulator configuration. For each system, a payload and desired position maneuver is specified and the performance of each system—specifically the time required for each system to achieve the maneuver—is noted and compared. This requires solving (3.30) for time, using $n = 1$ for the FRA and $n =$ (total number of gears) for the TBA[7]. Recalling that (3.30) is only valid for the acceleration portion of the maneuver, the symmetry of the speed response assures that the total maneuver time (i.e. acceleration and deceleration) is twice the value obtained from (3.30).

In this manner, motor-transmission combinations can be selected such that overall design requirements are met by the gross transmission parameters of the transmission-based system. In the next section, this approach is used to evaluate the feasibility of using transmission-based actuators in a specific distributed actuator robot manipulator.

[7]Note that (3.11) could also be used to solve for the maneuver time for the FRA.

3.3 Feasibility Study for Distributed Actuation

3.3.1 A Brief Introduction to *ORNL*'s Advanced Servomanipulator

To further study the *TBA* concept, it was decided to analyze an existing centralized-actuator design to determine if *TBA*'s of appropriate specifications would allow the design to be implemented with distributed actuators. The *Advanced Servomanipulator*, (*ASM*) [10] is a six degree-of-freedom (DoF) anthropomorphic telerobotic manipulator (Figure 3.3). The *ASM* is a high performance, low friction, high power manipulator with the capability of producing high tip velocities due, in part, to the centralized-actuator design configuration. Although the *ASM* is rather old (1985), it is a system for which detailed design data and performance specifications are available. For the purposes of this work, the *ASM* is a real system that is valid for comparative analyses because the *ASM* could *still* not be built with distributed actuation today.

The actuators for the *ASM* are identical permanent magnet DC motors with fixed-ratio gear reducers (in the form of internal arm gear trains). Thus, the *ASM* is seen to be made up of fixed-reduction actuators (*FRA*'s). The purpose of this analysis is to evaluate the feasibility of using *TBA*'s to realize a *distributed actuator ASM* design with equivalent payload and response characteristics.

3.3.2 *ASM* Baseline Design and Model

The *ASM* is used as a baseline design for which the (conceptual) distributed actuator system is to be compared on a performance basis. For joint actuation, we have seen that the *ASM* uses centralized identical motors with fixed-ratio gear reducers. Fig-

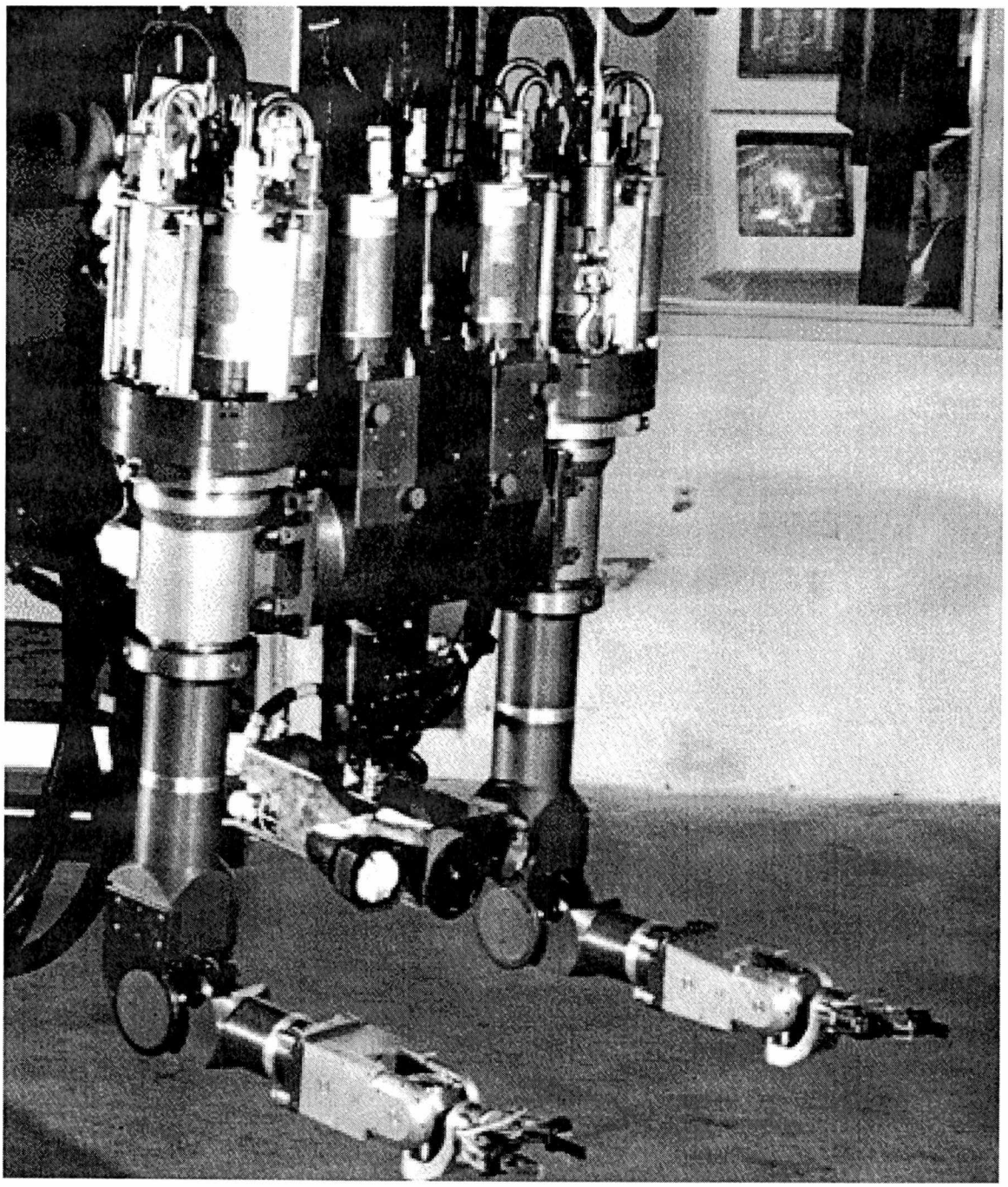

Figure 3.3: The Advanced Servomanipulator (*ASM*). (Photo courtesy of Oak Ridge National Laboratory)

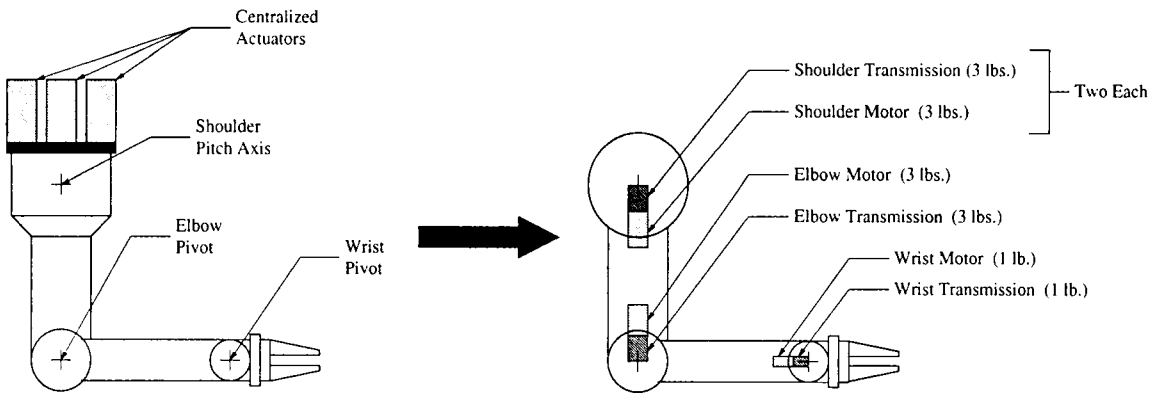

Figure 3.4: Schematic of current *ASM* design and a Distributed Actuator System

ure 3.4 shows schematic representations of both the *ASM* and a distributed actuator servomanipulator (*DAS*) conceptual design.

For simplicity, but without any loss of relevance, the feasibility analysis will use only the shoulder pitch joint with the rest of the arm fully extended. This configuration results in the largest joint torque requirements for any of the *ASM* joints. Using actual *ASM* design specifications [10], the effective (static) torque and the mass moment of inertia about the shoulder pitch-axis are estimated for a 35 lb design payload. For simplicity, it is assumed that the gravitational torque remains constant at its worst case value[8]. Using the maximum voltage torque-speed relation for the *ASM* motors, both the speed and position response of the system are obtained for a specified maneuver. The total travel time required for a given maneuver is numerically calculated from these results for use as baseline performance criteria.

[8]Non-linear loading is briefly discussed in Appendix B.

3.3.3 Modified *ASM* Model: Distributed *TBA* Design with Discrete Shifting

An equivalent *ASM* design is now imagined in which the servomotors and variable-speed transmissions are realized into compact modules located in the proximity of the joint axes. Key assumptions include:

- Actuators associated with each of the first 3 DoF (i.e. pitch DoF) are located in the arm extremities in the proximity of the respective driven joint.
- All physical parameters are left unchanged from the baseline case. This is a highly conservative assumption since the distributed actuator design requires no internal torque-tube transmission mechanisms.
- The transmission subsystem of each *TBA* has a mass equal to the motor for the particular joint. This is a reasonable assumption in the sense that the effective density of the motors is large due to the high-density magnets and windings.
- A multi-speed transmission can be designed, fabricated, and controlled within the manipulator low-level control architecture. In other words, for the feasibility analysis, we assume that a "black-box" transmission is obtainable on a small scale in hope of ascertaining the benefit that such a device could have for a robot system of this type.

After choosing a reasonable gear reduction span for the shoulder transmission subsystem we follow the procedure outlined in Section 3.2.1 and calculate the effective static torque and mass moment of inertia about the shoulder pitch axis *for each gear ratio of the transmission.* Using the approach outlined in Section 3.2.1 the speed and

Table 3.1: Motor parameters

Motor	Weight (lb)	Stall Torque, T_o (ft-lb)	ω_o (rpm)
ASM	8.2	4.2	1100
DAS	3	2.4	5400

position responses of the system are found using motor speed as shifting criteria. The total travel time for the specified maneuver is numerically solved and compared to the baseline case. In this manner, we can choose motor and transmission combinations that mathematically yield equivalent or superior dynamic performance to the baseline *ASM* design.

3.3.4 Feasibility Results

Feasibility is studied by comparing the baseline and *DAS* designs as large pitch-up maneuvers are performed with the arm fully extended. Concerning motor-transmission combinations, it should be emphasized that we generally select much "smaller" motors for use in the transmission-based actuators[9]. Since the manipulators are being compared using a "high" nominal payload, we are in essence seeking equivalency at the most stringent case for the *TBA*'s. Table 3.1 shows the motor parameters for both the baseline *ASM* and a sample distributed actuator servomanipulator (*DAS*) design using an off-the-shelf motor available from Electrocraft Corporation[10].

Figure 3.5 shows the *joint* torque-speed characteristics for both the baseline *ASM* and the *DAS*. The baseline design is marked and is the most flattened curve in the

[9] "smaller" in the sense that the motors are not only of less size but are low-torque, high-speed motors.

[10] ElectroCraft # 0243-02-014.

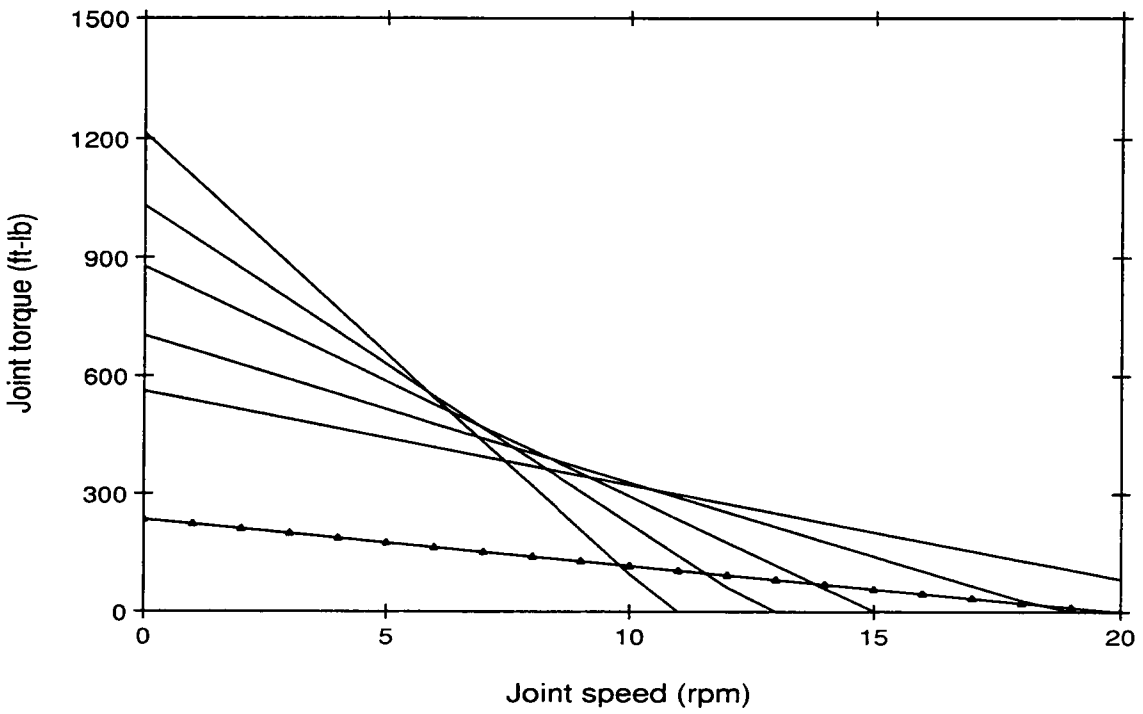

Figure 3.5: Joint torque-speed curves: *ASM* curve is marked.

figure. The other 5 curves represent the torque-speed relation in each gear for the 5-speed *TBA*. The gear reduction for the baseline system is fixed at 56:1, while the transmission-based system ranges from a maximum value of 500:1 to a minimum of approximately 250:1. We see that the transmission only alters the gear reduction by approximately a factor of two; hence this *TBA* can consist of a fixed reduction of 250:1 in-line with a transmission of total span 2.

Figure 3.6 shows a typical motor-speed response comparison. The inherent higher speed of the smaller motor is clear. Figures 3.7 and 3.8 show the *joint* speed and position responses of the two systems, respectively. Note from Figure 3.7 that the area beneath each curve represents the (arbitrarily chosen) specified pitch-up move of 40°. Also, please note from both Figures 3.7 and 3.8 that the required time of

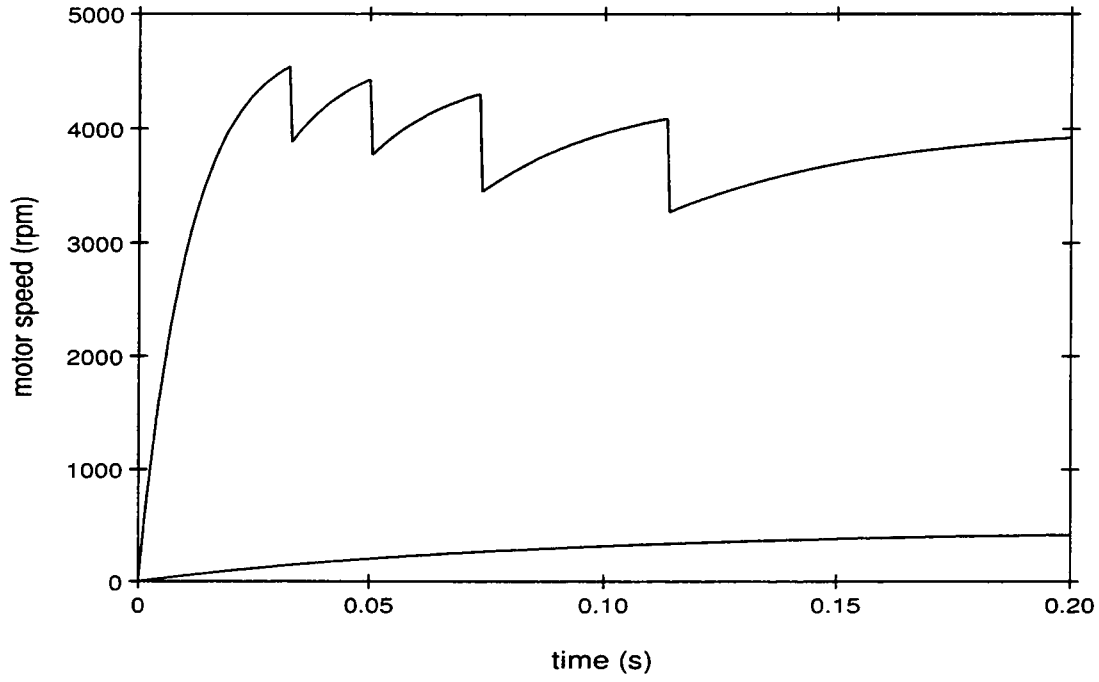

Figure 3.6: Motor speed comparison

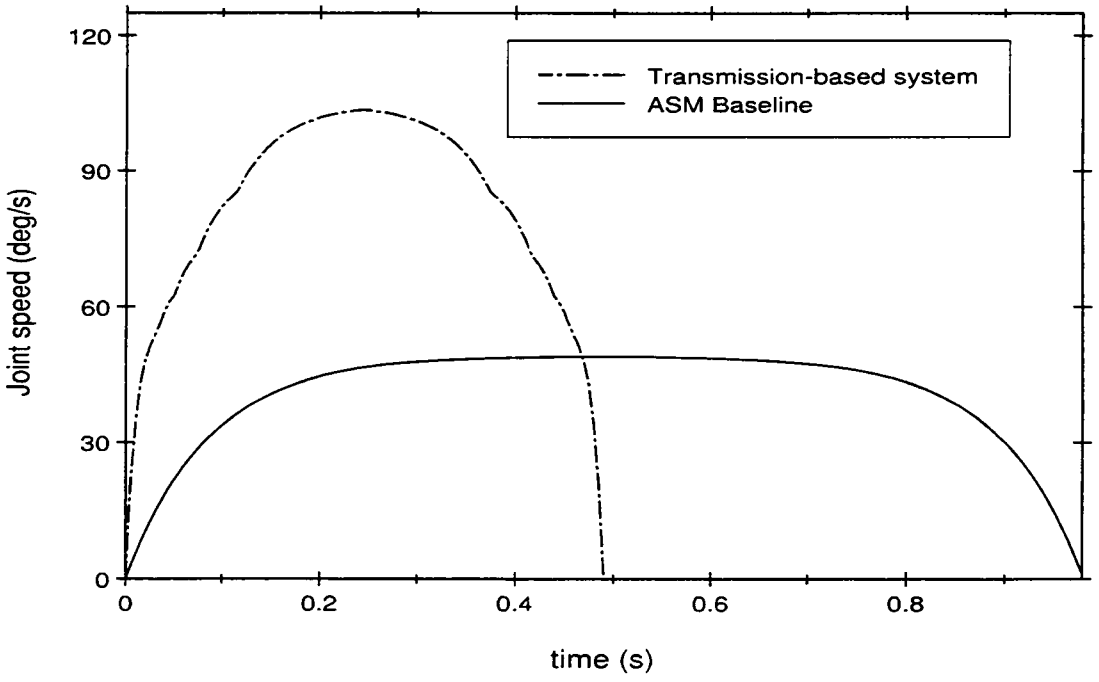

Figure 3.7: Joint speed response for a 40° maneuver

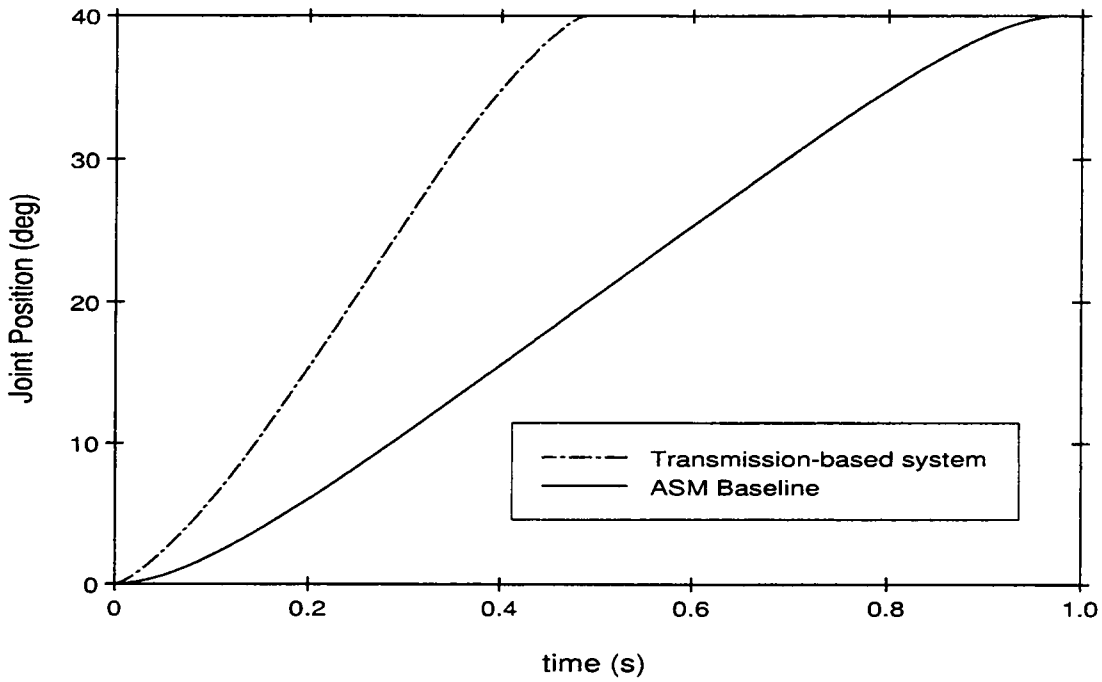

Figure 3.8: Joint position response for a 40° maneuver

maneuver for the *DAS* is approximately one half that required for the baseline *ASM* design.

These promising results were actually quite typical of the type of performance seen with well-chosen motor-transmission combinations for the *TBA*'s. In fact, the allocations for transmission parameters (e.g. weight, reduction span, etc.) could be altered such that the baseline and *DAS* designs had equivalent performance results. These results show that the idea of using *TBA*'s to simplify manipulator design and to expand the payload-response range is feasible in terms of the gross design parameters. There are of course many remaining issues regarding design optimization, compact multi-speed transmission development, and acceptable joint servo-control. Future research will focus on these areas.

3.3.5 Feasibility Conclusions

This analysis has evaluated the performance feasibility of using multi-speed transmissions to extend the payload range of electrical actuators. Transmission-based actuators (*TBA*) represent fundamental actuator technology which could change the nature of robot manipulator design. These results demonstrate that *TBA*'s should allow electrical actuators to extend into the performance range normally held by hydraulic actuators. *TBA*'s can also be used to address manipulator design requirements that have led to designs involving centralized actuators with complex drive trains (such as the *ASM*). This analysis is the first step toward the development of *TBA*'s and is based on two major assumptions: (1) compact (i.e. of the size of the servomotors) multi-speed transmissions can be designed and built, and (2) the gear changing of the multi-speed transmissions can be controlled through variable load conditions without disrupting overall manipulator motion quality and precision. Each of these assumptions is addressed in later chapters; Chapter 6 discusses some mechanical design concepts for the multi-speed transmissions, and Chapter 4 discusses low level transmission control.

Chapter 4

Low Level Joint Control

4.1 Overview

This chapter is a thorough investigation into low level transmission control as will apply to robotic applications. The introduction of a multi-speed transmission into an electric actuator design has interesting ramifications associated with robot control in terms of issues such as overall joint smoothness and accuracy, synthesis of logical shifting algorithms, and synthesis/design of mechanical transmission parameters. This chapter begins by discussing some overall control scenarios that are applicable to robot trajectory control. Next, logical minimum time shifting algorithms are developed using three parallel approaches: optimal control theory, calculus of variations, and (with some insight) standard calculus. It is shown that the resulting optimal shifting algorithms are developed in closed form and represent an efficient methodology for both online transmission control (in the case of continuously variable transmissions) and transmission parameter design (for all multi-speed transmissions). Use of the results of this chapter for transmission parameter design is discussed in Chapter 5.

4.2 Overall Control Scenarios

4.2.1 Introduction

As previously indicated, *TBA*'s can be based on either discrete-speed or continuously variable transmissions (*DST, CVT*). In either of these cases, the implications of transmission ratio variations are of considerable concern in robot control where, in general, the underlying joint servo control performance is of critical importance. The quality of the overall robot control, particularly trajectory control, depends on the joint level smoothness and accuracy over the full range of loading conditions. It is clear that changing gear ratio during trajectory maneuvers is disruptive to overall trajectory control—especially in the discrete-speed transmission case. Ideally, the speed ratio variations of the *TBA* should be transparent to the *overall* joint servo control. In other words, the servo control performance should not be significantly degraded by shifting actions, particularly with respect to the mission essential aspects of control precision and time response. Beyond the idealized system used in the analysis of the shifting strategies developed earlier, there exist a multitude of real-time control scenarios which are critical to the fundamental viability of the *TBA* concept. A discussion of several key aspects of the general robot trajectory control scenario in the context of *TBA*'s is presented.

4.2.2 Characteristics of Robot Control

Most robot tasks involve sequences of trajectory and tooling operations. Normally, a task operation involves start and completion phases which are connected by transition

phases. For example, in a simple pick-and-place task, the part to be moved is approached, grasped, moved to the desired location, and placed as required. Generally, precision control is required in the beginning and ending phases when the part is to be grasped and placed. This is required to assure that the part is acquired initially and deposited in the correct location within an acceptable tolerance. In contrast, the transition phase in which the part is being "flown" to the desired location is normally much less stringent in terms of accuracy. During this phase, the emphasis is more focused on the smoothness of operation to insure that undesirable vibrations and motions are not initiated. Additionally, the speed of operation during these phases has a direct correspondence to the accuracy requirements. Speeds tend to be slow during grasping and placing, while speeds are often maximized during transition such that task cycle time is minimized.

There is a natural match-up between transmission shifting behaviors and the fundamental task speed characteristics discussed above. A task trajectory will in general be comprised of a series of incremental changes in specific robot joints as shown in Figure 4.1. There is a period of acceleration, a period of constant speed at a desired angular rate and a period of deceleration. The shapes of the acceleration and deceleration regions can be based on polynomial functions which are intended to control jerk and other vibration inducing effects. The key point to Figure 4.1 is that speed ratio changes occur during the acceleration and deceleration phases before and after the part is in contact with the environment or other objects.

In pick and-place operations, it is not necessary to execute speed (i.e. *gear ratio*) variations during grasp and place since the precision requirements dictate low speed operation. It appears that the regime where speed changing will occur over a wide

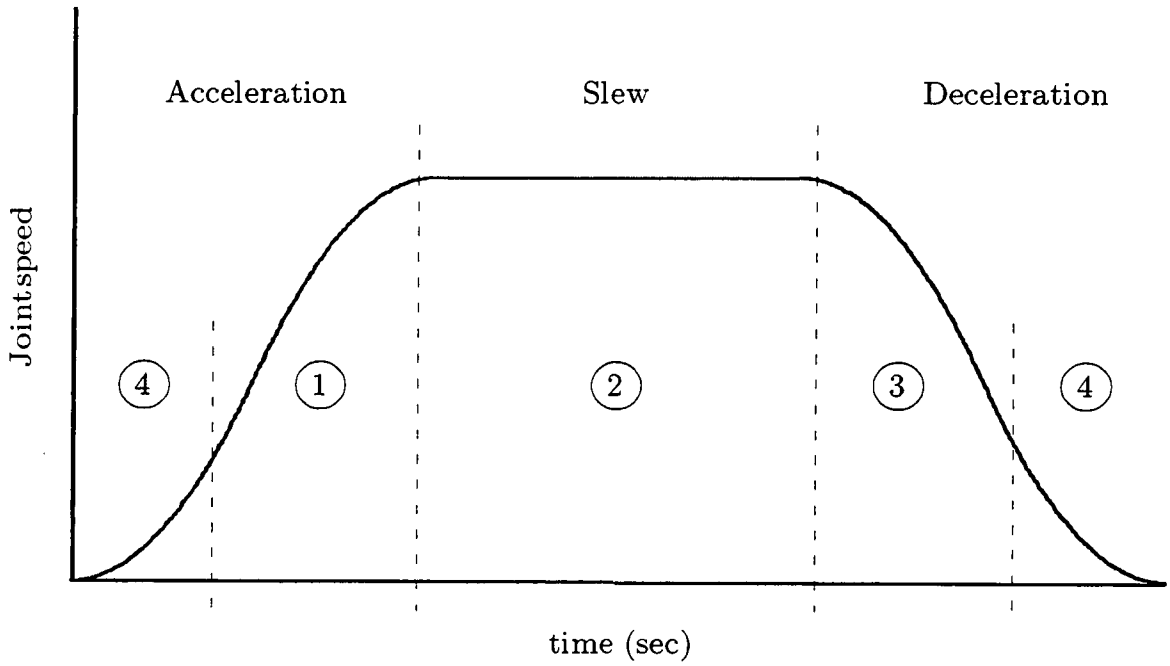

Figure 4.1: Joint Speed Task Trajectory

range is the transition phase where the part is being flown to a new location. The beauty of this fact is that in this phase precision control is not of great concern as long as smoothness and stability are achieved. In other words, the actuator will seldom, if *ever*, be required to implement speed change in the vicinity of a precision task.

4.2.3 General Control Objectives

Grasp and Place Phases: These are regions 4 in Figure 4.1. In this situation, it is desired to maintain high precision and stable servo-control under low speed operation. This will always be performed with a fixed value of gear reduction, most likely the highest ratio (lowest speed) selection. An adaptive control

scheme which is aware of the transmission ratio with appropriate gain changing may be needed.

Transition Phases: These correspond to region 2 and the connecting segments of regions 1 and 3 in Figure 4.1. Here we maintain smoothness and stability as the speed ratio (gear selection) varies over a large range. The situation is further complicated by the fact that manipulator mechanisms will *also* go through their largest configuration changes during this phase. The combined effect is that significant plant changes occur during the transition phase.

The transition phase could also be complicated by tracking precision in some applications (such as machine tools, for example). Tracking implies that it is not only necessary to get from point A to point B, but to accomplish the flight path with a measure of accuracy along the trajectory of the prescribed path. It is anticipated, however, that tracking accuracy is not nearly as stringent as the accuracy required for the grasping and placing of a part.

4.2.4 Generalization

It seems fundamental that machine operations tend to be slow and deliberate when precision is required and less so at other times such as transitions. This observation appears to reduce the challenges initially thought to be associated with *TBA* servo control. The most challenging joint-level control situations will occur at low-end fixed speed ratio conditions which are in essence identical to classical control objectives. Transition phase operations require less precision and will undoubtedly be more "tolerant" regarding control perturbations which may be associated with the altering of

gear ratio. In the transition phase, maintaining stability and smoothness with strict precision is far more tractable than maintaining stability, smoothness, *and* precision.

A "control regime partitioning" approach to low-level *TBA* control is an apparent method of attack. This approach should make robust control of the actuators more achievable and tractable, and has promising attributes for making the low-level control transparent to the overall system.

The foundations of the low level joint control for the transmission have been presented up to this point in this work. The next sections concentrate on the subject of transmission control with respect to the development of logical (and optimal) shifting strategies for the transmissions. In particular, since payload/response requirements are often critical to an overall actuator design, optimization of the shifting profiles is performed with respect to minimizing overall joint trajectory time. The algorithms are developed in a strict fashion for continuously variable transmission concepts using two parallel analytical approaches: optimal control theory and calculus of variations. Also, a correlation between a minimum time maneuver and a maximum acceleration maneuver is presented. The results are also extended for the purpose of developing optimal shifting algorithms for discrete-speed transmissions as well.

4.3 Optimal Control Analyses

4.3.1 Time Optimal Continuous Shifting Strategy

This section develops a continuous gear reduction strategy, which, when incorporated into a continuously variable transmission-based actuator, will execute a specified joint

trajectory in minimum time[1]. The optimal strategy is derived using both optimal control and variational calculus. The final result is a closed-form expression for the gear reduction versus joint speed that will, *for any rotational move*, provide a minimum-time path. In fact, the result is independent of the magnitude of the position change altogether. It will also be shown that a maximizing acceleration versus velocity gives the same joint trajectory—a minimum time path. Finally, a constraint will be shown that, if held intact, will guarantee that the strategy is associated with a local extremum.

4.3.2 Optimal Control Preliminaries

In optimal control problems, variables are considered either as *state* or *control* variables. The manipulation of control variables directly affects the state variables which are governed by first order ordinary differential equations. The problem is to find a suitable control for a desired result.

The simplest control problem is to select a piecewise continuous function $u(t)$, $t \in [0, t_{max}]$, to minimize (or maximize) [17, 18, 19]

$$\int_{t=0}^{t_{max}} L\left(t, y(t), u(t)\right) dt,$$

subject to

$$\frac{dy}{dt}(t) = g\left(t, y(t), u(t)\right), \quad t_{max}, y(0) : \text{fixed}, \quad y(t_{max}) : \text{free}.$$

For our purposes here, both the control variable $u(t)$ and the state variable $y(t)$ are at least piecewise continuous. In general, the fundamental step in using opti-

[1]An analysis developing a gear reduction strategy to match a trajectory performance is given in Appendix C

mal control theory is to "adjoin" the optimization integrand, $L(t, y(t), u(t))$ with the "constraint" $g(t, y(t), u(t))$ with an undetermined multiplier function $\lambda(t)$ forming the *Hamiltonian, H*:

$$H\left(t, y(t), u(t), \lambda(t)\right) \equiv L\left(t, y(t), u(t)\right) + \lambda(t) g\left(t, y(t), u(t)\right).$$

For an optimal control, $u^*(t)$, that yields an optimal (i.e. minimum or maximum) response $y^*(t)$, there is a continuously differentiable function $\lambda(t)$ such that $u^*(t)$, $y^*(t)$, and $\lambda(t)$ simultaneously satisfy the *state equation*

$$\frac{dy}{dt}(t) = g\left(t, y(t), u(t)\right), \quad y(0) = y_o,$$

the *adjoint equation*

$$\frac{d\lambda}{dt}(t) = -\frac{\partial H}{\partial y}, \quad \lambda(t_{max}) = 0,$$

and the *optimality condition*

$$\frac{\partial H}{\partial u} = 0,$$

for all $t \in [0, t_{max}]$. In the general case, the optimality condition is used to get the control u as a function of y and λ resulting in two simultaneous differential equations in y and λ. For a minimization problem, the optimal control $u^*(t)$ must minimize H with respect to u; thus

$$\frac{\partial^2 H}{\partial u^2} > 0$$

is necessary for a minimum. The converse is true for a maximization problem.

4.3.3 Calculus of Variations Preliminaries

A basic calculus of variations problem involves minimizing an integral of the form[2]

$$I = \int_{x=x_a}^{x_b} F\left(x, y(x), y'(x)\right) dx, \quad y(x_a) = y_a, \quad y(x_b) = y_b,$$

by making use of the *Euler-Lagrange differential equation*

$$\frac{\partial F}{\partial y} - \frac{d}{dx}\left(\frac{\partial F}{\partial y'}\right) = 0$$

on the integrand F of the integral [20]. The resulting second order ordinary differential equation, when solved, gives a family of optimal trajectories (or *extremals*) $y^*(x)$ for the general optimization problem. Application of two boundary conditions reduces the extremal family to the solution specific to the problem, if such a solution exists. Criteria for the extremal to represent a relative minimum or maximum can be found in any text on Calculus of Variations (e.g. [20, 21]) but will not be discussed here since we will address the point from an optimal control standpoint in the problem to be analyzed.

Note that in both this and the previous section, the discussions referred to the generalized problem statements– these brief overviews are just glimpses of the overall picture. These methods are merely formulations and simply lead to (generally) additional differential equations to solve such that the resulting solutions are optimized in some sense. Some cases can reduce down to additional *algebraic* equations that augment the governing differential equation. Indeed, this is the case for the problem to be presented.

[2]Here, a prime denotes differentiation with respect to the independent variable, x.

4.3.4 Problem Statement

The goal is to optimize a gear reduction strategy, say $N(t)$, such that the resulting rotational joint response of a transmission-based actuator will occur in minimum time. It can be shown that, for a *positively accelerating* load starting from rest, the governing differential equation for the *joint* speed $\omega(t)$ can be written as [22, 23, 24, 25]:

$$\left(I_m N^2(t) + I_{ext}\right)\frac{d\omega}{dt}(t) + \left(\frac{T_o N^2(t)}{\omega_o}\right)\omega(t) = T_o N(t) - T_{ext}, \quad t \geq 0, \tag{4.1}$$

subject to

$$\omega(0) = 0. \tag{4.2}$$

Here, I_m represents the mass moment of inertia of the motor, T_o and ω_o are the stall torque and no-load speed of the motor, and I_{ext} and T_{ext} are the external inertia and external torque about the joint axis. For compactness define the following terms:

$$A(N) \equiv I_m N^2 + I_{ext}, \tag{4.3}$$

$$B(N) \equiv \frac{T_o N^2}{\omega_o}, \tag{4.4}$$

$$f(N) \equiv T_o N - T_{ext}. \tag{4.5}$$

Using (4.3)-(4.5), (4.1) becomes

$$A(N)\frac{d\omega}{dt}(t) + B(N)\omega(t) = f(N), \quad \omega(0) = 0, \quad t \geq 0. \tag{4.6}$$

The final goal involves finding a trajectory for the gear reduction N---a continuous function of time, speed, etc.— such that the resulting *position response* $\theta(t)$

$$\theta(t) = \theta_o + \int_{\xi=0}^{t} \omega(\xi)d\xi \tag{4.7}$$

completes a desired position change (i.e. $\theta(t_{max}) - \theta_o$) in *minimum time.*

4.3.5 Optimal Analyses

4.3.5.1 Solution via Optimal Control

Since the objective is to minimize the total time of the rotational response (i.e. minimize t_{max}), the integral to be optimized is given by

$$t_{max} = \int_{t=0}^{t_{max}} dt, \tag{4.8}$$

subject to

$$\frac{d\omega}{dt} = \frac{f(N) - B(N)\omega}{A(N)}, \quad \omega(0) = 0, \quad t \geq 0. \tag{4.9}$$

Comparing this to the general case in Section 4.3.2, we have t as the independent variable, ω as the dependent variable, $L = 1$ and $g =$ RHS of (4.9). Adjoin (4.8) to (4.9) by forming the Hamiltonian as follows:

$$H(t, \omega, N, \lambda) = 1 + \lambda(t) \left(\frac{f(N) - B(N)\omega}{A(N)} \right). \tag{4.10}$$

A necessary condition for an optimum to occur is that

$$\frac{\partial H}{\partial N} = 0 = \lambda(t) \left[\frac{A(N) \left(\frac{\partial f}{\partial N} - \frac{\partial B}{\partial N}\omega \right) - (f(N) - B(N)\omega) \frac{\partial A}{\partial N}}{A^2(N)} \right]. \tag{4.11}$$

Since $\lambda(t) \neq 0$ and $A(N) \neq 0$, this reduces to[3]

$$A(N) \left(\frac{\partial f}{\partial N} - \frac{\partial B}{\partial N}\omega \right) - (f(N) - B(N)\omega) \frac{\partial A}{\partial N} = 0. \tag{4.12}$$

From the definitions (4.3)–(4.5), the required partial derivatives are explicitly

$$\frac{\partial A}{\partial N} = 2I_m N, \tag{4.13}$$

$$\frac{\partial B}{\partial N} = \frac{2T_o N}{\omega_o}, \tag{4.14}$$

$$\frac{\partial f}{\partial N} = T_o. \tag{4.15}$$

[3]Note that this step eliminates the need to solve a differential equation for $\lambda(t)$.

Using (4.3)-(4.5) and (4.13)-(4.15) in (4.12) gives

$$\left(I_m N^2 + I_{ext}\right)\left(T_o - \frac{2T_o N}{\omega_o}\omega\right) - \left(T_o N - T_{ext} - \frac{T_o N^2}{\omega_o}\omega\right) 2I_m N = 0. \tag{4.16}$$

Grouping like powers of N leads to the quadratic equation for the gear reduction:

$$N^2 + \left(\frac{2I_{ext}}{I_m \omega_o}\omega - \frac{2T_{ext}}{T_o}\right) N - \frac{I_{ext}}{I_m} = 0. \tag{4.17}$$

Define the following *constant* non-dimensional ratios:

$$\rho \equiv \frac{I_{ext}}{I_m} \quad \text{(Inertia ratio)}, \tag{4.18}$$

$$\sigma \equiv \frac{T_{ext}}{T_o} \quad \text{(Torque ratio)}, \tag{4.19}$$

such that the quadratic becomes:

$$N^2 + 2\left[\rho\left(\frac{\omega}{\omega_o}\right) - \sigma\right] N - \rho = 0. \tag{4.20}$$

It is clear from (4.20) that the optimal gear reduction is solely a function of the joint speed, ω, hence $N = N(\omega)$. The roots of (4.20) give the optimal continuous shifting strategy $N^*(\omega)$. Using the quadratic formula we have:

$$N^*(\omega) = -\left[\rho\left(\frac{\omega}{\omega_o}\right) - \sigma\right] \pm \sqrt{\left[\rho\left(\frac{\omega}{\omega_o}\right) - \sigma\right]^2 + \rho}.$$

Note that the discriminant is strictly positive, hence the negative radical corresponds to a negative root—regardless of speed—and must be discarded on physical grounds. We also note that

$$\left|\rho\left(\frac{\omega}{\omega_o}\right) - \sigma\right| < \sqrt{\left[\rho\left(\frac{\omega}{\omega_o}\right) - \sigma\right]^2 + \rho}, \quad \forall \rho, \sigma, \omega, \omega_o.$$

Hence one concludes that the positive radical always corresponds to a positive root—a physically realizable result. The final result for the optimal shifting strategy is

$$N^*(\omega) = -\left[\rho\left(\frac{\omega}{\omega_o}\right) - \sigma\right] + \sqrt{\left[\rho\left(\frac{\omega}{\omega_o}\right) - \sigma\right]^2 + \rho}, \tag{4.21}$$

with ρ and σ defined as shown in (4.18) and (4.19), respectively.

Finally, for the control trajectory $N^*(\omega)$ to truly correspond to a minimum time maneuver, the following relation must hold:

$$\frac{\partial^2 H}{\partial N^2} > 0, \quad \text{strictly.} \tag{4.22}$$

It is easy to show that this is always true since this relation reduces to

$$T_o N > T_{ext}. \tag{4.23}$$

This relationship always holds if our fundamental assumption of a positively accelerating load is intact. In other words, (4.23) (and subsequently (4.22)) always holds if the motor is capable of moving the load at all.

4.3.5.2 Variational Calculus Approach

Using a variational calculus approach, the integral to be minimized is of the form

$$t = \int_{\omega=\omega_1}^{\omega_2} F(\omega, N, N')d\omega \tag{4.24}$$

where we have (cleverly) chosen the joint speed ω as the independent variable. The integrand F is obtained directly from (4.9):

$$\frac{d\omega}{dt} = \frac{f(N) - B(N)\omega}{A(N)},$$

$$dt = \left[\frac{A(N)}{f(N) - B(N)\omega}\right] d\omega,$$

$$\int_{t=0}^{t_{max}} dt = \int_{\omega=\omega_1}^{\omega_2} \left[\frac{A\left(N(\omega)\right)}{f\left(N(\omega)\right) - B\left(N(\omega)\right)\omega}\right] d\omega,$$

Using the definitions (4.3)–(4.5) this becomes

$$t = \int_{\omega=\omega_1}^{\omega_2} \left[\frac{I_m N^2(\omega) + I_{ext}}{T_o N(\omega) - T_{ext} - \frac{T_o N^2(\omega)}{\omega_o}\omega}\right] d\omega.$$

Hence we find for the integrand F:

$$F = \frac{I_m N^2(\omega) + I_{ext}}{T_o N(\omega) - T_{ext} - \frac{T_o N^2(\omega)}{\omega_o}\omega} = F(\omega, N). \tag{4.25}$$

Since F is *not* a function of N', the Euler-Lagrange equation reduces to

$$\frac{\partial F}{\partial N} = 0. \tag{4.26}$$

With the Euler-Lagrange equation taking this form, the end result is an algebraic (instead of differential) equation for the optimal shifting strategy. Taking the required partial derivatives leads directly to the same solution for $N^*(\omega)$, i.e. (4.21).

4.3.6 Correlation to a Maximum Acceleration Maneuver

After carefully studying both of the foregoing analyses, it can be seen that "both" of the previous minimum time analyses correspond to *maximizing* the joint angular acceleration as a function of *joint speed* over the maneuver. This can be seen from[4]:

$$\frac{d\omega}{dt} = \alpha,$$
$$\int_0^t dt_o = \int_{\omega_o=0}^{\omega} \frac{d\omega_o}{\alpha(\omega_o)}.$$

Hence, time is minimized if the angular acceleration versus *speed* is maximized over the move. Writing the equation for the angular acceleration of the joint (in terms of A, B, and f of (4.3)–(4.5)) produces

$$\frac{d\omega}{dt} = \frac{f(N) - B(N)\omega}{A(N)} = \alpha(N(\omega)) = \alpha(N). \tag{4.27}$$

[4]Here, the subscript "o" simply denotes a dummy variable of integration.

Differentiating this expression with respect to N and setting the result to zero again leads to the quadratic equation for the optimal shifting strategy. Strictly, the condition that the solution corresponds to a extremal for acceleration is only true if:

$$\frac{d^2\alpha}{dN^2} < 0.$$

Again, the relation (4.23) assures that this is the case as long as the reflected motor torque exceeds the joint torque requirement at stall.

4.3.7 Demonstration of Results

With $N^*(\omega)$ known, the differential equation for the joint speed (4.6) becomes

$$\bar{A}(\omega)\frac{d\omega}{dt} + \bar{B}(\omega)\omega = \bar{f}(\omega), \quad \omega(0) = 0, \tag{4.28}$$

where

$$\bar{A}(\omega) \equiv A\left(N(\omega)\right), \tag{4.29}$$

$$\bar{B}(\omega) \equiv B\left(N(\omega)\right), \tag{4.30}$$

$$\bar{f}(\omega) \equiv f\left(N(\omega)\right). \tag{4.31}$$

Equation (4.28) is numerically solvable with a standard $4^{\underline{th}}$ order Runge-Kutta scheme. It is known from the physics that (4.28) is "friendly" in a numerical sense in that the coefficients $\bar{A}(\omega)$, $\bar{B}(\omega)$, and $\bar{f}(\omega)$ are continuous, non-zero functions of ω and are without singularities.

To demonstrate the effectiveness of $N^*(\omega)$, we compare four sets of numerical results for a single transmission-based actuator. The loading conditions corresponding

Table 4.1: System parameters

External Torque, T_{ext}	280 *ft-lb*
External Inertia, I_{ext}	34.5 *ft-lb-sec*^{2}
Motor Stall Torque, T_o	2.4 *ft-lb*
Motor No-Load Speed, ω_o	5400 *rpm*
Motor Inertia, I_m	4×10^{-5} *ft-lb-sec*^{2}

to an Advanced Servomanipulator (ASM) [10] shoulder pitch-up maneuver and the selected motor parameters are shown in Table 4.1.

Performance is compared using four gear reduction strategies assuming a speed range $\omega \in [0, \omega_{max}]$:

$$N_1(\omega): \quad N^*(\omega)$$

$$N_2(\omega): \quad N^*(\omega) + \varepsilon(\omega_{max} - \omega)$$

$$N_3(\omega): \quad N^*(\omega) - \varepsilon(\omega_{max} - \omega)$$

$$N_4(\omega): \quad \text{Linear over same range } N \in [N^*_{min}, N^*_{max}].$$

N_2 and N_3 are slightly perturbed above and below N^* respectively via a small parameter ε. This parameter is used such that the curves are perturbed more in lower speed ranges such that differences in the steady state responses are independent of the perturbation . These four strategies are shown for $\varepsilon = 50$, $\omega_{max} = 2$ (rad/sec) in Figure 4.2 [5]. The corresponding speed and position responses are shown in Figures 4.3 and 4.4, respectively.

Clearly, the plots show that N^* corresponds to a minimum-time move. Note that this is true regardless of the desired maneuver itself. The magnitude of the position change appears nowhere in the analysis. Indeed, the optimal strategy is dependent

[5] Although $\varepsilon = 50$ is not "small" relative to gear reductions on the order of 10^2-10^3, this somewhat high value was used by necessity such that the differences in the response plots were visible.

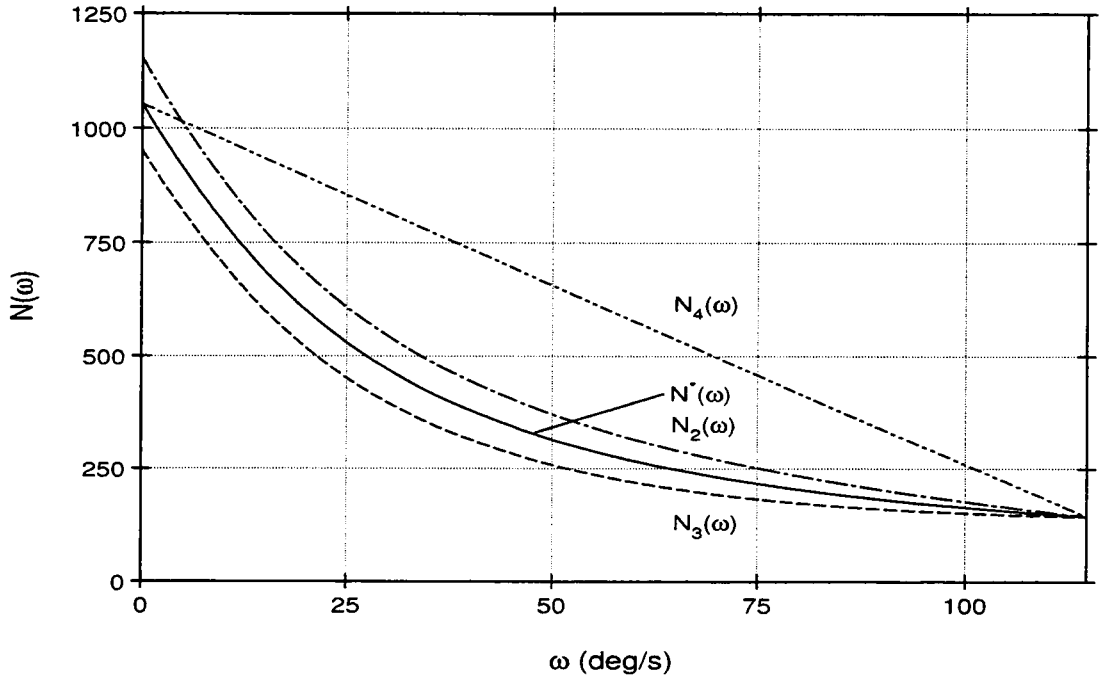

Figure 4.2: Gear reduction vs. speed. $N^*(\omega)$ is optimal.

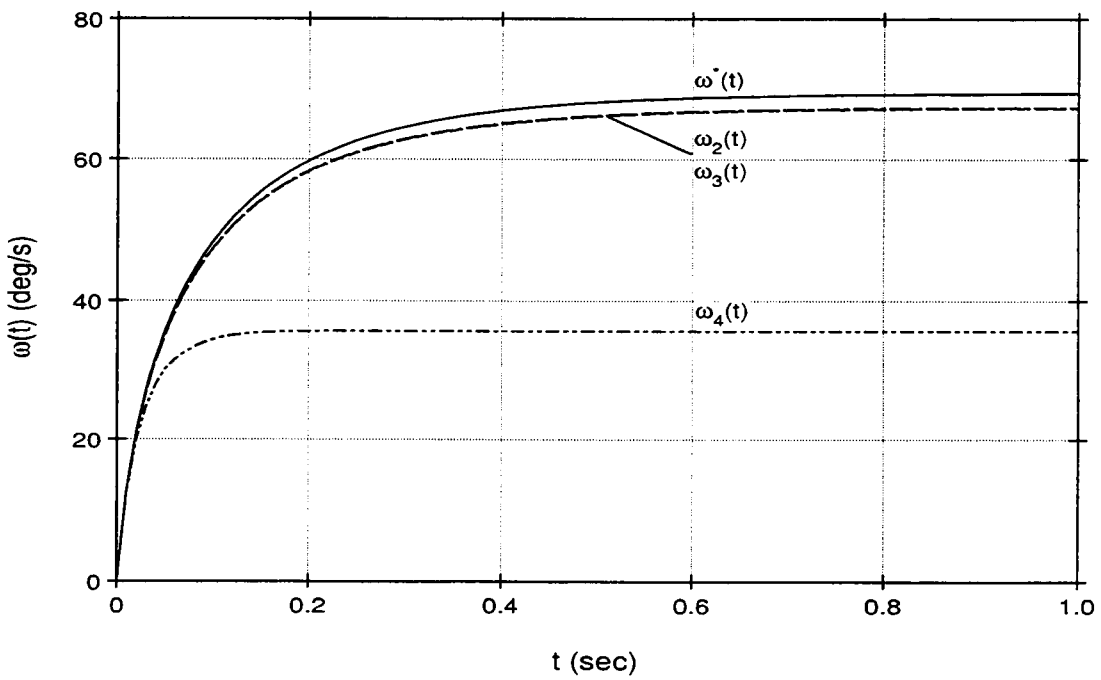

Figure 4.3: Joint speed response. $\omega^*(t)$ is optimal.

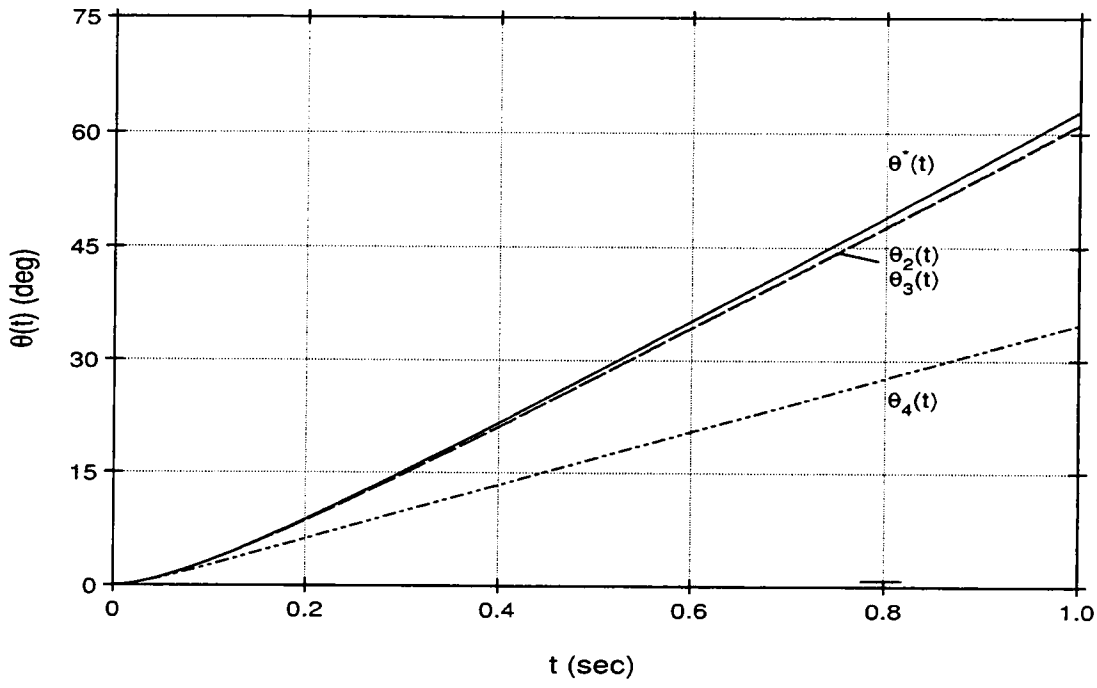

Figure 4.4: Joint position response. $\theta^*(t)$ is optimal.

only on the joint speed. Physically, transmission-ratio can be selected based solely on a joint speed and joint position reading. The latter is needed only to reverse the N^* trajectory for the deceleration portion of the maneuver. Finally, please note that the two responses corresponding to N_2 and N_3 are identical; this behavior is as expected in the vicinity of a relative minimum.

For a physical reason as to exactly why N^* provides the minimum time maneuver, examine a plot of the *motor* speeds for each case over the maneuver. With the joint speed response known, the motor speed response is simply given by

$$\omega_m(t) = \omega(t)N\left(\omega(t)\right), \quad t \geq 0. \tag{4.32}$$

Figure 4.5 shows the motor speed response for each of the four cases under investigation.

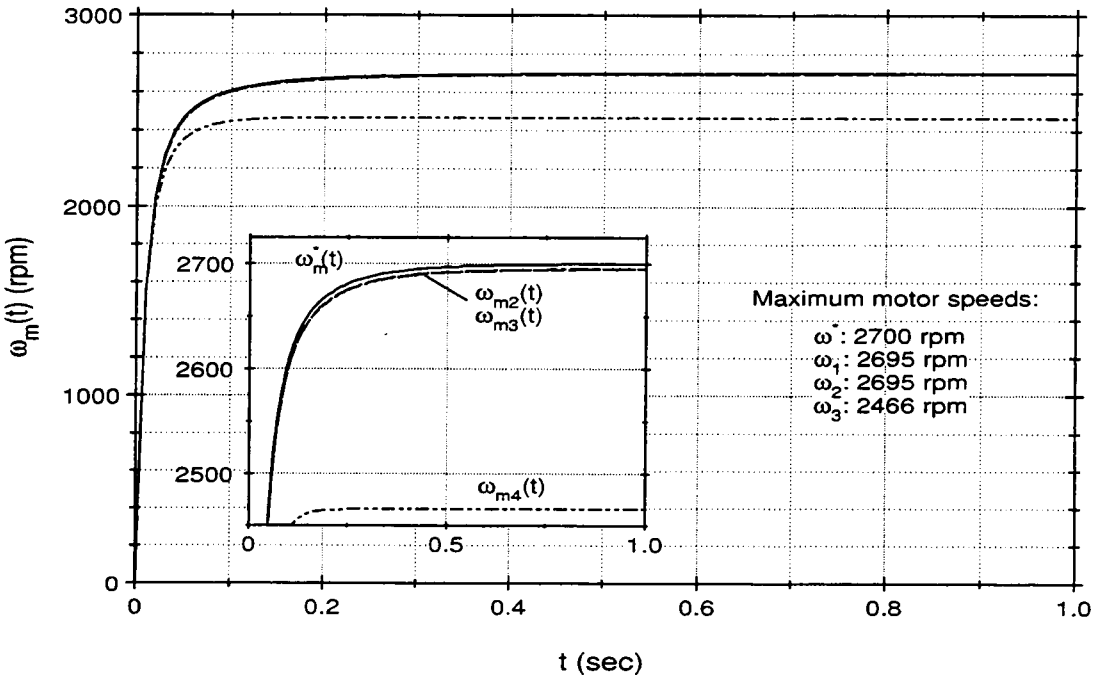

Figure 4.5: Motor speed response. Maximum motor power occurs at 2700 rpm

For cases 1–3, the curves are quite similar but are not identical. The maximum speed for case 1 is precisely 2700 rpm, which is exactly half of the free speed of the motor; this speed–$(\omega_o/2)$–is the speed at which the motor produces maximum power:

$$P(\omega) = T(\omega)\omega = T_o\omega - \frac{T_o\omega^2}{\omega_o},$$
$$\frac{dP}{d\omega} = T_o - \frac{2T_o\omega}{\omega_o} = 0 \Longrightarrow \omega = \frac{\omega_o}{2}. \tag{4.33}$$

Cases 2 and 3 (the two perturbed cases) again have identical responses and both reach a maximum motor speed of 2695 rpm—just short of the maximum power point. Case 4 is considerably slower and reaches a maximum speed of 2466 rpm. Hence we conclude that N^* is the optimal trajectory *because it allows the motor to reach and maintain its maximum power point.*

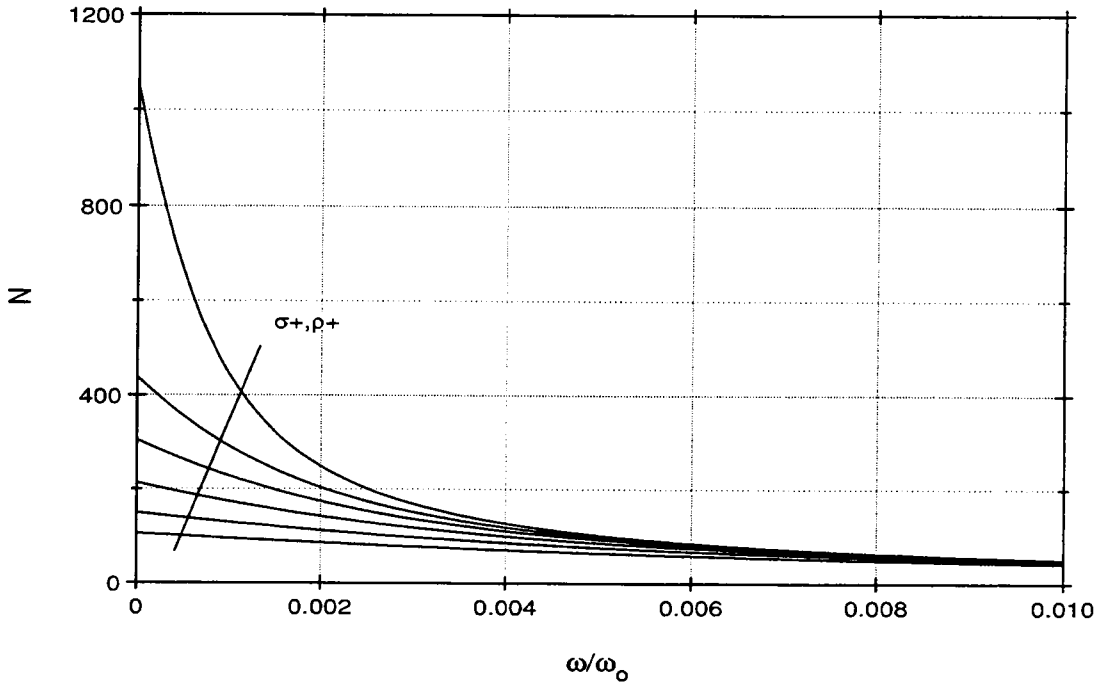

Figure 4.6: N^* vs. speed ratio. ($\sigma \leq 200$, $\rho \leq 10^6$).

4.3.8 Parametric Plots

In closing, a few general, non-dimensional plots of N^* are given as functions of (non-dimensional) speed, loading, and inertia. Figure 4.6 shows N^* as a function of non-dimensional speed. Please note that ω/ω_o will always be quite small for all reasonable situations since the ratio of joint speed to the free motor speed is small. Figure 4.7 shows how the maximum required gear reduction (i.e. $N_{max} = N^*(0)$) changes with loading and inertia. The plot shows that the relationship between N_{max} and torque ratio is approximately linear. Figure 4.8 shows similar information to Figure 4.7; this plot more clearly shows the relationship between N_{max} and inertia. It appears that N_{max} is approximately proportional to the square root of inertia ($N_{max} \propto \sqrt{\rho}$). Figure 4.9 verifies this graphically.

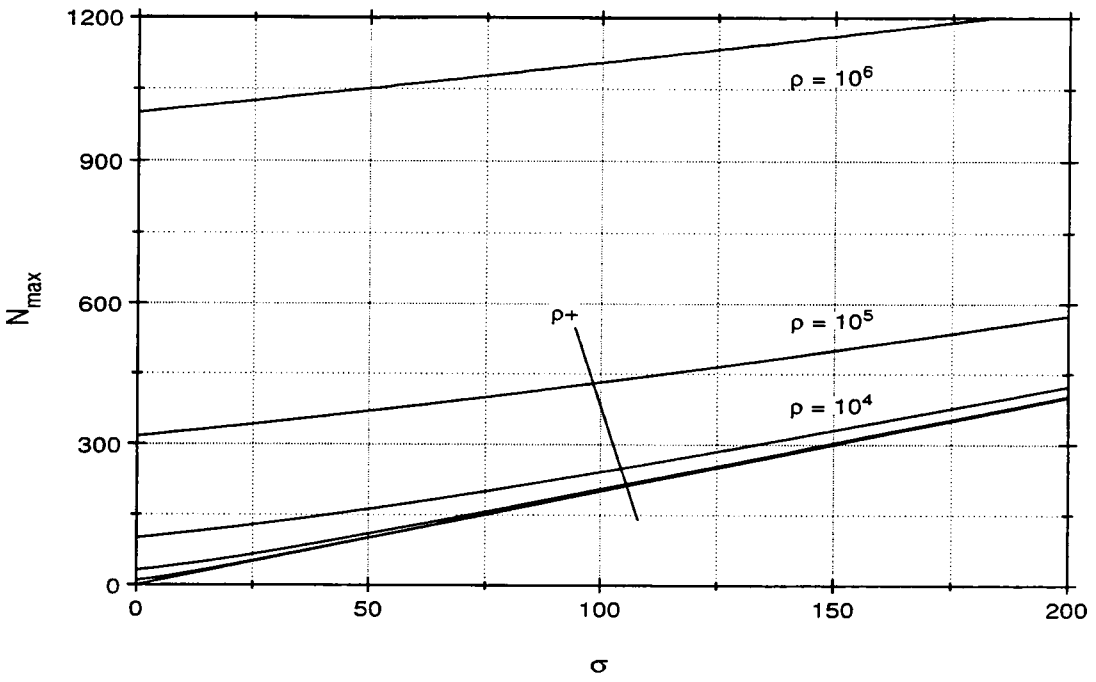

Figure 4.7: N_{max} vs. torque ratio, σ. ($\rho \leq 10^6$).

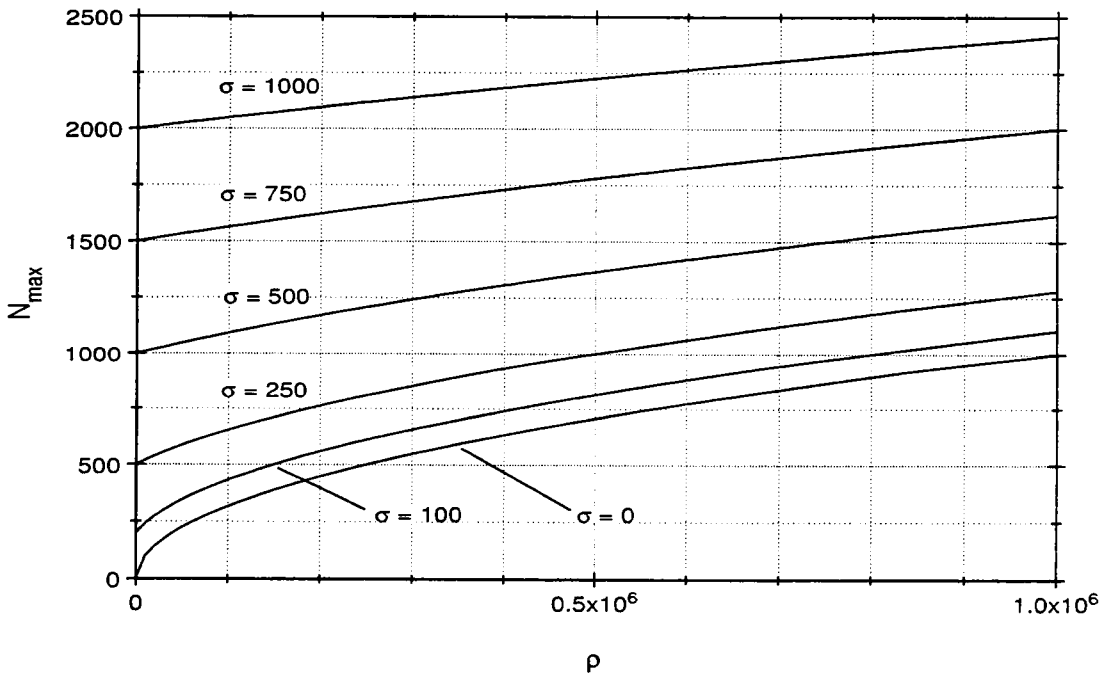

Figure 4.8: N_{max} vs. inertia ratio, ρ. ($\sigma \leq 1000$).

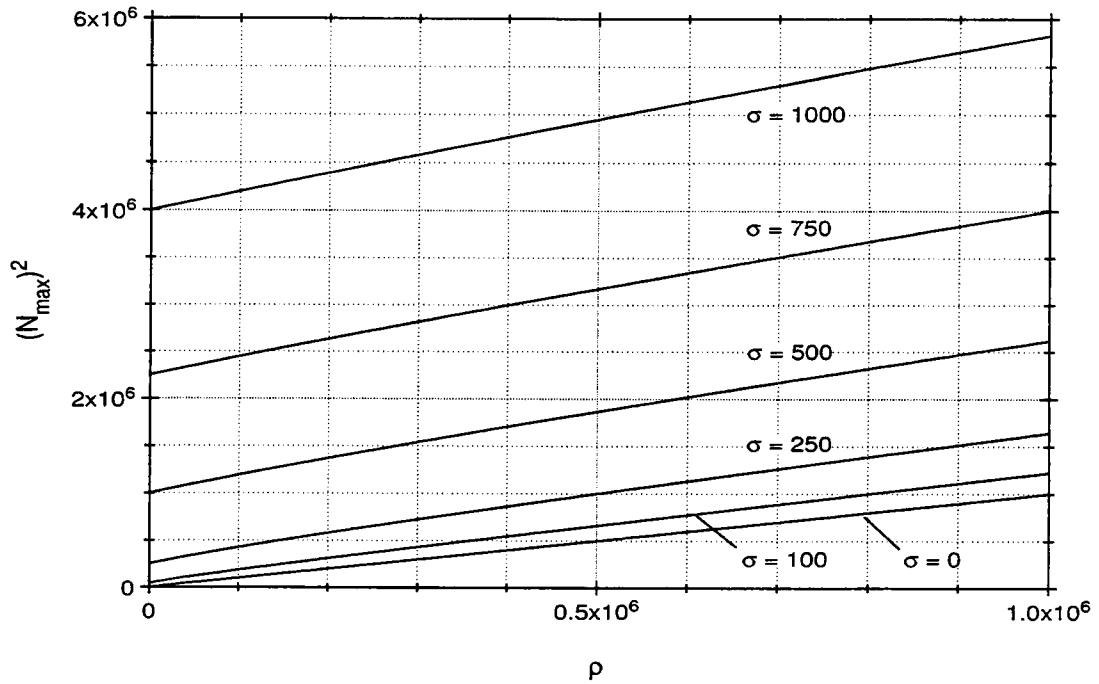

Figure 4.9: N_{max}^2 vs. inertia ratio, ρ. ($\sigma \leq 1000$).

4.3.9 Time Optimal Discrete Shifting Strategy

In this section, the formulations for the *CVT* optimal controls are modified to accommodate a discrete speed transmission with a finite number of gears. Mathematically, the assumption of a continuous (and smooth) curve for gear ratio inherent with a *CVT* allows for a robust design solution in that the end result encompasses both the entire required reduction range *and* a closed-form algorithm for shifting. For the discrete speed case, it is necessary to specify some of the transmission parameters and optimize a remaining parameter with respect to the others.

The most simple case to imagine is a two-speed transmission with two specified gear reductions N_1 and N_2. For the two speed case, there are three variables that can be tuned for a given loading and task-speed requirement: namely, N_1, N_2, and the

time (or perhaps speed) at which the transmission should be shifted. This problem is attacked assuming knowledge of the transmission ratios, external loading conditions, and motor torque-speed characteristics. In a manner similar to before, the goal is to optimize the shifting strategy such that the joint angular acceleration is maximized over the acceleration portion of the maneuver.

To begin, the joint angular acceleration can be written as

$$\alpha(\omega, \omega_s) = \alpha_1(\omega)u(\omega) + (\alpha_2(\omega) - \alpha_1(\omega))\, u\,(\omega - \omega_s)\,. \tag{4.34}$$

Here, α_1 and α_2 are the joint accelerations in first and second gear respectively. The Heaviside step functions $u(\omega)$ and $u(\omega - \omega_s)$ are simply used to form a piecewise continuous function for the overall joint acceleration versus speed. The expressions for the accelerations in each gear are analogous to before excepting that, in each case, the value of gear reduction N_j, $j = 1, 2.$ is constant.

$$\alpha_j(\omega) = \frac{f_j - B_j\omega}{A_j} \quad j = 1, 2. \tag{4.35}$$

Differentiating (4.34) with respect to the shift speed ω_s and setting the result to zero gives

$$\frac{d\alpha}{d\omega_s}(\omega) = (\alpha_1(\omega) - \alpha_2(\omega))\,\delta\,(\omega - \omega_s) = 0, \tag{4.36}$$

where $\delta(\omega - \omega_s)$ is a Dirac delta function triggered at the speed when shift should occur. Recalling the "sifting" nature of this function, it is known that it is non-zero *only* during the time of shift. Hence, we evaluate the above relationship at $\omega = \omega_s$, giving

$$\frac{d\alpha}{d\omega_s}(\omega_s) = (\alpha_1(\omega_s) - \alpha_2(\omega_s))\,(1) = 0. \tag{4.37}$$

This expression leads directly to an expression for the optimal shifting joint speed, ω_s^*:

$$\omega_s^* = \frac{A_1 f_2 - A_2 f_1}{A_1 B_2 - A_2 B_1} = \frac{f_2 - \frac{A_2}{A_1} f_1}{B_2 - \frac{A_2}{A_1} B_1} \tag{4.38}$$

The embedded non-dimensional ratio A_2/A_1 involves inertia and can be written simply as:

$$\Gamma(N_1, N_2) \equiv \frac{A_2}{A_1} = \frac{\frac{I_m}{I_e} N_2^2 + 1}{\frac{I_m}{I_e} N_1^2 + 1} \quad \Gamma \in (0, 1). \tag{4.39}$$

A few words about the interval over which (4.39) is valid should be mentioned. The ratio Γ is an inertial parameter that depicts a measure of the separation (in gear ratio value) between consecutive gears in the discrete transmission. The lower limit is open because the ratio can never be identically zero, although extremely separated gears could lead to low values. The upper limit is open because a value of $\Gamma = 1$ would correspond to two consecutive gears having the *same* gear ratio. For a discrete transmission, this is never the case. However, for a *continuously variable transmission*, an infinite number of gear ratios is available, indicating that the limit $\Gamma \approx 1$ corresponds to the *CVT* case. This will provide some reinforcement (and closure) to the optimization results presented for the *CVT* shifting strategy results.

Even though the interval over which (4.39) is valid (i.e. $\Gamma \in (0, 1)$) is mathematically true (as we previously discussed), on physical grounds the interval can be reduced to $\Gamma \in [0.5, 1)$. Even with incredibly high values for N_1 coupled with direct drive[6] for second gear (i.e. $N_2 = 1$), the ratio Γ stays above the lower limit of 0.5. With this physically justified modification of the interval, (4.39) becomes:

$$\Gamma(N_1, N_2) = \frac{\frac{I_m}{I_e} N_2^2 + 1}{\frac{I_m}{I_e} N_1^2 + 1} \quad \Gamma \in [0.5, 1). \tag{4.40}$$

[6]It should be noted that direct drive is not generally possible for manipulator loadings that are seen in large-scale robotics. Hence, direct drive is a logical absolute limit for the lowest gear ratio.

Recalling the definition of $B(N)$ and the analogous $B_j(N)$, we can nondimensionalize (4.38) with respect to the theoretical no-load speed. Define

$$b_j \equiv B_j \omega_o = T_o N_j^2, \quad j = 1, 2.$$

such that (4.38) becomes

$$\omega_s^* = \left(\frac{f_2 - \Gamma f_1}{b_2 - \Gamma b_1} \right) \omega_o.$$

Hence we can nondimensionalize (4.38) as:

$$\frac{\omega_s^*}{\omega_o} = \frac{f_2 - \Gamma f_1}{b_2 - \Gamma b_1}. \tag{4.41}$$

Please note that all of the following speeds have been *joint speeds.* It is advantageous to adapt the shift speed to the motor axis. This is simply done and allows the equation to provide an algorithm for optimally shifting gears while monitoring motor speed. To this end, recall[7]:

$$\omega_{motor} = \omega_{joint} N_1.$$

Using this, (4.41) becomes the nondimensional equation relating optimal motor shifting speed to the spacing between the gears:

$$\frac{\omega_{motor,s}^*}{\omega_o} = N_1 \left(\frac{f_2 - \Gamma f_1}{b_2 - \Gamma b_1} \right). \tag{4.42}$$

Recall the following definitions:

$$f_j \equiv T_o N_j - T_{ext} \quad j \in [1, 2],$$

$$b_j \equiv T_o N_j^2 \quad j \in [1, 2].$$

[7]The derivation assumes shifting is occurring from first to second gear. In general, however, the motor speed is the joint speed times the current value of gear ratio.

Using these definitions, (4.42) becomes

$$\begin{aligned}
\frac{\omega^*_{motor,s}}{\omega_o} &= N_1\left(\frac{(T_oN_2 - T_{ext}) - \Gamma(T_oN_1 - T_{ext})}{T_oN_2^2 - \Gamma T_oN_1^2}\right) \\
&= \frac{T_oN_2N_1 - T_{ext}N_1 - \Gamma T_oN_1^2 + \Gamma T_{ext}N_1}{T_oN_2^2 - \Gamma T_oN_1^2} \\
&= \frac{N_2N_1 - \frac{T_{ext}}{T_o}N_1 - \Gamma N_1^2 + \Gamma\frac{T_{ext}}{T_o}N_1}{N_2^2 - \Gamma N_1^2} \\
&= \frac{N_2N_1 + (\Gamma-1)\frac{T_{ext}}{T_o}N_1 - \Gamma N_1^2}{N_2^2 - \Gamma N_1^2} \\
\left(\frac{\omega^*_{motor,s}}{\omega_o}\right)^- &= \frac{\frac{N_2}{N_1} + (\Gamma-1)\frac{T_{ext}}{T_oN_1} - \Gamma}{\left(\frac{N_2}{N_1}\right)^2 - \Gamma}.
\end{aligned} \tag{4.43}$$

This is the final equation for the optimal motor shifting speed for a discrete transmission. It denotes the speed at which the motor should shift into the next gear. Hence, this is the speed of the motor just *before* the shift occurs[8]. The speed of the motor *after* the next gear is engaged is simply given by:

$$\left(\frac{\omega^*_{motor,s}}{\omega_o}\right)^+ = \frac{N_2}{N_1}\left(\frac{\frac{N_2}{N_1} + (\Gamma-1)\frac{T_{ext}}{T_oN_1} - \Gamma}{\left(\frac{N_2}{N_1}\right)^2 - \Gamma}\right). \tag{4.44}$$

General equations analogous to (4.43) and (4.44) are

$$\left(\frac{\omega^*_{motor,s}}{\omega_o}\right)^- = \frac{\frac{N_{j+1}}{N_j} + (\Gamma-1)\frac{T_{ext}}{T_oN_j} - \Gamma}{\left(\frac{N_{j+1}}{N_j}\right)^2 - \Gamma}, \quad j = 1, 2, \ldots, n. \tag{4.45}$$

$$\left(\frac{\omega^*_{motor,s}}{\omega_o}\right)^+ = \frac{N_{j+1}}{N_j}\left(\frac{\frac{N_{j+1}}{N_j} + (\Gamma-1)\frac{T_{ext}}{T_oN_j} - \Gamma}{\left(\frac{N_{j+1}}{N_j}\right)^2 - \Gamma}\right), \quad j = 1, 2, \ldots, n. \tag{4.46}$$

These equations are a bit complex and deserve attention. As we have mentioned before, Γ (an inertial parameter) is never identically equal to unity because that would indicate that two consecutive gears have the same ratio. In the limit, though,

[8]Denoted by the superscript "-".

a *CVT* satisfies the condition of $\Gamma \approx 1$ because, for an "infinite" number of gear ratios, any two consecutive "gears" will have approximately the same value of gear ratio.

Also note the term in (4.45) and (4.46) involving the external torque. This is the only term in the equation that involves the static torque; all of the other terms are functions of inertia only. The point to notice is that within the term is a ratio of torques—the ratio of the external torque to the maximum reflected[9] holding torque that the motor can provide within the current gear. For all reasonable motions, this term will be small, because if the external torque is approaching the maximum torque that the motor can provide, then the gear ratio is insufficient for the maneuver and should be increased. This is a design issue, and the assumption is that the gears have been well selected for their payload/speed requirements. At this point, (4.45) and (4.46) deserve discussion.

It is interesting to examine high values of Γ because it reinforces the optimization work performed in earlier sections. For the moment, suppose that $\Gamma \approx 1$; (4.45) and (4.46) will reduce to:

$$\left(\frac{\omega^*_{motor,s}}{\omega_o}\right)^- \approx \frac{\frac{N_{j+1}}{N_j} - 1}{\left(\frac{N_{j+1}}{N_j}\right)^2 - 1}, \quad j = 1, 2, \ldots, n. \tag{4.47}$$

$$\left(\frac{\omega^*_{motor,s}}{\omega_o}\right)^+ \approx \frac{N_{j+1}}{N_j}\left(\frac{\frac{N_{j+1}}{N_j} - 1}{\left(\frac{N_{j+1}}{N_j}\right)^2 - 1}\right), \quad j = 1, 2, \ldots, n. \tag{4.48}$$

Figure 4.10 depicts this somewhat "hypothetical" situation graphically. It is somewhat academic in two ways: (1) $\Gamma \approx 1$ never occurs for a discrete transmission, and (2) if Γ *did* approach unity then the plot shrinks down to a point. However, even

[9]That is, with the mechanical advantage of the transmission accounted for.

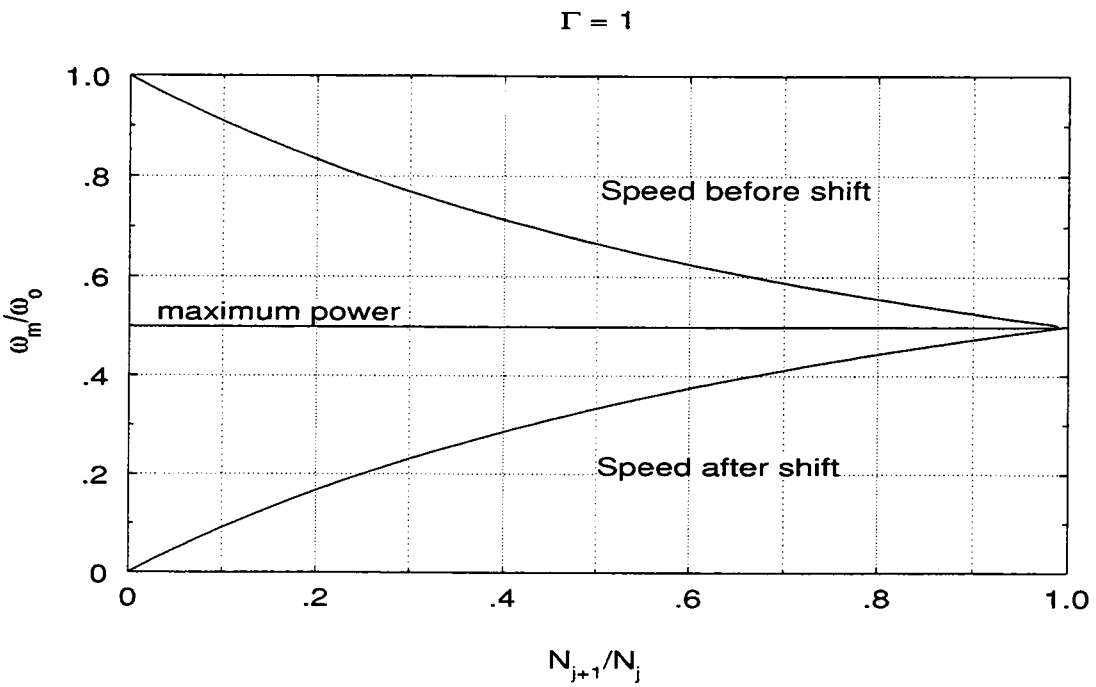

Figure 4.10: Optimal discrete shifting speeds for "hypothetical" case $\Gamma \approx 1$.

in light of all of this, Figure 4.10 shows one significant point[10]. In the figure, the top curve represents the speed (strictly, the ratio of the motor speed to its maximum speed) at which the transmission should be shifted as a function of the separation of the gears N_{j+1}/N_j, where "j" is the current gear. Similarly, the lower curve is the speed of the motor after engagement of the new gear, gear "$j+1$". Note that the curves are symmetric about the line where the speed ratio is 0.5. This corresponds to the speed at which the motor produces maximum power. The point where the two curves meet on the right side of the plot represents the limiting case corresponding to a *CVT*. Figure 4.10 shows that, for time-optimal performance, a *CVT should continually shift while the motor is held at the maximum power point.* This verifies the results of Section 4.3.1, and demonstrates a nice correlation between the continuous

[10]The exact point that the plot would shrink to (pun intended).

and discrete shifting profiles.

Also note in Figure 4.10 that the symmetry of the plot denotes that the motor speeds before and after shift form a "speed bandwidth" about the maximum power point. What this means is that the motor spins up past the maximum power point to accommodate the shifting of the gears. In this manner, the motor continually "straddles" the maximum power point until all gears have been shifted. In the final gear, the motor would be run up to maximum power and kept there for the remainder of the acceleration portion of the maneuver. Figure 4.11 shows this on a motor torque/power vs. speed diagrams. The main issue to be seen here is the fact the optimal shifting (for maximum acceleration/minimum-time-moves) has *everything* to do with the maximum power point of the motor. As we have seen, a CVT places and maintains the motor at its maximum power point throughout the move. So, a CVT would have zero "speed bandwidth" if shown in Figure 4.11. A discrete transmission, on the other hand, must shift between gears with finite "spacing" or ratio separation between them. To accommodate this, the motor "straddles" the maximum power point. The larger the separation between the gears, the larger the speed bandwidth. If the gear spacing is quite wide, then the motor has to move considerably beyond the maximum power point to accommodate the shift. This can be thought of with another car analogy; if the driver wishes to shift from first gear to *third* gear directly, he has to spin the engine up a lot faster than he would for a simple shift into second.

It is imperative that Figure 4.11 be fully understood before looking at more realistic situations (i.e. Γ not approaching unity). Recalling that Γ is an inertial parameter, it will be seen that the plots in Figure 4.10 are changed because inertial effects are included. We will see that, especially for high gear reductions, the inertial effects are

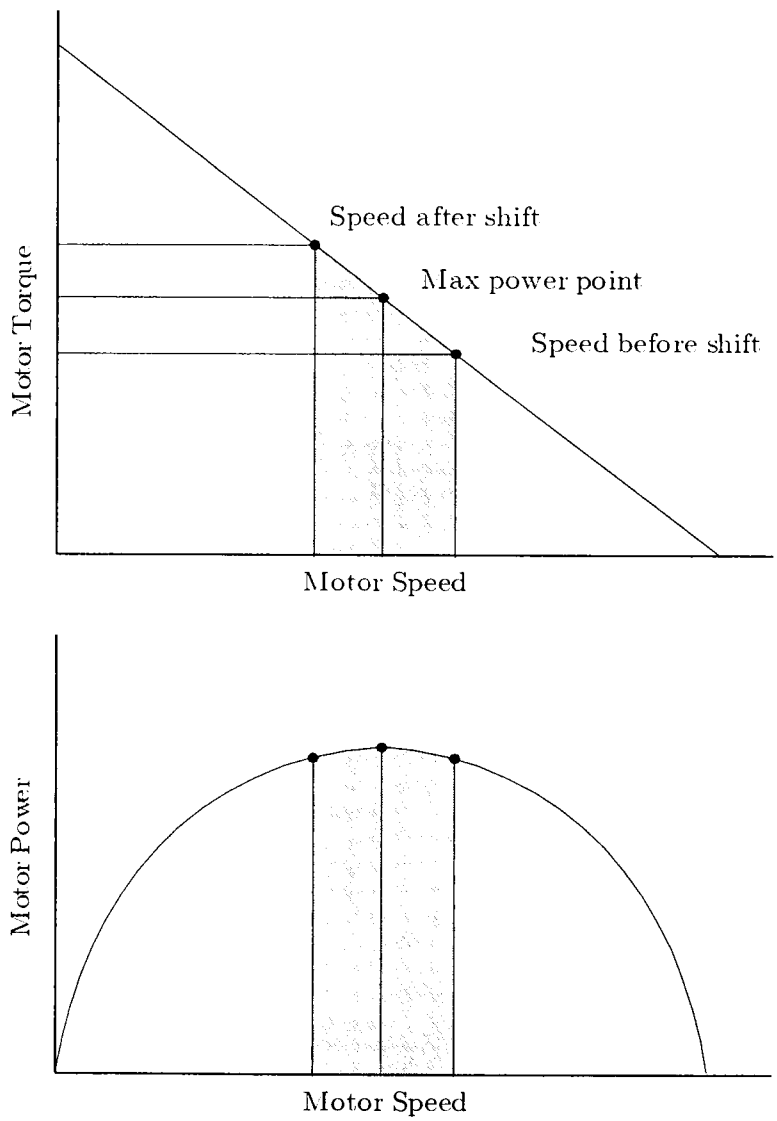

Figure 4.11: Optimal shifting points for a hypothetical discrete transmission

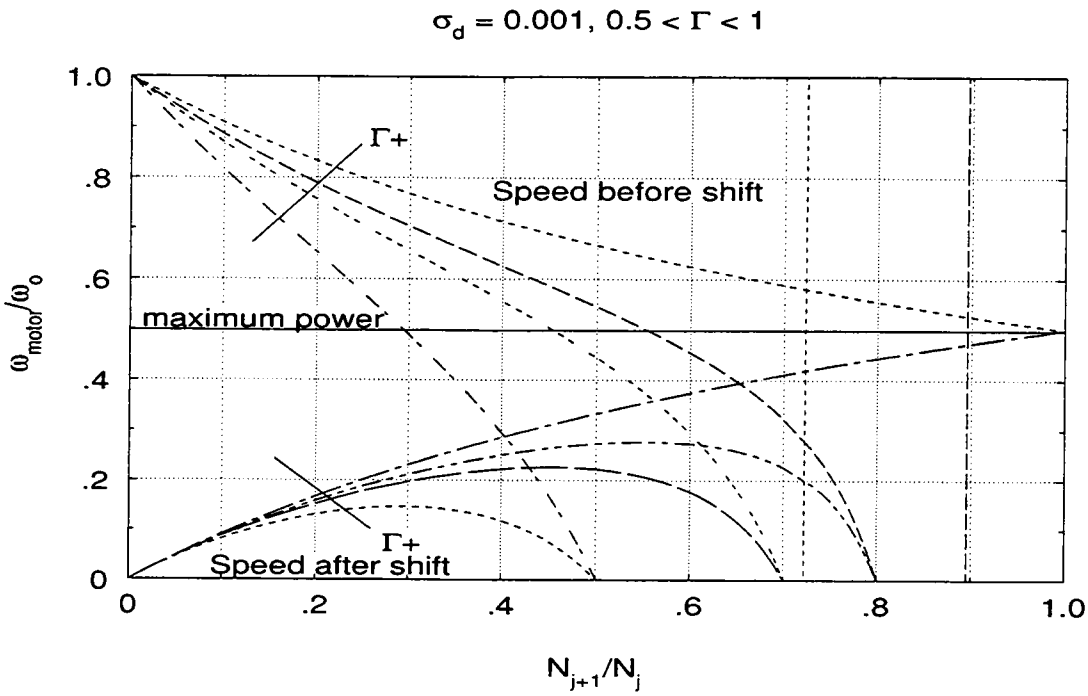

Figure 4.12: Discrete transmission optimal shifting curves. $\Gamma \in [0.5, 1)$, $\sigma_d = 0.001$.

significant to the optimal shifting times. In essence, for high gear ratios, the motor inertia itself—when transmitted through the gear train—has a dominant effect on the joint dynamics. The optimal curves will change to accommodate this effect.

The following are several plots showing how the shifting curves change with both Γ and the torque ratio $\sigma_d = T_{ext}/T_o N_j$. This definition expresses a similar parameter to an earlier section—the ratio of the external torque to the maximum torque that the motor can provide in the engaged gear. All of the following plots are for $\Gamma \in [0.5, 1), \sigma_d \in [0.001, 0.25]$. The range on torque ratio (i.e. σ_d considers mechanical advantage at stall ranging from 4:1 to 1000:1. For reference, the "CVT" case remains on all of the plots. Figures 4.12 through 4.15 show how the optimal shifting curves vary with respect to these parameters. As can be seen in the figures, the general effect that the inertial parameter Γ has on the curves is a downward translation in

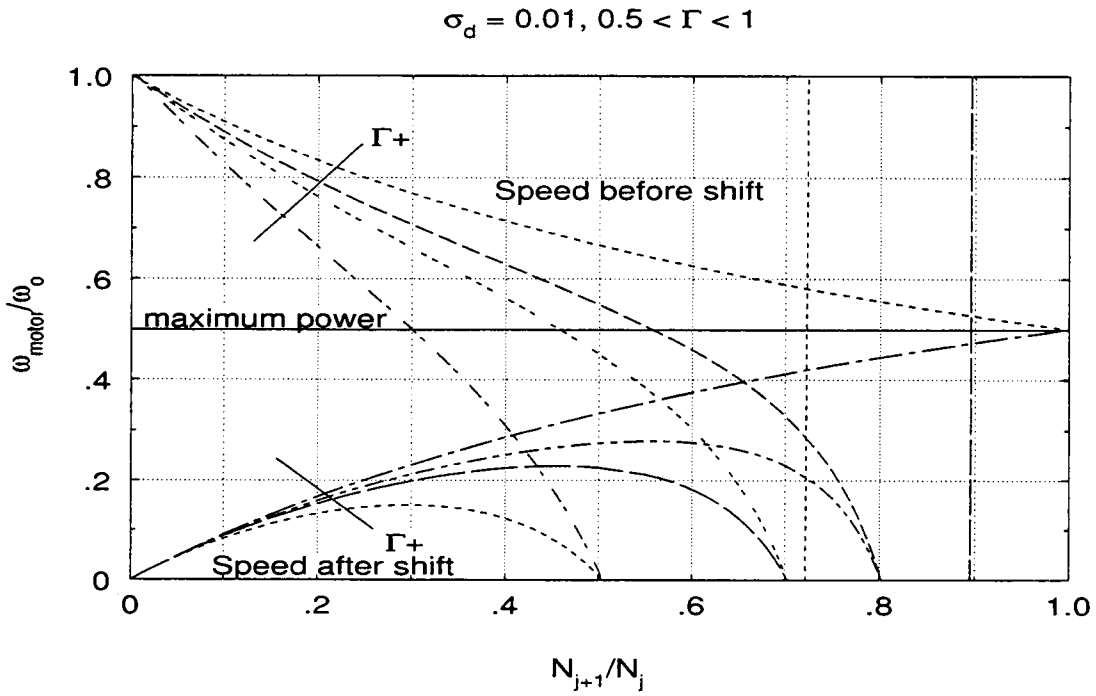

Figure 4.13: Discrete transmission optimal shifting curves. $\Gamma \in [0.5, 1)$, $\sigma_d = 0.01$.

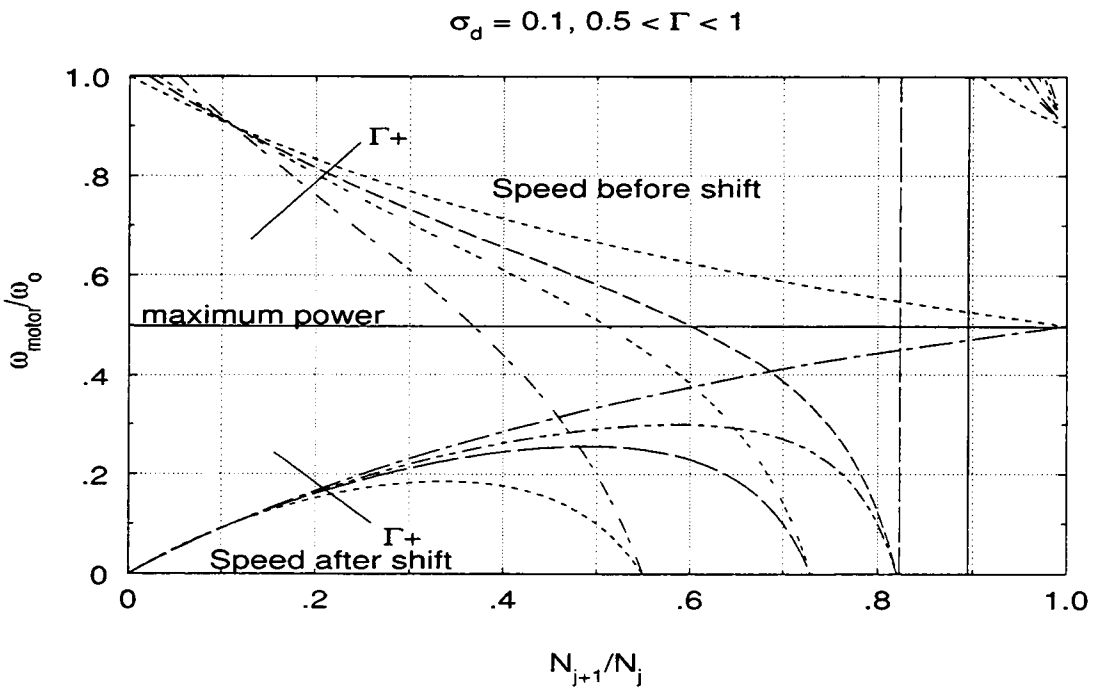

Figure 4.14: Discrete transmission optimal shifting curves. $\Gamma \in [0.5, 1)$, $\sigma_d = 0.1$.

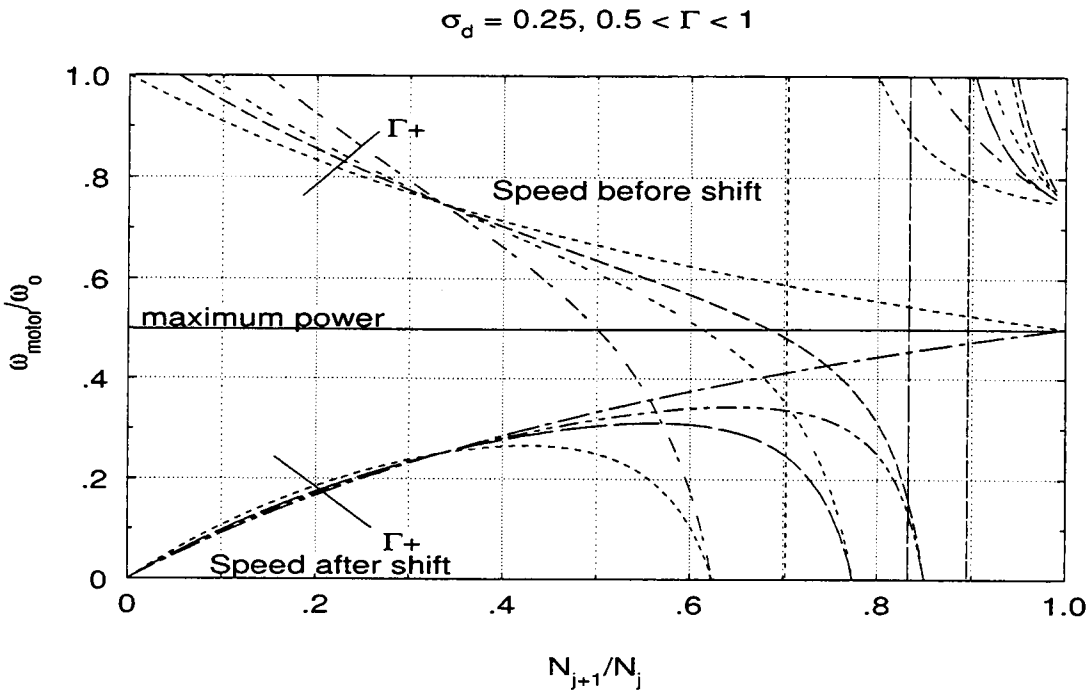

Figure 4.15: Discrete transmission optimal shifting curves. $\Gamma \in [0.5, 1)$, $\sigma_d = 0.25$.

the shift speed. For particularly high gear ratios, the shifting speeds are quite lower than is seen for lower ratios. In fact, some combinations of gear spacing, Γ (an inertial parameter), and σ_d (a torque parameter) can lead to operating points that do *not* straddle the maximum power point. Most of these points, however, consider gear spacings that are much too small for consideration in a discrete transmission (i.e. high values on the horizontal axis). Although interesting over the entire range, the above plots are only realistic (in terms of building actual transmissions with discrete gear spacings) in the range $N_{j+1}/N_j \in [0.25, 0.75]$. Beyond this range, the gear spacings are either too far apart to be reasonable (analogous to shifting from first to *fifth* gear in a car) or are too close to be useful[11] (analogous to a car having $\gg 5$ speeds).

An interesting point to the results is that the entire algorithm is based on gear

[11]...and buildable.

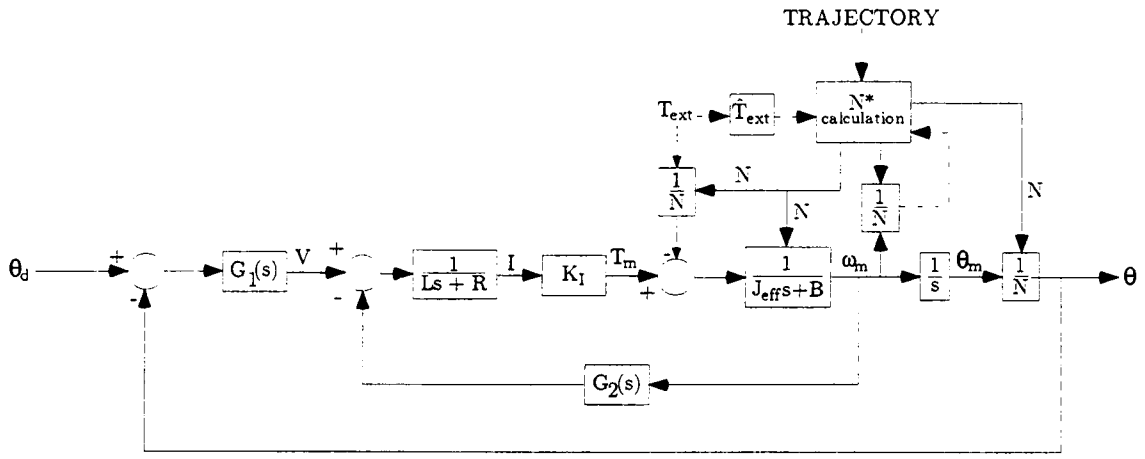

Figure 4.16: Modified control architecture for variable gear reduction

spacing. The gears need not be sequential (i.e. "neighboring") gears. As long as the ratio separation is known, the algorithm will determine an optimum speed at which to shift.

4.4 Modified Control Architecture

With low level control strategies (i.e. shifting strategies) developed for the transmissions, an outline of a modified control architecture that could be investigated in the future is presented. This is depicted in Figure 4.16. As shown in the figure, the fundamental idea is to augment a conventional PD joint servo architecture with calculations which determine an instantaneous gear reduction that is optimal in some sense. This requires that the effective joint inertia and external torque be known. Joint inertia can be determined through the manipulator Jacobian and current joint positions (from joint position sensors). Depending on joint friction, T_{ext} can be estimated through joint motor currents (i.e., torque) with some degree of precision. If a

six-axis wrist force-moment sensor is available, T_{ext} can be estimated via the sensor output and the manipulator Jacobian. An interesting idea would be to consider the gear reduction, N as a system parameter that varies over a known range (as would be the case for a designed transmission), and to design the controller using Quantitative Feedback Theory (QFT) such that those parameter variations introduced minimal disturbances to the overall system and the system is continually stable. In essence, QFT is used to design the compensation functions $G_1(s)$ and $G_2(s)$ such that, for any value of gear ratio in the specified range, the system performs smoothly and remains stable. This would be an interesting investigation that the author would have liked to complete; this investigation could not be completed due to time constraints. However, for someone adept at using the QFT toolbox in $MATLAB^{TM}$, this idea could be investigated for feasibility in a relatively short period of time.

4.5 Conclusions: Control Considerations

This chapter has addressed some of the more fundamental issues concerning multi-speed transmission control in a robotic system. Particular attention has been paid to assessing how and *when* the transmission trades torque capacity for speed capacity. For acceleration, the transmission starts at a maximum value and reduces gear ratio to trade torque capacity for speed capacity as the joint begins to move. A CVT can operate smoothly between a maximum and minimum speed ratio, and it has been shown that for maximum joint acceleration, the joint-level CVT shifting forces the motor to achieve and maintain its maximum power point. Realization of a CVT-based actuator conceptually allows a manipulator like the ASM to be re-

designed with distributed actuation. In fact, even with distributed actuation, the speed performance of a single *TBA* on the *ASM* shoulder joint would outperform the *two* tandem servomotors on the baseline system. Results such as these are very encouraging and indicate that the transmission mass and volume are not as critical as it was initially assumed.

The analysis for optimization of *CVT* shifting has been extended to optimize the shifting profile (specifically, the motor speed at which the shift should occur) of a discrete-speed transmission. The shifting curves, as expected, are functions of the joint loading, inertia, and gear separation. Unlike the *CVT*, a transmission with a distinct number of gears cannot allow a motor to continually run at its maximum power point due to the jump discontinuities in the gear ratio profile; the shifting profile is a *piecewise* continuous curve, and the "jumps" in ratio demand that the motor "straddle" the maximum power point. In other words, during shifting, the motor will spin past the maximum power point such that, after the shift has occurred, the motor rpm will be *below* the maximum power point such that the motor can remain in the vicinity of maximum power. A *CVT* is indeed the limiting case where the "vicinity" is extremely narrow (mathematically of zero-width). For a discrete transmission, the "speed bandwidth" or "vicinity" size is proportional to the ratio separation between the gears—the wider the separation, the wider the band. Inertia in the system has the effect of lowering the speeds at which the motor should be shifted; this is due to the fact that—especially for high gear ratios—the reflected rotor inertia dominates the system and reduces the need to spin the motor to such high speeds before shift. This effect is somewhat analogous an energy storage problem seen in [26], where *CVT*'s coupled with energy storage for automobile applications were studied.

From an overall control standpoint, we have shown that there is a natural matchup between transmission shifting behaviors and the fundamental task-speed characteristics. In high precision situations, joint speed is invariably slow and hence a high (constant) gear ratio will be used in this phase. Thus, for precision maneuvers, the transmission is held fixed and the overall joint control is essentially the same as for currently available fixed reduction actuators. Conversely, when high speed is desired, such as flight of a part from one point to another, it is logical that precision is no longer nearly as vital and the transmission can manipulate the speed ratio to spin the motor up to its maximum power point. Once that point has been achieved, the transmission ratio is held essentially constant, and the controls are again similar that of a simple gearmotor. It is only in the transition phase, where the ratio of the transmission is changing over a wide range, that the control objectives will be significantly different from classical control objectives. A partitioning approach to the low level *TBA* control is a logical methodology for making the multi-speed transmissions essentially transparent to the overall manipulator control system.

Chapter 5

Transmission Parameter Design

5.1 Introduction

This chapter continues the discussion of the concepts introduced in Chapter 4 in terms of *using* the results to select transmission ratios for a particular application. Essentially, a particular application will have necessary payload-response requirements, and, to meet these requirements a sufficient motor-transmission combination must be designed. The optimal analyses of Chapter 4 offer great assistance in motor selection in that the optimal shifting profiles—when coupled with a particular motor—will put an absolute constraint on the maximum acceleration performance of the motor. Hence, as a first iteration, motors may be selected from industrial specifications and modeled to ascertain the absolute bound on their acceleration and response time performance. Several motors may be candidates for the engineering application at hand, but the following arguments all apply to any of the motors. Once a candidate motor is selected, the optimal shifting curves—both continuous and discrete-speed—are known. However, the optimization process leaves the transmission ratios completely open; this is especially true in the *CVT* case. In a real engineering design situation, the designer must select a range of gear ratios which the transmission can mechani-

cally provide; until this decision is made, the transmission itself cannot be built. For example, for a given torque/inertia loading and a selected motor, the optimization of Section 4.3.1 will yield an optimal shifting profile that has both a maximum and minimum gear ratio that is perfectly suited for the situation. If the loading or inertia changes, so does the optimal shifting profile. From an engineering design standpoint, a continuously variable transmission can only provide a smooth shifting profile (and an infinite number of gear ratios) between a maximum and minimum value of gear reduction. Hence, the engineer must select the maximum and minimum gear ratios apriori. Section 5.2 discusses maximum/minimum gear ratio selection.

Once the overall range of gear ratios has been chosen, the next design question to address concerns the selection of the "intermediate" gear ratios. For a continuously variable transmission, this is of little concern since a *CVT* can provide an infinite number of ratios within the transmission bounds. However, since the optimal profile leaves the maximum and minimum gear ratios open during the optimization process, there may be a need to look at the effects of *constraining* the optimization procedure to remain within those bounds. This is an interesting topic and is discussed in Section 5.3.1.

Discrete-speed transmissions, on the other hand, have a finite number of available gear ratios available within the transmission bounds. The engineer must not only select how many gear ratios to put into the transmission, but he must also select the "ratio separation" between each gear. In the analysis of Section 4.3.9, the optimal shifting curves were determined with respect to the motor speed at which the transmission should shift. One of the most important factors in the end result of the optimization was the separation between the engaging and disengaging gears

(i.e. N_{j+1}/N_j, where $(j+1)$ represents the gear to be engaged and j represents the gear to be disengaged during shift). The designer must use the optimal curves of Section 4.3.9 to make decisions concerning the gear ratio values to be put into the transmission. There are interesting concepts to think about, however, concerning the optimal profiles of Section 4.3.9 for the engaging/disengaging gears. There was no constraint in the analysis that demanded that the gears be consecutive; in other words, there was no constraint in the analysis that limited the transmission to only shifting from first gear to second gear, second gear to third gear and so on; shifts can *skip* gears (such as shifting from first gear to third gear, for example). This idea also has some interesting implications and is the subject of Section 5.3.2.

When thinking about the concept of using variable-ratio or multi-speed transmissions, one might ask what the advantage of one type of transmission (i.e. CVT or DST) is over the other. There are a multitude of issues to consider when deciding between the two concepts including factors concerning mechanical issues such as weight, space, complexity, and cost, along with performance issues such as smoothness during shifting and robustness to variations in loading conditions. It will be shown in Section 5.4 that there are clearly a few tradeoffs between the two concepts and the deciding factors between the two will be determined by the specific critical requirements of the application.

Overall, this chapter is an introductory discussion into a multitude of further research projects that could be drawn from this work. Clearly, the inclusion of a multi-speed transmission into an electro-mechanical drive introduces many new research and development issues concerning actuator synthesis. It is the hope of the author that this chapter will spark the interest of a future researcher towards the continual

development of this concept.

5.2 Selection of Maximum/Minimum Gear Ratios

In this section, we address some issues concerning the selection of the maximum and minimum gear ratios that will be incorporated into a transmission—either *CVT* or *DST*. As was seen in Chapter 4, for a selected motor and given payload response requirement, there is an optimal way to manipulate mechanical advantage (i.e. shift the transmission) such that the joint acceleration is maximized and, hence, the maneuver time is minimized. The optimization process, however, leaves the range of available gear reductions completely open. In an engineering application, the first objective for designing a transmission is to synthesize a set of transmission bounds—the maximum and minimum gear reductions available within the transmission—such that the mechanical design of the transmission can begin.

The maximum gear reduction will correspond to the maximum amount of mechanical advantage that the transmission will be able to provide. This ratio, whether it be in a *CVT* or *DST* setting, will be used only in situations where exceptionally high loading is present. In accelerating a load from rest, this gear will be thought of as "first" gear in both the *DST* and *CVT* situation. The minimum gear reduction, on the other hand, corresponds to the minimum amount of gear reduction that the transmission will provide. This ratio may be used when external loadings are exceptionally low, when the arm is in steady state motion (e.g. slew), or for high speed situations (as in travel between tasks, as the loading allows). In any case, these two

ratios define the absolute envelope which limits the range of mechanical advantage and speed reduction that the transmission can provide.

5.2.1 Maximum Gear Ratio Selection

5.2.1.1 *CVT* case

The maximum gear ratio, obviously, is selected based on the payload/response requirements. But more specifically, the maximum gear ratio is selected based on the performance requirements corresponding to *maximum* joint loading. In the robotics case, maximum joint loading most often corresponds to maximum end-effector payload.

To begin synthesis of the maximum gear ratio, an absolute worst case static loading situation for the joint should be determined. This will involve not only using the maximum payload, but also placing the arm in the configuration which produces maximum gravitational torque to the joint. This loading scenario should be considered constant in its worst case position such that the loading represents an absolute limit to the amount of external torque and inertia put upon the joint. This is exactly the procedure that was done in Chapter 3 for the *ASM*. The continuous optimization process of Section 4.3.1 will yield a continuous curve of the gear reduction N versus the joint speed ω (hence $N = N(\omega)$). The value of gear reduction corresponding to *zero* joint speed (i.e. joint is static) is the maximum gear reduction value:

$$N_{\max} = N^*(\omega = 0).$$

For a continuously variable transmission approach, the value of $N_{\max}$ is obtained, in general, by coupling a *CVT* with a fixed gear reducer. For example, if the maximum

ratio needed was 100:1, a *CVT* capable of 4:1 (or, the *CVT* is capable of manipulating ratio by a factor of 4) would be coupled to a 25:1 fixed gear reducer. Once this maximum ratio is defined, the optimal continuous shifting curve is completely defined for maximum loading. Hence, both the maximum ratio and intermediate ratios are defined for the *CVT*[1]. It should be noted, however, that the optimization of Section 4.3.1 will give *different* values of $N_{\max}$ for different loading situations. When the transmission is to built, however, the maximum gear ratio value is *fixed.* This effectively constrains the optimal shifting profile to have an upper bound determined by the selected design value for $N_{\max}$. For loadings that are below the maximum design scenario, this has no effect on the optimal profile; since the profile starts at $N_{\max}$ and shifts closed-loop as joint speed is monitored, the end result is that the transmission simply shifts more rapidly. However, if the maximum design loading is exceeded[2], the same optimal shifting algorithm applies with one major exception: if the algorithm calls for a gear ratio higher than the design value of $N_{\max}$, then the design value is held until the algorithm commands a shift into a lower ratio. This is analogous to a saturation nonlinearity. Essentially, the maximum gear ratio is held until the joint speed is sufficient to allow for shift into lower ratios as dictated by the optimal algorithm, equation (4.21).

5.2.1.2 *DST* case

The situation for selecting maximum gear reduction for a discrete-speed transmission is similar to that for a *CVT* . The worst-case maximum loading scenario is set up in

[1]The minimum ratio selection for both continuous and discrete transmissions will be discussed in Section 5.2.2.

[2]This should not happen if the "worst case" situation is correctly analyzed.

exactly the same way as was done for the *CVT* case. However, the optimal shifting strategy for discrete transmissions (Section 4.3.9) defined the speed shifting speed of the motor with the (separation between) gear ratios *known*. Therefore, the discrete optimization cannot be used to synthesize gear ratio values. However, the continuous optimal shifting profile can be used to gain some insight as to what the maximum ratio should be. Just as was done for the *CVT* case, (4.21) will indicate the absolute maximum gear ratio that should be used for the transmission. It should be pointed out, however, that the value predicted by (4.21) will most likely be too high. This is because a *CVT* instantaneously shifts "out" of "first" gear, whereas a *DST* cannot. As we have seen, the discrete optimal algorithm, (4.43), will dictate that the transmission shift out of first gear when the motor reaches the vicinity of maximum power; the size of the bandwidth around maximum power is dependent upon the gear spacing, but regardless, (4.43) will lead to an extremely short time of engagement in first gear if the value predicted by (4.21) is chosen. The author has observed that a considerable lower value of gear ratio must be used for maximum reduction such that the time of engagement isn't unreasonable. In essence, the optimal continuous shifting curve of Figure 4.2 must be approximated discretely in some sense. This could be an interesting future investigation. It is possible that gear ratios and shift times could be considered as individual parameters to be optimized. For example, for a two speed transmission, an optimal profile would consist of three parameters: N_1, N_2, and ω_{shift}. The optimization would be numerical by necessity, and would be strongly dependent on the loading conditions. For the purposes of a parametric study, however, an analysis of this type could offer great insight.

5.2.2 Minimum Gear Ratio Selection

Selection of the minimum value of gear ratio is not as vital as selection of the maximum ratio because the minimum ratio only puts a limit on maximum speed. The minimum ratio (*high* gear) always corresponds to the lowest dynamic joint loadings. Further, the minimum ratio can be *avoided* if the loading is too high for engagement. This is in striking contrast to the maximum ratio (low gear). If the loading is too high for maximum reduction, there is no alternative; maximum gear ratio must be maintained until the loading levels are reduced sufficiently to allow for shifting into higher gears. The fact that the minimum ratio (high gear) can be avoided is interesting in that, if space and weight considerations allow, an "overdrive" gear can be included in the transmission for high speed situations (such as travel between two tasks, flight of a light part from point "A" to point "B", etc.). This "overdrive gear" isn't really a gear in the *CVT* case, as much as it is a lower bound on the gear ratio the transmission is to provide. In the *DST* case, the overdrive gear could very well be a gear that is only engaged in very low payload situations (perhaps a free arm, for example).

In either case, the minimum gear reduction can be chosen in a manner analogous to that for the maximum gear ratio. Instead of visualizing the worst-case scenario for the joint loading, the "best" case scenario is imagined. This must be realistic; obviously, the arm configuration can be arranged such that, at a particular instant, there is *zero* torque load on a particular joint. A best case scenario may be considering the joint loading at zero payload and full extension (this would be very conservative), or some other low joint loading situation (such as low payload and no gravitational loading). Regardless, the minimum ratio for this type of situation would strictly be for an overdrive gear used in low loading situations.

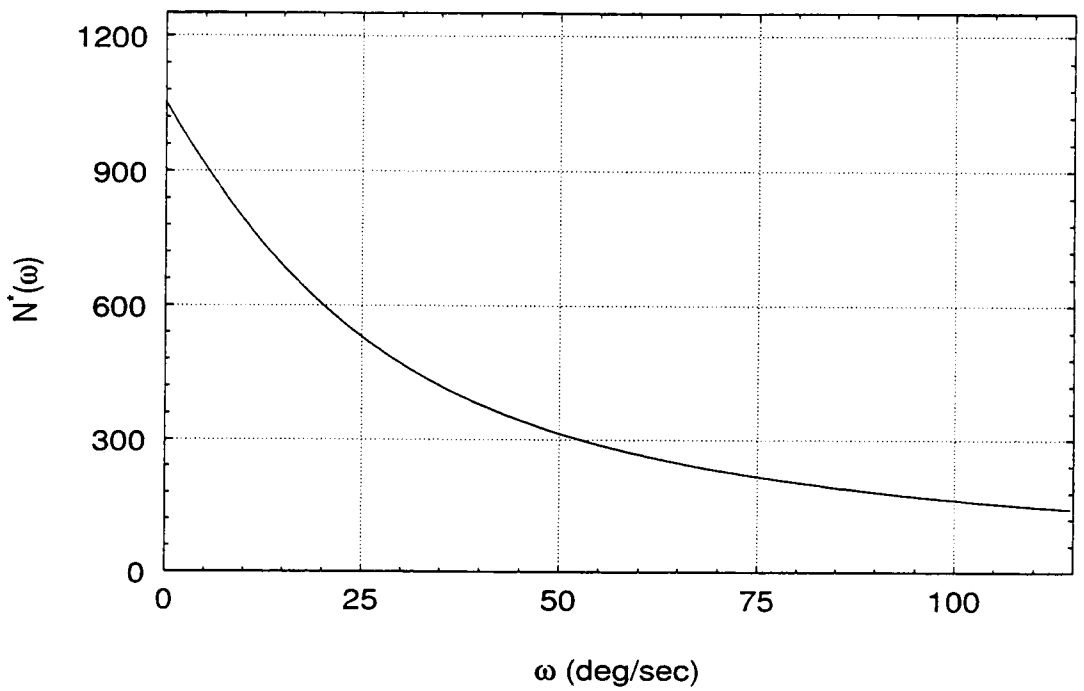

Figure 5.1: Optimal shifting strategy vs. joint speed

For a minimum gear reduction under nominal loading, the continuous optimal shifting strategy again provides the answer. The interesting point is that (4.21) provides the answer for both the continuously variable *and* discrete-speed transmission concepts. The reason is this: whether the transmission-based actuator is using a continuous or discrete transmission, the "final" or "steady state" gear ratio is the *same*. For the *CVT* case, the transmission smoothly shifts from maximum reduction to minimum reduction as the joint accelerates, while a *DST* does the same thing in discrete steps; regardless of the type of shifting, the final transmission ratio is the same. Figures 5.1 and 5.2 show the optimal continuous shifting strategy versus joint speed (Figure 5.1) and versus time (Figure 5.2) for the distributed actuator system studied in Chapter 3. Recall that Figure 5.1 is simply a plot of (4.21). This simply shows how the transmission shifts as a function of the joint speed, ω. Figure 5.2 on

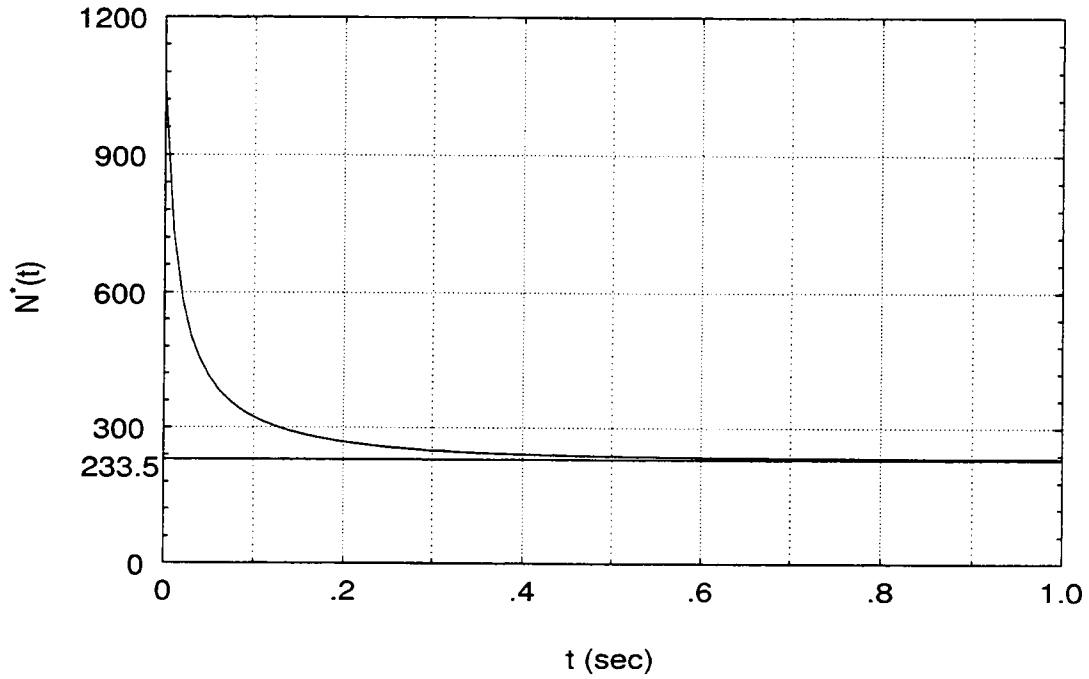

Figure 5.2: Optimal shifting strategy vs. time

the other hand, is a plot of the gear reduction as a function of *time*; this shows the evolution of the gear reduction provided by the transmission over the move. Since (4.21) is a function of joint speed, a steady state value of joint speed (i.e. zero acceleration) will correspond to a steady state value of gear reduction (i.e. N_{minimum}). Even though the plots of Figures 5.1 and 5.2 are for a continuously variable transmission, it can be argued that the final result—the minimum gear reduction—applies to discrete transmissions as well. Regardless of whether the shifting profile is continuous or discrete, the end result—for a given loading situation—will be a motor driving a load with a final, *fixed* amount of gear reduction. The minimum gear reduction shown in Figure 5.2 is the minimum gear ratio value that the engineer would want to put in the transmission if the loadings are those outlined in Chapters 3 and 4.

The nice fact about this result is that (4.21) is a *closed form* solution for the

optimal gear reduction versus joint speed. A simple simulation using this strategy will yield the joint speed versus time; this plot will invariably have a steady state speed, and this speed, when inserted back into (4.21) will give the minimum value of gear reduction needed for the transmission under loading. As mentioned before, a purely overdrive gear could be added by using the same procedure with no end effector and/or gravitational loading.

5.3 Transmission Ratio Design

5.3.1 Continuously Variable Transmissions

With the transmission bounds (i.e. maximum and minimum gear reductions) defined, the transmission can be physically designed. In the CVT case, there is no concern for designing the "intermediate" transmission ratios since a CVT is capable of delivering an infinite number of gear ratios between the maximum and minimum values. However, the optimization of Section 4.3.1 will give different results for the optimal shifting profile depending upon the loading conditions. For intermediate ratios, this is of no concern for a CVT; however, the maximum and minimum gear ratio values are physically fixed when the transmission is built. In particular, the maximum gear ratio is of the greatest concern. For loadings that are lower than the design values for $N_{\max}$, the transmission will simply shift more quickly into lower gears. However, for loadings that are higher than the design value for $N_{\max}$, the transmission has "nowhere to go". The only means the transmission has is to hold the gear ratio at $N_{\max}$ until the joint loadings reduce sufficiently to allow shifting into lower gears. This is analogous to a saturation nonlinearity. It may be of interest to simulate this

scenario to quantify the effect of holding the gear ratio fixed temporarily. Another interesting idea would be to go through the optimization process with a constrained set of trial functions (i.e. the class of available test functions is reduced to only include curves which meet the initial "saturation" constraint). The optimization would be purely numerical, but it would be interesting to see the effects of the constraint on the final shifting results. The author anticipates that the optimal profile will simply minimize the saturation period. The lower limit could also be constrained; however, this limit only puts a bound on the maximum speed of the actuator. While it is true that, in general, a well designed transmission should not encounter loads outside of the design space, a simulation of this type could be of interest.

5.3.2 Discrete-Speed Transmissions

Unlike the *CVT* case, a discrete speed transmission will only have a finite number of available ratios between the maximum and minimum value. Maximum reduction will always correspond to first or "low" gear, and minimum reduction will always correspond to "high" or "last" gear. For a two speed transmission, the story is over; the two gears would be designed to approximate the results of Figure 5.2. The high gear is picked as the steady state value of N^* as shown in Figure 5.2; hence the gear ratio[3] for high gear would be $N_{\min} = 233.5$. The low gear, on the other hand, must be selected a bit more arbitrarily. In the figure, $N_{\max}$ is around 1000:1. However, as mentioned earlier, this value will most likely be too high because the optimization was performed assuming *continuous* shifting. With continuous shifting, the maximum

[3]All values for gear ratio are subject to slight approximations needed to physically build the trains. This is strictly a function of the number of teeth on the gears

ratio is "disengaged" all but instantaneously; a discrete transmission cannot shift out of the gear that quickly, and any time spent in such a high value of gear ratio will be lost time at the joint. With such a high gear ratio, the motor spins up to steady state speed very quickly, and acceleration delivered to the joint ceases. That is exactly the reason that the *CVT* changes ratio so rapidly early in the maneuver. The ratio must continually be lowered such that joint acceleration may continue. Since a *DST* cannot continually shift, a compromise in ratio must be made for high gear.

A gear ratio, definitely lower than 1000:1 (for this example), is selected using Figure 5.2 as a guide. Again, the designer wishes to approximate the curve in the figure as closely as possible with a discrete number of steps. For a two-speed transmission, the curve is approximated with simply a high and low gear. High gear will be the same regardless of the number of gears; the "overdrive" gear is simply that. Selection of the maximum gear reduction is somewhat arbitrary, but suffice it to say that 1000:1 is (way) too high and 300:1 is too low. Say, for example, a value of $N_{\max} = 600 : 1$ is chosen. The approximate curve is then a step function initially at $N = 600$, finally at $N = 233.5$ with a shift time (actually a shifting speed) determined by the optimal algorithm, described in (4.45).

The design process is similar for a *DST* having more than two gears. Again, high gear remains the same: the steady state value in Figure 5.2. The low gear (maximum reduction) can also be chosen in a similar manner. In essence, the main idea is to approximate the curve of Figure 5.2 as closely as possible with a finite number of steps. Once the gear ratios are selected, the optimal shift speeds are immediately determined via (4.45).

Another interesting bit of future work would be a parametric study on approxi-

mating Figure 5.2 in different ways. This could be used to give a quantitative measure of how the number of gears and their spacing affects the overall joint performance. Most likely, it will be found that only a few gears—say 2 to 5—are needed to approximate the continuous curve very well. Most likely, a *DST* will only have a small number of gears because, beyond, say, five gears, the spacing between the gears is so small that the shifting must occur too rapidly. This was hinted at Figures 4.12 through 4.15. It would still be interesting to see a quantitative study on these effects.

Another interesting aspect for *DST*'s is that individual gears can be designed for different tasks. With this concept, a *DST*can be thought of as multiple fixed reduction actuators connected together. For some applications, this may be the best way to design the transmission. For example, if a machine will, in general, see only three distinct loading conditions (0, 10, and 20 *lbs* of payload, for example) then one way to design the transmission is to optimize three separate gear ratios: one for each loading situation. In essence, this is a modular design allowing three distinct fixed-reduction actuators to be packaged in one actuator system. Optimization for a single gear ratio allows the motor to reach and maintain its maximum power point. The details of this are given in Appendix D. Essentially, for a given loading condition, the optimal gear reduction for a single gear is the ratio that allows the reflected torque to be the torque delivered by the motor at maximum power.

5.4 *CVT* vs. *DST*: The Best Transmission for the Job

The question about which type of multi-speed transmission to choose, either *CVT* or *DST*, is strongly dependent on the application. If the smoothness of operation is imperative during shifting, then a *CVT* has an obvious advantage in that the shifting profile is continuous and smooth (of the general appearance of Figure 5.2). Other issues such as mechanical complexity may come into play. *CVT*'s, while relatively simple on a mechanical scale, are inherently friction drive. This can lead to limitations on the reflected torque capacity. Clearly, if friction drive is undesirable, then *DST*'s have the distinct advantage since they are completely comprised of toothed gears.

Mathematically, it is clear that *CVT*'s are much more elegant. This may be part of the reason that engineers have been chasing the idea for over one hundred years. Given the right application, a *CVT* could be a beautiful choice for the transmission system; a *CVT* offers inherent modularity, flexibility in use, and smoothness of operation. The modularity is seen the most when considering the infinitum of gear ratios available within the transmission bounds. In that light, *CVT* is infinitely many fixed reduction actuators in parallel. However, the *CVT* may be "more" transmission than is needed in some applications. In some situations, only a few gears may be needed. It is clear that the shifting profile of Figure 5.2 can be approximated with a high-low gear set. Hence, the design process, although completely rooted in *CVT* mathematics, can often lead to a *discrete speed transmission* solution for the actuator!

For a quick glance into this, consider the same motor chosen for the transmission-based system in Chapters 3 and 4. Using the discrete-speed optimization algorithms developed in Chapter 4, a comparison between a *DST* and *CVT* (both optimized) can

Table 5.1: Maneuver time comparison: *DST* vs. *CVT*

N_1	N_2	time (s)
1000	233.5	0.821
800	233.5	0.807
750	233.5	0.803
500	233.5	0.770
400	233.5	0.759
300	233.5	0.782
233.5	233.5	0.874

be made. As discussed earlier, for the *DST*, the minimum value of gear ratio is chosen as 233.5 (see Figure 5.2). The selection of the maximum ratio is a design choice, but a logical value can be found by sweeping several candidate values. Table 5.1 shows the maneuver times for several *DST*'s (optimized with respect to shifting) for the same 40° shoulder pitch-up maneuver investigated throughout this work. The maneuver time for the optimized *CVT* actuator is around 0.74 s. Clearly, a two-speed *DST* is very competitive in terms of maneuver time. If the nominal loading is reasonably close to invariant for a particular application, the a *CVT* actuator is difficult to justify. For loadings varying over a wide range, *CVT* may be a more robust solution.

Implementation of either type of transmission will involve many factors that are application specific. It is safe to say, however, that the general trend will be to use *CVT*'s in applications where loadings change over wide ranges and extremely smooth operation is required *at all speeds*[4]. Likewise, for situations having relatively constant joint loadings, a *DST* will be an effective transmission system for the *TBA* application.

[4]If smoothness of operation is only required at low speeds, then a *DST* will work just fine; the transmission ratio is simply held fixed during this phase.

5.5 Summary

This chapter has discussed *using* the results of Chapter 4 to synthesize gear ratios to be physically built in the transmissions. Specifically, the maximum and minimum ratios are found first such that the overall transmission ratio range is defined. The minimum ratio is found in the same manner for both continuously variable and discrete-speed transmissions; it is simply the steady state gear ratio that results when (4.21) reaches steady state speed. The maximum gear ratio is calculated in a straightforward manner for a CVT; since the maximum gear reduction always occurs at zero joint speed, (4.21) is evaluated at $\omega = 0$ with the worst case loading conditions assumed for torque and inertia. A DST on the other hand, should *not* use this ratio; as discussed in Section 5.3.2, the maximum ratio (and intermediate ratios) are always selected such that the continuous shifting profile (e.g. Figure 5.2) is approximated in some sense.

With the transmission bounds (maximum and minimum ratio) selected, the CVT space is complete. However, once the transmission is built, the maximum and minimum ratios are absolute and fixed bounds. Equation (4.21) gives different values for different loadings; however, once the transmission is built, the bounds on maximum and minimum ratio cannot be broken. For lower loadings than the design value, this will simply result in the transmission shifting more quickly than normal. For loadings higher than the design value, the transmission will have no alternative other that to remain at maximum ratio until the loading reduces to a value sufficient to allow shifting into higher gears.

It has been demonstrated that the DST involves a bit more work in that the intermediate ratios must also be defined by the designer. In essence, the gear ratios

should be chosen such that the curve of Figure 5.2 is approximated as closely as possible. This can be an iterative process, since the ratio selection and optimal shifting times are inherently coupled. The shift times come from the optimal shift *speeds* given by (4.45).

Some interesting areas of future work come from this chapter. In particular, a parametric study of gear ratio selection along with the number of gears would provide a quantitative look at the effects of additional gears, wider gear spacing, etc. It is possible that the parameters themselves can be optimized. Recall that the discrete optimization presented in this work required knowledge of the ratio separations apriori. A numerical parametric optimization of the gear ratios and the shift speeds may be possible. The number of parameters (ratios and shift speeds) is, in general, $2j - 1$, where j is the number of gears in the transmission. An interesting avenue to explore would be to quantify the effects of skipping gears. It was never assumed in the analysis presented here that the gears in the DST would be consecutive. There may be situations (especially for low payloads) where "running through the changes", or shifting through all of the gears isn't necessary or even efficient.

This chapter has more clearly defined how the results of Chapter 4 are used to synthesize transmission ratios for applications. It not only showed the distinct differences in continuously variable and discrete-speed transmissions, but also that, depending on the application, one concept may have distinct advantages over the other. It is interesting that the entire synthesis of gear ratio selection is based on results from an optimization process based on CVT's, but the results—especially concerning minimum reduction or "high gear"— are completely applicable to both CVT's and DST's. The choice of which transmission is implemented will have to

do with factors such as size, weight, robustness, and smoothness of operation among other factors.

Chapter 6

Transmission Hardware Conceptual Designs

6.1 Planetary Gear Trains: Discrete Speed Transmissions

Perhaps the most simple multi-speed (or multi-gear) transmission is just a two-speed transmission. This denotes that the transmission itself has two distinct gear ratios. Of course, the transmission can be designed to have any distinct number of gear ratios, but the principles are all the same.

Multi-speed transmissions are generally composed of compound planetary (or "epicyclic") gear trains. In these transmissions, the gears *always* remain in mesh. Planetary gear trains are multi-degree-of-freedom systems, so multiple gear ratios (i.e. ratio of input to output speeds) are obtainable by simply engaging and disengaging different members of the train. For example, a simple planetary set is a two degree-of-freedom system and hence requires two inputs for a predictable output. A brake can introduce one of the two required inputs by imparting zero velocity to a member of the train, while the other input is provided by the driver (i.e. prime

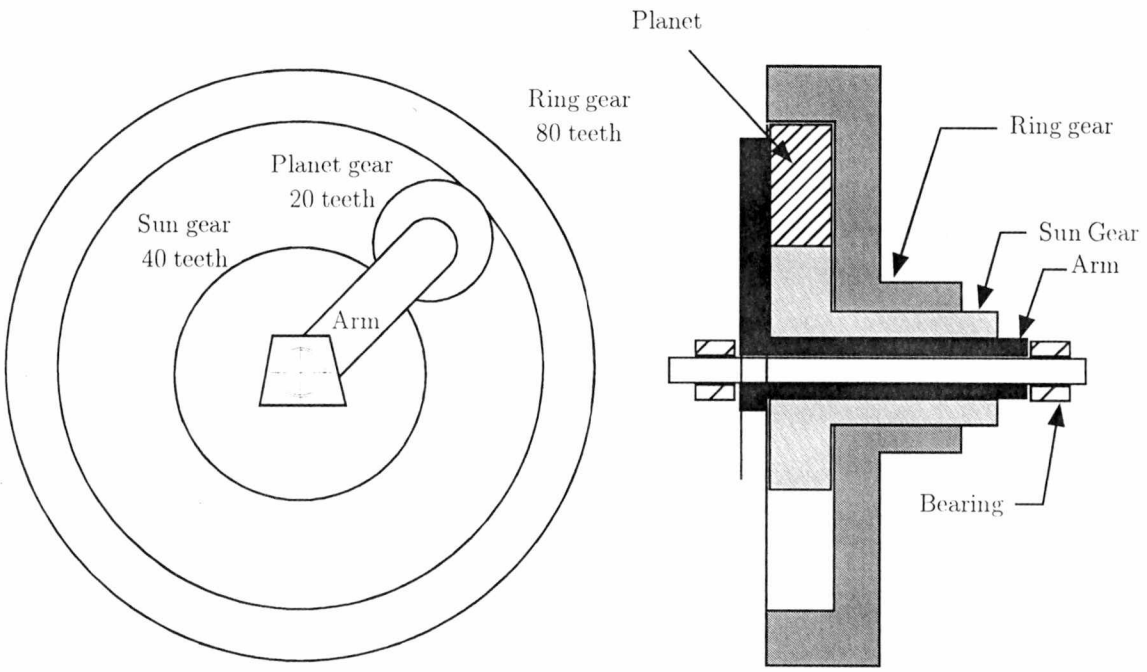

Figure 6.1: A basic planetary gear train

mover). Figure 6.1 shows a basic planetary gear train. The selection of the two input gears is left to the designer. The gearset shown in Figure 6.1 could easily use any two of the ring gear, sun gear, and arm as inputs while accessing the remaining as the output. If, for example, the sun gear and arm are chosen as inputs with the ring gear as output, for the geometry shown the gear ratio from arm to ring is +1.25:1 and from sun to ring +2.5:1.

Planetary gear trains have several advantages over conventional gear trains. Perhaps the most important is that they can be made extremely compact. In other words, planetary trains can offer a lot of gear reduction in a small amount of space. Secondly, planetary gear trains are *reverted* gear trains by default, meaning that the axes of input shaft and output shaft are coincident. Concentric shafting is an especially nice feature for electric machines in general since it can allow the overall actuator (motor

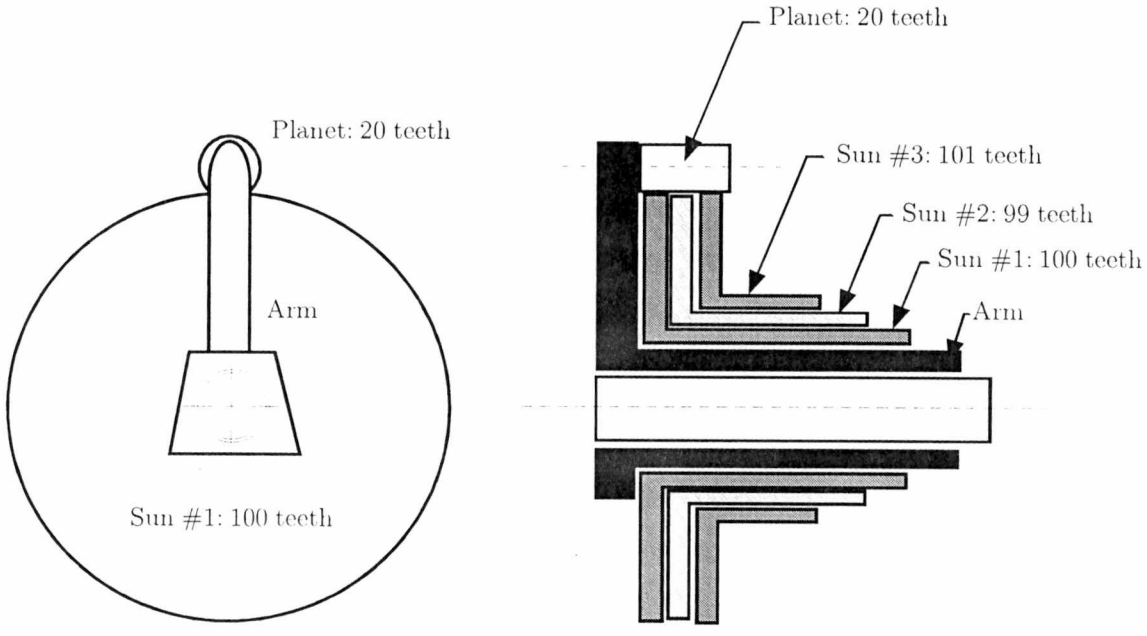

Figure 6.2: A compound planetary gear train

+ transmission) to also be made as compact as possible. Finally, planetary trains can be made such that concentric, bi-directional outputs can be generated with a single unidirectional input. This feature makes planetary trains especially popular in vehicle automatic transmissions.

There is a nice example given in [27] that beautifully illustrates several of these advantages. The compound planetary train is shown in Figure 6.2 and is sometimes referred to as "Ferguson's paradox". The two inputs for the gearset are the second sun gear (it is held fixed) and the arm (it is the driver). The outputs are the sun gears 2 and 3. The reason for the name has to do with the available outputs. For the geometry shown, the gear train has a ratio of 100:1 with output available in both directions *simultaneously*. For example, for a counterclockwise 100 rpm input to the arm, a counterclockwise output of 1 rpm is available from gear 3 and a *clockwise*

output of 1 rpm is available from gear 2. The gear ratio of 100:1 is a much higher ratio than can be obtained with a conventional train of similar sized gears (i.e. gears with 100 teeth and 20 teeth).

In general, clever gearset designs with gears having nearly the same number of teeth can allow very high gear ratios to be obtained. Because of the properties of the involute tooth profile, gears with slightly different pitch diameters (hence nearly the same number of teeth) can still mesh smoothly with a coupler gear; the coupling gear in Figure 6.2 is the planet gear. The discrepancy in pitch diameters leads only to slightly different pressure angles for each gear.

6.2 Continuously Variable Transmissions

6.2.1 Van Doorne Push-Belt *CVT*

By far the most commonly recognized *CVT* is the Van Doorne "push belt" *CVT* [28, 29, 30, 31]. This transmission is shown schematically in Figure 6.3.

The concept of a variable pulley *CVT* is well over one hundred years old. Originally, the torque was transmitted from the input to the output pulleys via tension in a V-belt. Continuous changing of the speed ratio is achieved by changing the spacing between the pulleys; this changes the where the belt rides on the pulley and hence effectively changes the pulleys pitch radii. As with all *CVT*'s, ratio can smoothly change between a maximum and minimum value.

The majority of the evolution of "belt-based" transmissions has been centered around the belt itself. Lost motion and stretching of the belt were among many of the problems associated with the dual pulley concept.

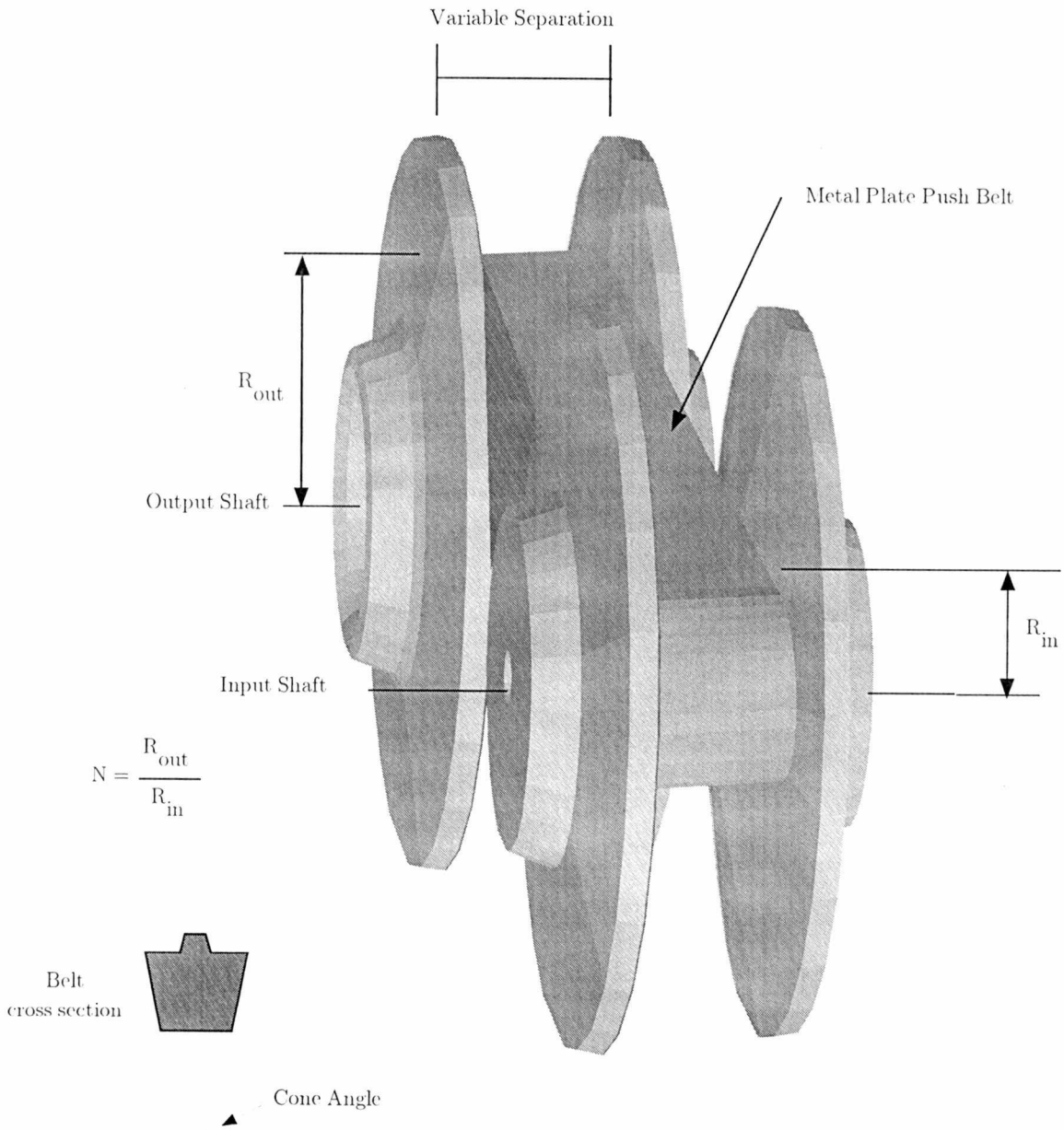

Figure 6.3: Van Doorne "push belt" *CVT*

In attempts to improve the dual pulley concept, a major conceptual change over the years has been the development of "push-belt" technology for the Van-Doorne idea. A push belt transmits torque through compression rather than tension[1]. Hence, a "push-belt" really isn't a belt, but a load-bearing structure that is virtually rigid axially and somewhat flexible transversely. This is possible because the belt is actually composed of a series of hardened plates. Each plate transmits force along the axis of the belt cross section by thrusting against its forward neighbor. The plates are held in place by a steel band that supplies just enough pre-tension to force the plates to follow their path around the pulleys.

The majority of literature on specific *CVT* designs is focused on the Van Doorne concept; however, the number of papers is still scarce. Of the papers that are specific to the Van Doorne idea, the majority address issues with the effectiveness of the belt itself, particularly with respect to slip characteristics [32]. The problem of slip leads to a low torque capacity on the automotive scale. The belt technology is still under investigation, and literature indicates that concepts being pursued involve improved plate geometries and dry belt designs [33].

The metal push belt *CVT* has been developed to the point of automotive applications, most recently being seen in automobiles from Honda, Ford, and Subaru [31, 34, 35, 36]. The concept may not be as compatible with robotic applications for several reasons. Primarily, the compressive force pressing the pulleys against the belt may be excessively high. Second, the belt *CVT* is generally a "wet" belt system in that the entire apparatus exists in a lubricating bath; this could be very restrictive concerning weight actuator weight restrictions. However, a dry belt design may

[1]It's amusing to note that use of a push belt turns "pulleys" into "pushies".

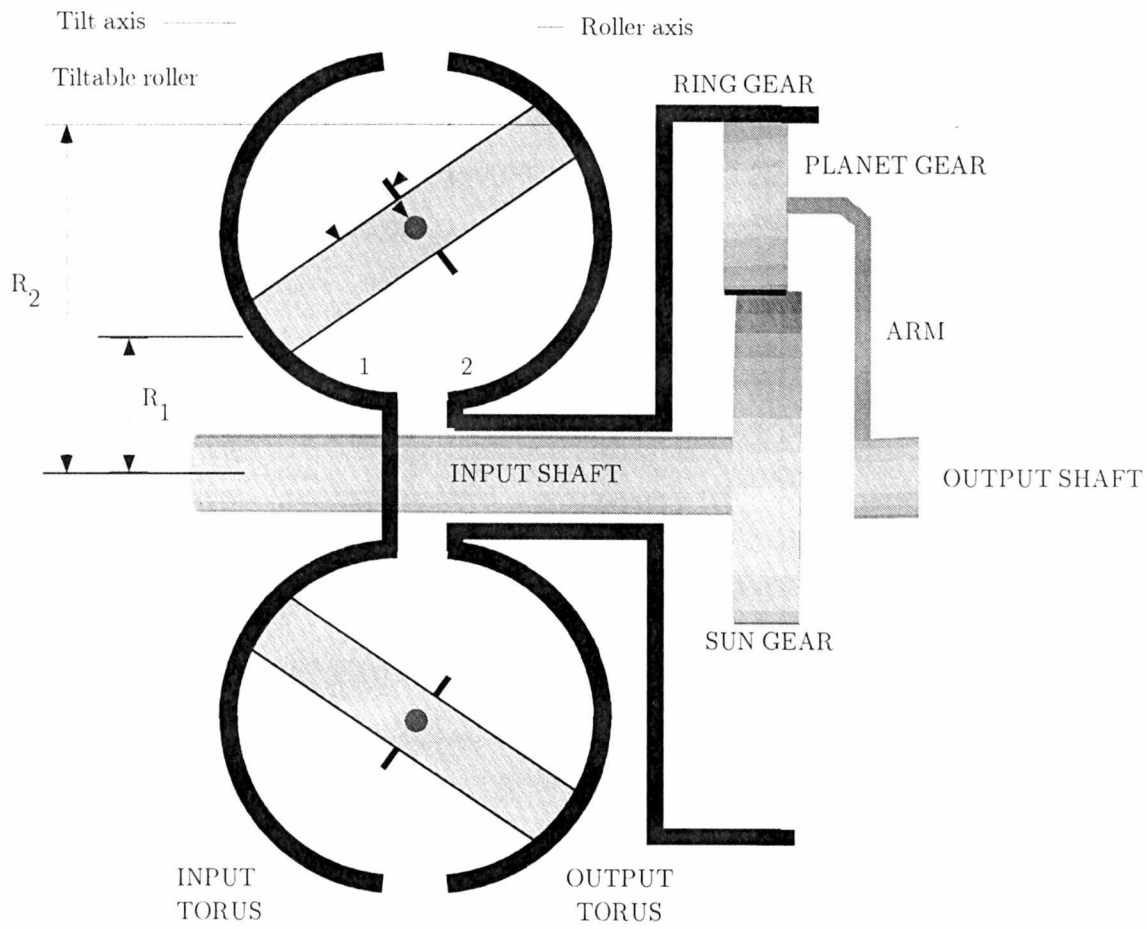

Figure 6.4: Split toroid *CVT*

be possible. Finally, the axes of the input and output shafts for this type of transmission are not coicident. Even though the transmission could be reverted, again it seems advantageous to choose a transmission concept that is inherently "in-line". The remaining *CVT* concepts to be discussed all have in-line input and output shafts.

6.2.2 Split Toroid Type *CVT*

Another *CVT* configuration is shown schematically in Figure 6.4. As with the Van-

Doorne belt drive, this transmission concept has been pursued in automotive research [37, 38, 39, 40]. Some literature refers to this type of drive (and all others except Van Doorne) simply as a traction drive. In Figure 6.4, the continuously variable drive unit is composed of two toroidal discs coupled together by a pivotal traction roller. The transmission ratio is smoothly altered by changing the angle of the coupling roller. In Figure 6.4, the transmission is not only continuously variable, but what is termed as *infinitely* variable. The term generally refers to a CVT design that is capable of zero output motion and reversed output motion without changing the motion direction of the prime mover. Since gear ratio is generally defined as the ratio of input speed to output speed, mathematically, a zero output speed would apply an "infinite" gear ratio. This is the origin of the name, but it does not imply that the transmission ratio increases without bound with respect to torque. The torque limitations on this type of system are directly associated with the limitations on the friction drive concerning slip.

The transmission of Figure 6.4 is infinitely variable because it is "input coupled" to a planetary gear train. The planetary train is uses inputs from both sides of the $CVT$and couples them together such that the final output speed is a function of the ratio of the two inputs. With any input-coupled $CVT$and planetary combination, it is always possible to arrange the gear train such that a zero output speed point exists. Such an arrangement is impossible with an output-coupled system. Input and output-coupled system schematics are shown in Figure 6.5.

It is imperative to understand that "infinitely" variable transmission refers only to the speed ratio side of the argument. In a general sense, when gear ratio, speed ratio, transmission ratio, etc. are defined in textbooks—and research papers— the

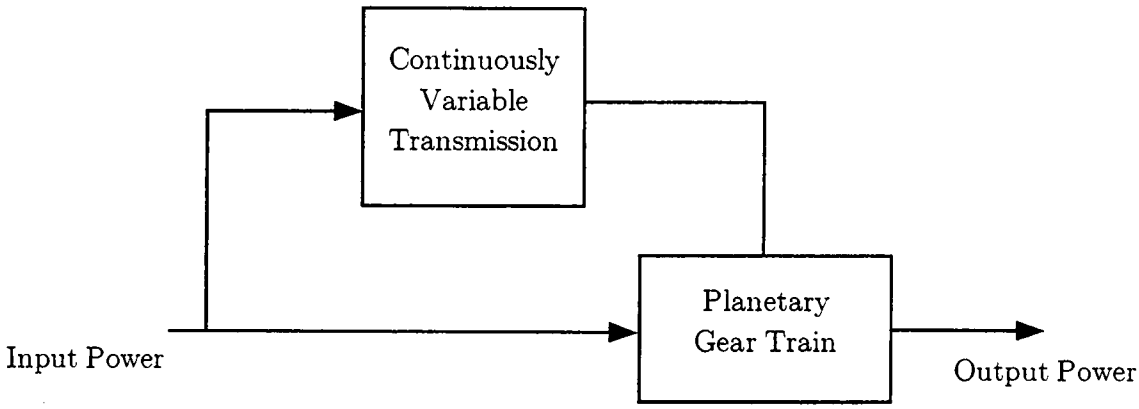

(a) Input-coupled configuration

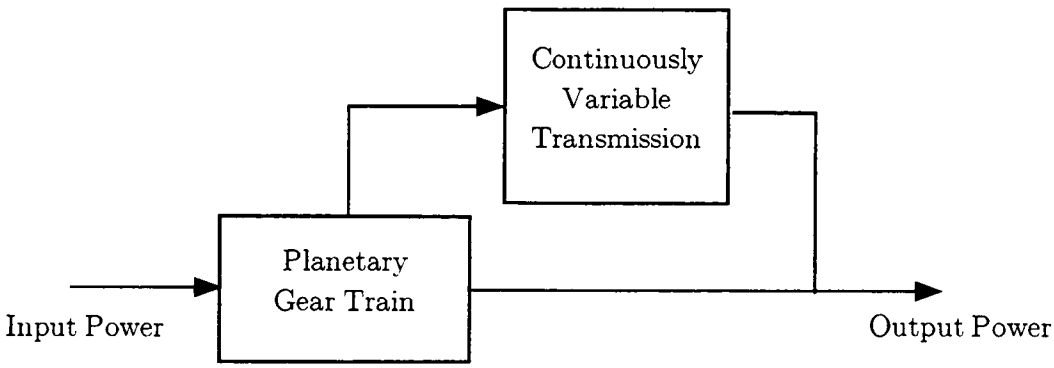

(b) Output-coupled configuration

Figure 6.5: Input and output coupled transmission schematics

terms are used interchangeably. In reality, there are a few cases where the terms are emphatically *not* interchangeable. In most references, when a transmission's "ratio" is defined, it is tacitly assumed that speed ratio and "gear ratio" imply the same principle. In most cases, this is true. For example, for a standard gear train, albeit standard or planetary, the derivations for the ratio of the train are generally defined as:

$$\text{Gear Ratio} = \frac{\text{Input Driver Speed}}{\text{Output Driver Speed}}.$$

While this is true for the overwhelming majority of systems, it is *not* true for all systems. It is a mistake to assume that a geared system, whether hard geared or friction drive (as with a *CVT*), has the capability of manipulating both mechanical advantage (i.e. *gear* ratio,) and speed ratio. In fact, there are a handful of systems for which this fact is untrue. It is the estimation of the author that many "transmission" conceptual designs have failed because of the misunderstanding of this fact; this research work lost many hours by assuming that speed ratio manipulation implied torque ratio manipulation also.

For a standard gearset, say simply, a set of spur gears with relative diameters of 2:1, the immediate implication is that not only will speed be altered by a factor of two with a train of this type, but also torque. For most gear trains, this is true. However, the painfully tacit assumption that makes this assumption hold is that the gears, whatever their fashion, be capable of reacting some portion of the torque via strict relations to geometry, or via reactions due to certain linkages being connected to *ground*.

With the so-called "infinitely" variable transmission concept that we have introduced in this section, ideas may arise as to why a zero speed point can occur.

Mathematically, specifically due to geometry, it first appears that the input coupled planetary set simply matches the input and output speeds of the *CVT* (a toroid-base *CVT-IVT* in the case of Figure 6.4), in such a manner that the output speed may be zero for a non-zero—or moving—input. This statement is true. However, even though this mathematically implies that the "gear" ratio is infinite, it is not the case. It's not even close. For some systems, speed ratio and gear ratio—a parameter that literally defines a transmission—are not intimately coupled; in fact, for some systems they are not coupled at all. The next section discusses an actuator concept that was exciting to investigate because of its robustness concerning manipulation of speed ratio (and, perhaps mistakenly, gear ratio). Upon closer investigation, it is found that the coupling of two motors with a two degree-of-freedom planetary set *does* offer an incredibly simple and robust *speed reducer*. Sadly, however, the extension to "torque multiplier" is not feasible strictly due to physics alone. The actuator will be discussed in the next section. The point to remember is this:

> No matter what any elementary text states concerning gearing, speed ratio and gear ratio, that is speed ratio and its connection to torque multiplication, are *not necessarily* intimately connected as the inverse of each other.

6.2.3 Dual Motor Actuator

A concept for what was initially thought to have promise as a "dual motor *CVT*-based actuator configuration is shown in Figure 6.6. Obviously, there is no friction drive in the schematic; thus, the transmission ratio surely cannot be changed contin-

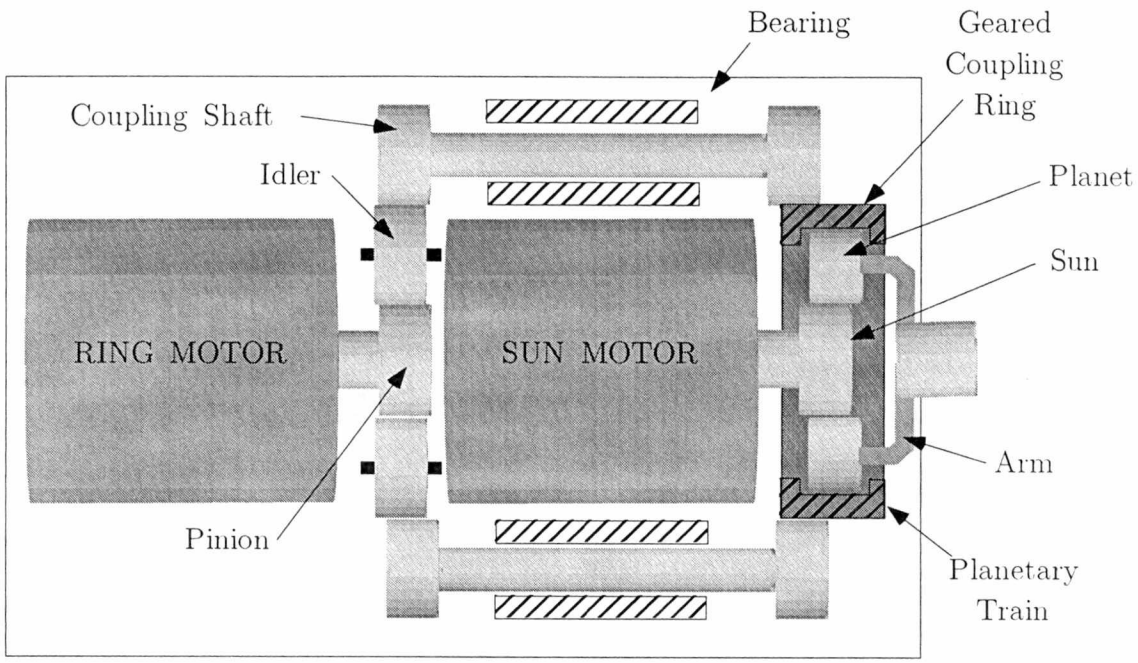

Figure 6.6: Dual motor actuator

uously..., or can it? The idea arose from the toroid-based *CVT* actuator of Figure 6.4. The toroid actuator, and infinitely variable actuators in general, seemed interesting because they incorporated a clever use of a planetary gearset to couple the input and output speeds of a *CVT*. With the idea of the transmission in hand, the weakest link of the transmission system seemed to be (as with all *CVT* concepts) the friction drive itself. It has been written [41] that a geared *CVT* (i.e. a *CVT* based on gearing versus friction or cyclic concepts[2] is the engineering version of the Holy Grail. Being enthusiastic, however, the author pursued this new idea. Since the planetary set simply matches two distinct inputs (as all planetary sets do) to give a desired input, then do the inputs necessarily have to come from the same driver motor? The

[2]Here, cyclic is not to be confused with epicyclic. Cyclic transmissions create variable geometries in sine wave generating mechanical mechanisms that can continuously adjust the angle of the sine wave to create varying output speeds [33, 42].

answer to that question is a resounding "no", but the ramifications are not simple.

It must be kept in mind, that the majority of *CVT* research (along with that of infinitely variable transmissions and the like) has been focused toward the automotive (or at least vehicle) industry. It is most likely a fair statement that most applications of that level cannot "afford" to have two motors. However, for the robotic and/or industrial actuator application, we have determined that the overall actuator power and torque density are the critical factors in the design situation. As we saw in our feasibility study with the Advanced Servomanipulator, even assumptions of transmission masses on the order of the masses of the driver motor themselves were not overly restrictive in the overall performance, if the actuators could alter mechanical advantage in a strategic manner. The conclusion was that, if the concept would actually work, having two motors and a coupling epicyclic train would be well within our design constraints.

This led to an exciting question. "Could a dual-motor actuator emulate an infinitely variable transmission-based system (of the type of Figure 6.4) *without* a friction drive?" In other words, "is a hard-geared system capable of continuously variable gear ratio manipulation?"

The answer is sobering, and hindsight is definitely "20/20" vision. If the fundamental (and common!!) assumption of the basic equivalence (strictly, the basic "hard-wired" relationship) of speed ratio and gear ratio is accepted, then analysis will predict that it is not only possible, but easily implementable. In detail, if from the beginning, the ratio of the input speed to output speed (and, tacitly, the output torque to input torque) is redefined as a parameter called gear ratio N (assumed continuously variable), then the analysis will predict that intelligent control of the

two motor speeds can be coupled with a well designed epicyclic train to yield a continuously variable (and infinitely variable since zero output speed is possible) system. What an exciting result! And what a disappointment.

Speed ratio and torque ratio are not always intimately connected. One is not always the reciprocal of the other. Even though the dual motor concept is capable of manipulating speed ratio—just as the toroid-based CVT is capable of doing—it is emphatically *not* capable of manipulating torque ratio. For the toroid based system, the torque is multiplied as speed is reduced because of geometry. For the dual motor system, no such geometry is available to manipulate torque; the amount (i.e. ratio of the total amount) of torque going to each driver motor is *solely* a function of the size of the gears—specifically diameter, and equivalently, the number of teeth on the gears. No amount of speed manipulation can change this fact, and the disappointing result is that torque ratio cannot be altered for the overall actuator even though speed ratio can be altered to any degree within the torque limits of the driver motors. This is simply because, in the dual motor system, speed ratio is altered by essentially using one motor as a driver and one motor as a brake. While this arrangement can manipulate speed completely, it cannot alter torque at all. Is the actuator infinitely variable in a "speed ratio sense"?—YES. Does this affect torque ratio?—NO. The toroid based system—or any system which input-couples a true CVT to a planetary set—can alter speed ratio and torque ratio simultaneously only because the torque is altered with geometry. Whether it is a variable diameter pulley as with Van Doorne or a split toroid, the geometry is what maneuvers the torque flow through the system. The dual motor system doesn't have the capability to multiply torque—it isn't a transmission.

The immediate question, once the disappointment has faded somewhat, is how to take the perceived promise of the dual motor concept to a working system that can manipulate both speed and torque. The answer that seems most obvious is that the actuator must have *independent* control of both the speed ratio and torque ratio. The solution is that a motor (or two motors) must still be driven through a true transmission of some sort. In a later section, we will discuss a possible solution to this actuator crisis.

6.2.4 Planetary Cone *CVT*

Another transmission configuration is shown in Figure 6.7. This transmission is based on a set of planetary cones. Essentially, the friction-drive cones are equivalent to variable diameter planets for a planetary set. As arranged in Figure 6.7, the output of the system is the arm which taps the motion of the friction drive planets relative to the rotationally fixed ring. Also note that the input is a geared ring-planet set. As the effective diameter of the cone planets is changed, so is the relative planet motion and output motion. This concept is a clever version of an epicyclic train; indeed, it is a continuously variable planetary set.

This leads to an interesting idea; since a planetary set was used in the dual motor concept to blend the two motor outputs into a single output, a variation on this planetary cone concept could be used for the same purpose. Further, since this planetary set has the capability of continuously manipulating speed *and* torque, this concept could allow either a single or dual motor actuator to smoothly trade torque and speed. In other words, a idea of this type could correct the fatal flaw of the

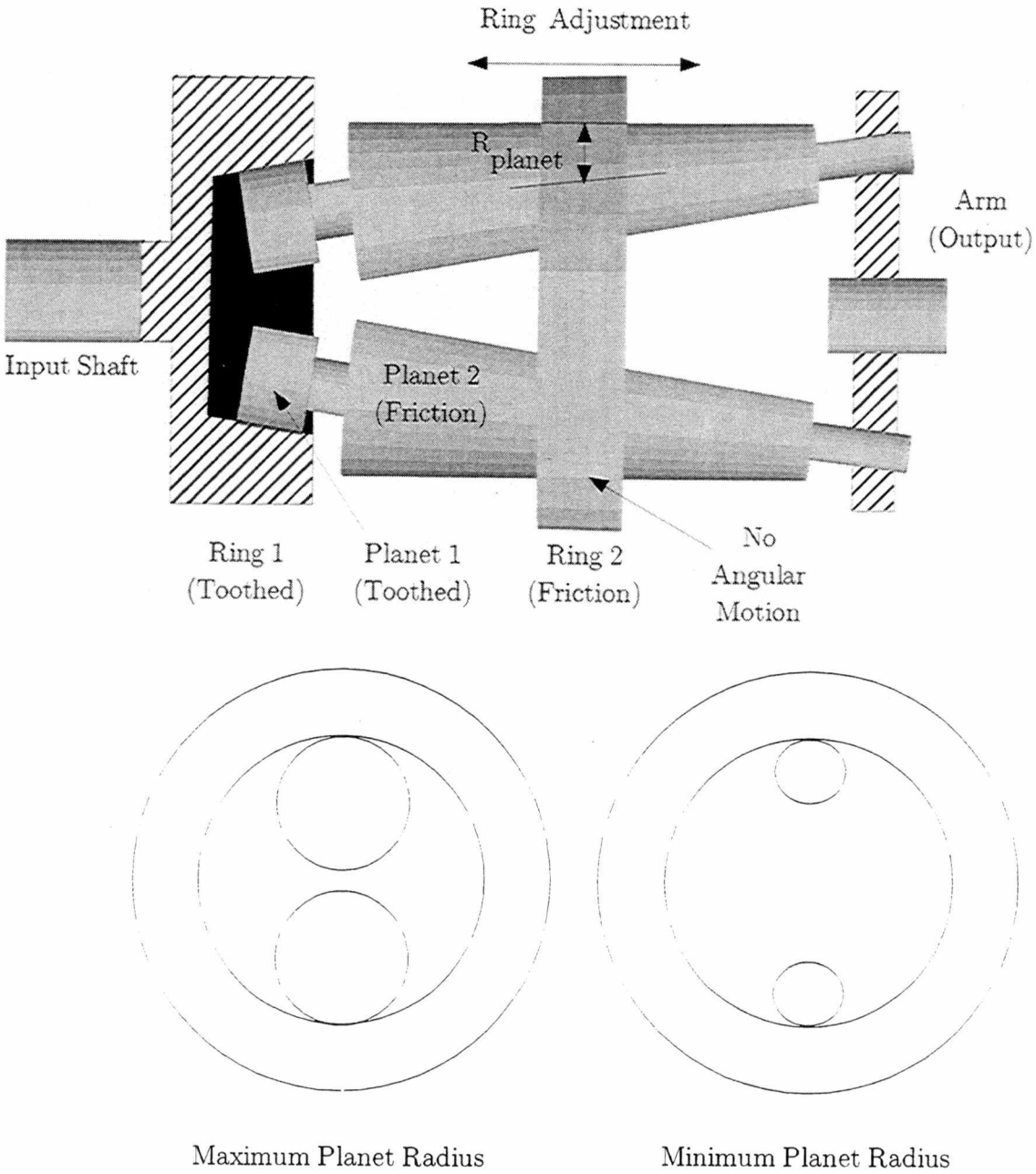

Figure 6.7: Planetary cone *CVT*

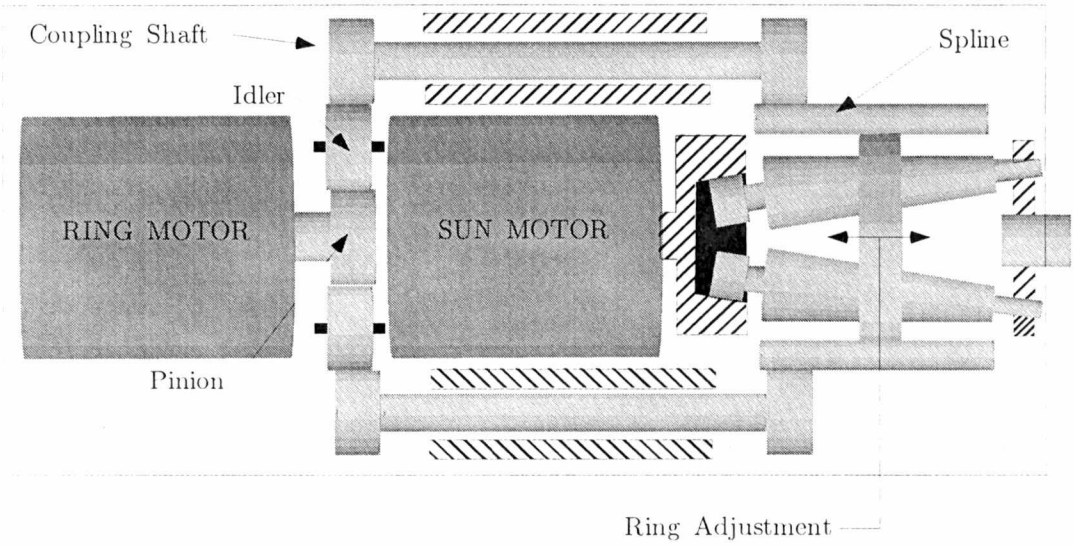

Figure 6.8: Dual motor planetary *CVT* Actuator

dual motor actuator of Section 6.2.3. A continuously variable planetary set with two motors as inputs offers a wide range of speed and torque possibilities. With the train fixed in ratio, the two motors can manipulate speed (but not torque) by simultaneous control of the motor speeds as discussed in Section 6.2.3. When the train is adjusted, torque can also be manipulated (simultaneously) and the actuator becomes a *CVT*-based actuator. This is discussed in detail in the next section.

6.2.5 Dual Motor Planetary *CVT* Actuator

The concept for a dual planetary actuator (with the ability to manipulate speed *and* torque) is shown in Figure 6.8. First, it should be emphasized that the planetary cone system could be used with a single motor; this section looks at the dual motor

case in an effort to resurrect some of the lost research work that led to Section 6.2.3. The transmission itself is changed from that of Section 6.2.4 because the friction ring is allowed to have motion (controlled by the ring motor) as opposed to being fixed as in Figure 6.7. This just changes one of the required two planetary train inputs from a constant value of zero to a variable (and controllable) value that is delivered by the second motor.

The discussions of Section 6.2.3 all apply to this actuator as well, except that the disappointing news about torque manipulation has been eliminated. This actuator has many interesting avenues that could be investigated if prototyped. First, there are *three* inputs to the system that must be controlled: the two motor speeds and the transmission ratio. It is interesting to think of the different control modes that might be used. For example, the actuator could be used simply as a speed reducer (i.e. the train ratio is fixed) in situations where feasible. The actuator could also be used as a "single motor" actuator by fixing one of the two motors; fixing the ring motor (hence the friction ring), for example, would form an equivalent transmission system to that of Section 6.2.4. The relative sizes of the motors could be another interesting area to investigate. It's possible to arrange the nominal transmission ratio such that one motor might be significantly smaller than the other in the actuator. The amount of torque going to each motor is always within the band specified by the cone transmission, but the effective torque at each motor axis could possibly be adjusted with fixed gear reducers, for example. Of course, efficiency gones down with every gear mesh, so too many reducers may be to much of a constraint on overall actuator power efficiency. At any rate, these are all interesting ideas that could use further investigation.

Chapter 7

Conclusions

7.1 The Fundamental Idea of *TBA*

This work has thoroughly investigated the concept of incorporating variable gearing or multi-speed transmissions into electric actuators for both robotic and industrial applications. The transmission-based actuator (*TBA*) concept is based on the idea that incorporation of multi-speed transmissions will allow the torque and speed capacity of the actuator motor to be manipulated over the course of a joint maneuver. By this, we have seen that torque capacity can be exchanged for speed capacity (and vice-versa) as joint motions begin and inertial effects allow dynamic torques to be reduced. As joint accelerations decrease, subsequently the dynamic torque requirements reduce in such a way as to allow the actuator motor to be capable of driving the load with less mechanical advantage (gear ratio). This translates to the transmission logically shifting to lower gear ratios as the joint moves such that (no longer needed) torque capacity is exchanged for increased speed capacity.

7.2 The Initial *TBA* Study

The initial feasibility study for the *TBA* concept looked at an existing manipulator design—ORNL's Advanced Servomanipulator—and evaluated the performance and design potential that multi-speed transmissions could bring to the field. From the standpoint of overall manipulator design, it was envisioned that *TBA*'s could eliminate centralized actuation for many manipulator classes; the actuators were envisioned as directly coupled to the joint in what is termed *distributed actuation*; this has the effect of eliminating the transmission of torque through manipulator joints and, as a general idea, uncoupling the overall arm design from the actuator drivetrain details. In other words, distributed actuation could allow the arm to be at least "first cut" without significant regard to actuator details concerning weight, space, drivetrains, etc. Obviously, this could introduce a quantum improvement in overall manipulator simplicity and cost.

The initial study revealed exciting results in that, even from a trial-and-error standpoint of selecting motor-transmission combinations, coupled with extraordinarily conservative assumptions concerning loading and inertia, the *TBA* concept could allow not only a distributed actuator system (in the *ASM* class to be feasible, but could also allow the *TBA* system to outperform the baseline in terms of both load *and* speed capacity. We later discovered that the initial study, as impressive as the results were, only represented the "tip of the iceberg". The initial study assumed fairly crude shifting profiles for the transmissions; the next phase of the dissertation revealed that logical shifting profiles could introduce huge increases in actuator performance. As an added bonus, the optimized shifting profiles removed any fundamental need for trial-and-error selection of motor-transmission combinations by providing an absolute

upper performance bound for a motor.

7.3 Transmission Shifting Strategies

We have seen that the transmission shifting strategies, for both continuously variable and discrete speed transmissions, are indeed logical and can be optimized. In this work, the shifting strategy was optimized with respect to the acceleration delivered to the joint and, hence the required maneuver time. In both cases, the optimal shifting curves[1] were centrally involved with allowing the motor to run in the vicinity of its maximum power point.

For the *CVT* case, the optimal shifting curves allowed the motor to reach and maintain its maximum power point for the entire acceleration portion of the maneuver. Hence, for the vast majority of the maneuver, the motor is running at constant speed and delivering maximum power. The continuously variable transmission, with its capability of providing seamless shifting (and an infinite number of gear ratios) within its maximum/minimum ratio values, smoothly alters gear ratio such that the motor can maintain maximum power, even in the case of variable loading. Indeed, the optimal shifting algorithm, (4.21), was derived with no assumptions as to the variance of the loading and inertia.

For the *DST* case, the optimal shifting was found in terms of both "gear separation"[2], loading, and inertia. Since a *DST* can only provide a *finite* number of gear ratios within the transmission bounds (i.e. maximum and minimum reduction), a

[1]Shifting curves tacitly means "gear ratio versus joint speed" for the *CVT* case and shifting *motor speeds*" for the *DST* case.

[2]Gear separation is defined as the ratio of the gear value to be engaged to the gear value of gear to be disengaged. Mathematically, N_{j+1}/N_j where "j" is the current engaged gear.

DST is incapable of allowing a motor to identically maintain its maximum power point during shifting. With discrete shifting, there is a finite "separation in gear ratio" between consecutive gears (see Figure 2.1; because of this separation, the motor must be spun *past* the maximum power point such that the finite shift may be accommodated. The result is that, during shifting, the motor is continually running the in the neighborhood of maximum power, but is never remaining at maximum power as long as there is another gear to be engaged. The "neighborhood" of maximum power is actually a speed bandwidth around the maximum power point of the motor; the width of the band is directly proportional to the gear separation. Indeed, if there is no gear separation—as is approximated by a *CVT*—the bandwidth is zero and represents the limiting case of continuously variable, or seamless, shifting.

It is extremely encouraging that, in studying the two transmission concepts in parallel, the optimization results are so intimately connected. The derivation of the analytical solutions looks completely different for each case, but the results are completely consisent. For a DC motor under constant voltage conditions, the maximum power point has everything to do with optimized transmission shifting for maximum acceleration (minimum time) joint trajectories.

As mentioned in the previous section, the optimal shifting strategies eliminate the fundamental trial-and-error approach to selecting motor-transmission combinations in that the transmission shifting strategies are known and an absolute performance bound for any motor is immediately attainable for any given loading situation. For any motor and loading condition, the optimal performance (on an acceleration basis) is directly obtained by numerical solution of the differential equation of motion with the optimal shifting profile (gear ratio versus joint speed) included. Since the

result is *CVT* based, the motor performance is maximized, the transmission shifting is maximized, and hence the *actuator performance* is maximized. The resulting performance (response time, maximum speed, etc.) is an absolute upper bound on motor performance. This can greatly reduce the time required for motor selection.

7.4 Selection of Physical Transmission Parameters

In the mechanical design phase of the transmission, we have seen that decisions must be made to physically define:

1. the transmission bounds (maximum and minimum available gear ratios), and
2. whether the transmission is to be a *CVT* or a *DST*, and
3. (if the transmission is a *DST*,) the number of available gear ratios, and
4. (if the transmission is a *DST*,) the ratio values of each gear in the transmission.

With respect to each of these issues, we have shown that the optimization results of Chapter 4 provide a definitive set of guides for for physically selecting transmission parameters. The transmission bounds are selected based on the maximum acceleration optimal shifting profiles. For a *CVT* the maximum reduction is directly available when maximum loading/inertia in the manipulator workspace is introduced in equation(4.21) at zero joint speed. And, as discussed in Chapter 5, adjustments must be made to this value if the transmission to be used is a *DST* for accommodation of the finite number of gears available. For the minimum gear reduction under nominal loading, we have seen that the result is fundamentally the same for both the

CVT and *DST* cases. Since minimum reduction corresponds to "high" gear, the final gear can simply be thought of as the "steady state" gear; Figure 5.2 demonstrates that the final gear is essentially reached within a fraction of a second; for a *DST* the curve of Figure 5.2 should be approximated as closely as possible with a finite number of steps; clearly, the "final" step would be the final, steady state gear ratio shown for the *CVT* case shown the figure.

It was also mentioned in Chapter 5 that an "overdrive" gear could be incorporated into the transmission design for modularity. This gear could be used in situations where high speeds are desirable (such as in travel between two tasks, for example). For the *CVT* case, this only involves lowering the minimum available gear value (the lower transmission bound). The value could be obtained from a simulation solution similar to Figure 5.2 with zero payload, zero gravitational loading, etc. Likewise, the steady state value can be used to design a physical "overdrive" gear in a *DST*.

Finally, we noted that any multi-speed transmission can be considered a finite (in the case of *DST*) or infinite (in the case of *CVT*) number of fixed reduction actuators "in the same box". Just as a single gear ratio can be optimized with respect to a nominal loading (as seen in Appendix D), so can each of the *DST* gears for a discrete range of nominal loads. It is a wonderfully interesting result to recognize that a *CVT* is an infinite number of optimized fixed reduction actuators within a nominal loading range. Indeed, since the optimal single gear ratio allows the motor to run steady state at maximum power for the nominal loading, the *CVT* guarantees that, as long as the loading falls within transmission bounds, the steady state ratio is optimal!

7.5 Transmission Design Ideas

The physical layout of multi-speed transmissions is an area which is well documented and researched mostly because of the automotive industry. The key points to be focused on concerning transmission design concepts will involve issues such as size, scaling, flexibility, and efficiency among others. The overall concepts, however, especially concerning size, weight, scaling, and the like remain equally encouraging for *TBA* implementation because inherently, transmissions deal in *ratios* which indicates that components only need to maintain their relative sizes to provide the desired train ratios.

In Chapter 6, we looked at some fundamental multi-speed transmissions along with a few new conceptual ideas that could be exciting to pursue. The most basic transmissions discussed were planetary transmissions which are the foundation of virtually every multi-speed transmission (i.e. *DST*) in existence. The advantages of planetary sets are numerous including compactness, stiffness, and inherent *revertedness*[3]. Since multiple speeds can be obtained in multiple directions with planetary sets and brakes, these type of trains are extremely popular in many applications—especially vehicle applications. Multi-directional outputs for single inputs could have interest implications in an industrial machine or robotic application.

Several *CVT* designs were also introduced; the most widely known *CVT* is undoubtedly the Van Doorne "push belt" *CVT*. Based on a semi-rigid mechanical belt system, arrangements of this type have seen several automotive applications over the years. However, problems with a strict Van Doorne arrangement could arise since hydraulics are generally used to generate interfacial forces between the transmission

[3]A reverted gear train implies that the axes of the input and output shafts are coincident.

belt and the pulleys; this defeats the entire purpose of *TBA*'s concerning expanding the electric actuator range. For the ranges of loadings seen in robotics, however, hydraulics may not be required, so the Van Doorne arrangement, or a modified version of it, may be feasible. A major disadvantage is this *CVT* is not reverted.

Other *CVT*'s are numerous and have one common element: they are all friction drive. Some transmissions are based on "sloppy" teeth interaction are "semi-*CVT*", but are extremely inefficient. Of the true *CVT*'s we presented, two main concepts were focused upon: the Split-Toroid *CVT*, and the Planetary Cone *CVT*. Again, both are friction drive, but both offer interesting possibilities. Both of these transmissions, when arranged correctly with a planetary set, can provide multiple output speed directions for a single input speed.

A new idea for an actuator combined a failed effort (a dual motor actuator that—it turned out—could only manipulate speed ratio but not torque ratio) with one of the *CVT* concepts[4] resulting in a combined actuator that could have incredible ranges in both torque and speed capacity. This "Dual motor planetary *CVT* actuator" could be made extremely compact and has the advantage of a redundant mode of control since the two motors can be controled independently of one another. This offers an incredible amount of manipulation power concerning speed control. Further, as with any actuator, the introduction of multiple gear ratio values greatly expands the usable range of the actuator.

[4]Any feasible *CVT* concept could be used.

7.6 Future Work

With this being somewhat of a pioneering effort toward development of this idea, there have been times where the research seemed endless to the point of being overwhelming. By this, we mean that each "avenue" of the research led to exciting results with implications that could open doors for continued research. In most cases, the only resort was to pick one and run with it until results were found. In some cases, the results weren't so exciting (particularly the investigation—details and pain of which were mostly omitted—of Section 6.2.3). However, in most cases, the results—when finally obtained—were exciting and opened doors for multitudes of possible future research work. Some of these ideas were mentioned in the dissertation body. We summarize a few of them here, basically in the order which they appeared in the dissertation

Discrete transmissions: Independent parameter optimization: Is it possible that the transmission parameters for a *DST* could be optimized independently? That is, for say a two-speed transmission, can three parameters N_1, N_2, and the time or speed of shift be optimized independently?

***DST* shifting: Parametric study for skipping gears:** Since the optimization of Section 4.3.9 required knowledge of gear separations (hence relative knowledge of gear ratios), the result is optimized with respect to that knowledge. However, there is no assumption that the engaging and disengaging gears need be consecutive. A study of performance with various gear separations would be interesting.

Constrained continuous shifting simulation: The continuous optimization pro-

cedure of Chapter 4 put no constraints on the bounds of the transmission. From a parameter design standpoint, this is just as needed since the transmission ratios have yet to be designed. However, once the transmission bounds have been physically set, the optimization regime is effectively constrained. For example, for a given loading situation, the optimal algorithm, (4.21) could request gear ratios outside of the transmission bounds. Physically the only alternative is to "saturate" the transmission in the direction that the algorithm wants. For ratios higher than the transmission bounds, the transmission must hold at the maximum reduction until the loading reduces to a level consistent with the transmission range. A quantitative study of this saturation type of effect would be useful.

Quantitative study of optimal discrete profile For designing the parameters of a *DST*, the major objective is to approximate a figure similar to Figure 5.2 "as closely as possible" with a finite number of gears. A quantitative study of a procedure for that approximation (number of gears, method of ratio selection, etc.) could be extremely useful in *DST* parameter design.

Closed loop controller design Especially in the *DST* case, the disturbances with respect to abrupt changes in gear ratio could have abrupt effects on the overall manipulator performance. A controller design using a robust method such as Quantitative Feedback Theory (QFT) could be a nice first cut at investigating low level control.

Physical engineering transmission design Selection, design, and prototyping of a multi-speed transmission is an obvious next step in the research. The proto-

type could be used as a testbed for current and future research results, especially concerning control algorithms.

These are just a few of the ideas that have been considered both during this research and for future investigations. Undoubtedly, focus on any of the above concepts will lead to a multitude of other questions to be answered.

7.7 The Challenges Ahead

As with any research project, the scope of the work has to be well defined such that sufficient focus can be given to the critical investigations of the work. The transmission-based actuator concept has numerous challenges in front of it if it is to be incorporated into the industrial machine and servoactuator realm. However, all of the challenges are mere details in comparison to the main challenge: staying focused on the fact that, undoubtedly and without question, the introduction of a multi-speed transmission into a system makes the system more robust in terms of both the speed range and loading range that the system can handle. That fact, above all others, should be firmly planted in anyone who pursues this idea further. This truth is evidenced completely by the automotive industry and their continual pursuit of better, more robust, and more efficient drivetrains.

Note that many of the assumptions in this dissertation were conservative, simplified, and even non-realistic in the sense that loadings are *not* generally constant, torque-speed curves for motors aren't exactly linear, motors have a multitude of non-linearities inherent to their control, etc. The list goes on and on. But the focus of this work was to evaluate the *TBA* concept *from the ground up*. There were so many

fundamental questions that needed to be answered:

- Can transmissions be scaled down?
- Would transmissions with certain weight/size assumptions and available ratios allow distributed actuation in an *ASM*-type manipulator class?
- Could the *ASM* baseline performance be matched? Exceeded?
- How does the designer logically select motor transmission combinations?
- How *should* continuously variable transmissions shift?
- How should discrete speed transmissions shift?
- Can the shifting be optimized in some sense?
- Do *CVT*'s and *DST*'s have any analogous behavior in how they shift?
- How do you pick gear ratios?
- How do you select the number of gears to put in the transmission?
- What are some possible designs for *TBA* transmissions?
- Are there possibilities for new transmission concepts (and are new concepts really needed)?

All of these question were answered, at least in part, in this work. And few if any of them would have been answered if focus had been lost. Focus on the fact that the introduction of a transmission has *got* to be an improvement in the actuator. Any of the assumptions that were made in this work could be expanded further to make the

situation more realistic, interesting, or both. But the procedures that were used in this work will undoubtedly be fundamentally the same as for any future investigation. For example, we once received a question as to how realistic a linear torque-speed profile assumption for a motor actually was. The answer is "pretty close" but that's irrelevant. If a more realistic torque speed relation is known, then by all means use it; the procedures are fundamentally unchanged. We can guarantee, however, that second order effects such as slight nonlinearities in the torque-speed relation will not effect the overall feasibility of the *TBA* concept.

The overall theme of this dissertation can be summarized quite concisely.

1. Use a multi-speed transmission if at all possible

2. Design the transmission parameters such that the motor runs in the vicinity of maximum power

3. Keep it simple, and answer the fundamental questions

It is sincerely hoped that this project is indeed a pioneering effort for transmission-based actuators in that the concept is pursued fully, even to the point of incorporation into a multitude of machines, both robotic and industrial. The concept could revolutionize actuator technology and industrial machines in general. The challenges will undoubtedly be in the application specific details such as selection of transmission configuration, transmission bounds, specific gear ratios, motor-transmission combinations, and controller configurations. The main challenge, however, will not to lose the big picture: transmissions can revolutionize electric actuators.

Bibliography

Bibliography

[1] J. M. Hollerbach. A comparative analysis of actuator technologies for robotics. *Robotics Review*, pages 298–342, 1991.

[2] Electro-Craft Engineering Handbook. *DC MOTORS, SPEED CONTROLS, AND SERVO SYSTEMS.*

[3] J. M. Hollerbach. A recursive lagrangian formulation of manipulator dynamics and a comparative study of dynamics formulation complexity. *IEEE Transactions on Systems, Man, and Cybernetics*, pages 730–736, November 1980.

[4] H. Asada and K. Youcef-Toumi. *DIRECT DRIVE ROBOTS: THEORY AND PRACTICE.* MIT Press, 1987. p. 39.

[5] R. C. Dorf. *MODERN CONTROL SYSTEMS.* Addison-Wesley Publishing, New York, NY, 1989.

[6] I. S. Larman. Choosing the drive system for the right application. *IMechE European Conference on Electrics versus Hydraulics versus Pneumatics*, 11(1):99–104, 1985.

[7] J. J. Craig. *INTRODUCTION TO ROBOTICS.* Addison-Wesley Publishing, 1986.

[8] H. Asada and T. Kanade. Design of direct drive mechanical arms. *ASME Journal of Vibration, Acoustics, Stress, and Reliability in Design*, 105(3):312–316, 1983.

[9] Y. Koren. *ROBOTICS FOR ENGINEERS.* McGraw-Hill Book Co., 1987.

[10] H. L. Martin and D. P. Kuban et al. System design requirements for the Advanced Servomanipulator slave, 1985. AIMS-SDR-2.1, Oak Ridge National Laboratory.

[11] W. P. Seering. *CONCISE INTERNATIONAL ENCYCLOPEDIA OF ROBOTICS: APPLICATIONS AND AUTOMATION*, pages 1044–1052. Wiley and Sons, 1985.

[12] W. P. Seering and V. Scheinman. *MECHANICAL DESIGN OF AN INDUSTRIAL ROBOT*, chapter 4, pages 29–79. Wiley and Sons, New York, 1985.

[13] M. Thomas, H. C. Yhan-Chou, and D. Tesar. Optimal actuator sizing for robotic manipulators based on local dynamic criteria. *ASME Journal of Mechanisms, Transmissions, and Automation in Design*, 107:163–169, June 1985.

[14] Drive-All Manufacturing Company, Harbor Beach, Michigan. *DRIVE-ALL INDUSTRIAL TRANSMISSIONS*, 1998.

[15] Turner Uni-Drive Company, Kansas City, Missouri. *TURNER UNI-DRIVE: MULTI-SPEED TRANSMISSIONS FOR INDUSTRY*, 1998.

[16] Andantex U.S.A. Inc., Wanamassa, New Jersey. *HEYNAU POWER TRANSMISSION*, 1998.

[17] M. I. Kamien and N. L. Schwartz. *DYNAMIC OPTIMIZATION*. North-Holland, 1986.

[18] Arthur E. Bryson and Yu-Chi Ho. *APPLIED OPTIMAL CONTROL: OPTIMIZATION, ESTIMATION, AND CONTROL*. Blaisell Publishing, 1969.

[19] Andrew P. Sage. *OPTIMUM SYSTEMS CONTROL*. Prentice-Hall, 1968.

[20] Robert Weinstock. *CALCULUS OF VARIATIONS*. Dover Publications, 1974.

[21] I. M. Gelfand and S. V. Fomin. *CALCULUS OF VARIATIONS*. Prentice-Hall, 1963.

[22] W. R. Hamel and T. C. Widner. Transmission-based electrical actuators: A concept for improving robot manipulator performance. In *IEEE International Conference on Robotics and Automation*, pages 2204–2211, Albuquerque, New Mexico, 1997.

[23] T. C. Widner and W. R. Hamel. Fundamental control concepts for implementation of transmission-based actuators in robotics and automation. In *IEEE International Conference on Robotics and Automation*, Leuven, Belgium, 1998.

[24] T. C. Widner and Hamel W. R. Control concepts for transmission based actuators in robotics. In *IEEE International Conference on Intelligent Robots and Systems*, Victoria, B.C., Canada, 1998.

[25] T. C. Widner and W. R. Hamel. A multi-speed transmission approach to electric actuation in robotics. Submitted to the IEEE/ASME Transactions on Mechatronics, 1999.

[26] F. S. Jamzadeh. *POWER TRANSMISSION OPTIMIZATION WITH AND WITHOUT ENERGY STORAGE.* Ph.D. dissertation, Mechanical Engineering, The University of Wisconsin, Madison, 1983.

[27] R. L. Norton. *DESIGN OF MACHINERY: AN INTRODUCTION TO THE SYNTHESIS AND ANALYSIS OF MECHANISMS AND MACHINES.* McGraw-Hill Book Co., 1992.

[28] J. D. Micklem. Modelling of the steel pushing v-belt continuously variable transmission. *Proceedings of the Institute of Mechanical Engineers*, 208(1):13–, 1994.

[29] J. D. Micklem. Belt torque loss in a steel v-belt continuously variable transmission. *Proceedings of the Institute of Mechanical Engineers*, 208(2):91–, 1994.

[30] M. Guebeli. Maximum transmission efficiency of a steel belt continuously variable transmission. *Journal of Mechanical Design*, 115(4):1044–1048, December 1991.

[31] Honda Civic HX CVT. Road and Track, April 1996. Page 61.

[32] H. Kim and J. Lee. Analysis of belt behavior and slip characteristics for a metal belt CVT. *Mechanism and Machine Theory*, 29(6):865–876, 1994.

[33] SwRI transmission technology section white papers, 1998. Website address: `http://www.swri.org/atts/whpapers/vartrans.htm`.

[34] Continuously variable transmissions. Mechanical Engineering, March 1991. Page 64.

[35] Is CVT the car transmission of the future? Mechanical Engineering, November 1994. N 11, Page 64.

[36] E. Markland. Dual-mode improves CVT efficiency. *Professional Engineering*, 113(3):27–28, July 1991.

[37] H. Tanaka and M. Eguchi. Stability of a speed ratio control servomechanism for a half toroidal traction drive CVT. *JSME International Journal Series III*, 36(1):135–, March 1993.

[38] H. Tanaka. Power transmission of a half toroidal traction drive CVT. *JSME International Journal*, 38(4), 1995.

[39] Hirohisa Tanaka et al. Half toroidal traction drive continuously variable power transmission for automobiles. *JSME Series C: Dynamics*, 38(4), 1995.

[40] M. Nakano. Dynamic characteristics of speed ratio control of the halt toroidal CVT for passenger cars. Proceedings of SAE. Paper No. 901761.

[41] Question and answer board, the Power Transmission Homepage, 1998. Website address: `http://www.powertransmission.com`.

[42] R. P. Jones, I. F. Kuriger, and M. T. G. Hughes. Modelling and simulation of an automotive powertrain incorporating a Perbury continuously variable transmission. *Proceedings of the Institution of Mechanical Engineers*, 1986.

[43] J. I. Frankel and M. Keyhani. A global time treatment for inverse heat conduction problems. *Journal of Heat Transfer*, 119:673–683, 1997.

[44] J. I. Frankel and M. Keyhani. A new approach for solving inverse solidification design problems. *Numerical Heat Transfer*, 30, Part B(2):161–178, 1996.

[45] J. I. Frankel and G. E. Osborne. A new time treatment for solving partial integro-differential equations of radiative transport. *IMA Journal of Numerical Analysis*, 19:91–103, 1999.

[46] T. J. Rivlin. *THE CHEBYSHEV POLYNOMIALS.* Wiley and Sons, New York, 1974.

[47] T. J. Rivlin. *AN INTRODUCTION TO THE APPROXIMATION OF FUNCTIONS.* Blaisell, London, 1969.

[48] E. W. Cheney. *INTRODUCTION TO APPROXIMATION THEORY.* McGraw-Hill, New York, 1966.

Appendices

Appendix A

Discrete Shifting: Angular Momentum Considerations

The following is a discussion concerning the validity (actually accuracy) of a few assumptions made in Chapter 3 during the development of the discrete-speed transmission model. It has been mentioned that (3.18) is only approximate. This discussion shows that the error in this approximation is negligible for the purposes of this work.

The essential assumptions (and approximations) in (3.18) can be summarized by

$$\frac{{\omega_m}^+}{{\omega_m}^-} = \frac{N_{j+1}}{N_j}, \quad (j = 1, 2, \ldots, n-1), \tag{A.1}$$

$$\frac{{\omega_{load}}^+}{{\omega_{load}}^-} = 1, \quad \text{(all shifts)}, \tag{A.2}$$

where superscripts $^-$ and $^+$ denote before and after the transmission shift, respectively.

By the conservation of angular momentum, the validity of these assumptions can be checked. Consider gear "j". The system angular momentum (before shift) can be written as follows:

$$\bar{H}^- = I_m \, {\omega_m}^- + I_{ext} \, {\omega_{load}}^- ; \tag{A.3}$$

The motor speed and load speed (during engagement of gear "j") is given by

$${\omega_m}^- = N_j \, {\omega_{load}}^- . \quad (j = 1, 2, \ldots, n). \tag{A.4}$$

Hence the system angular momentum before shift is explicitly given by:

$$\bar{H}^- = (I_m N_j + I_{ext})\, {\omega_{load}}^-, \quad (j = 1, 2, \ldots, n). \tag{A.5}$$

Similarly, the angular momentum after shift (gear "$j+1$") is given by:

$$\bar{H}^+ = (I_m N_{j+1} + I_{ext})\, {\omega_{load}}^+, \quad (j = 1, 2, \ldots, n-1). \tag{A.6}$$

Conservation of angular momentum demands that (A.5) and (A.6) be equal:

$$\bar{H}^- \equiv \bar{H}^+.$$

Combining (A.5) and (A.6) gives:

$$(I_m N_j + I_{ext})\, {\omega_{load}}^- = (I_m N_{j+1} + I_{ext})\, {\omega_{load}}^+, \tag{A.7}$$

from which directly comes

$$\frac{{\omega_{load}}^+}{{\omega_{load}}^-} = \frac{I_m N_j + I_{ext}}{I_m N_{j+1} + I_{ext}}. \tag{A.8}$$

It also follows that

$$\frac{{\omega_m}^+}{{\omega_m}^-} = \frac{N_{j+1}}{N_j}\left(\frac{I_m N_j + I_{ext}}{I_m N_{j+1} + I_{ext}}\right) \tag{A.9}$$

These expressions are approximated very closely by the assumptions of Chapter 3 unless the gears are widely separated (i.e. $N_{j+1} \ll N_j$). This is illustrated with an example.

The system parameters used for the motor and external inertia in this work are given by $I_m = 0.00004$ and $I_{ext} = 34.5$ ft-lb-sec^2, respectively. The gear spacings used throughout this work were bound by[1]:

$$\frac{N_{j+1}}{N_j} \in [0.5, 1). \tag{A.10}$$

[1]The upper bound is open because this discussion only concerns discrete-speed transmissions.

In Chapter 3, Section 3.3.4, the *DST* was shifted through five gears from a maximum reduction of around 500:1 to a minimum reduction of around 250:1. The five gears were used to keep the gear spacing down. Clearly, a worst case scenario is to shift the transmission over the same span of gear ratio in only *one* shift. So, considering a two-speed transmission ($j = 1, 2.$), the transmission bounds are given by $N_1 = 500$ and $N_2 = 250$. Using these values, (A.8) becomes

$$\frac{{\omega_{load}}^+}{{\omega_{load}}^-} = \frac{(0.0004)(500) + 34.5}{(0.0004)(250) + 34.5} \approx 1.0003, \quad \text{(assumed 1)}. \tag{A.11}$$

Similarly, (A.9) becomes

$$\frac{{\omega_m}^+}{{\omega_m}^-} = \frac{250}{500}\left(\frac{(0.0004)(500) + 34.5}{(0.0004)(250) + 34.5}\right), \approx 0.5001 \quad \text{(assumed 0.5)}. \tag{A.12}$$

Since this *is* a worst case scenario, clearly the assumptions of Chapter 3 are valid for the actuator comparative analyses of this work.

Appendix B

Joint-Level Model with Non-Linear Loading

B.1 Introduction

This research in fundamental robot actuator technology has involved the concept of incorporating multi-speed transmissions into electric servomotor drive systems. In particular, the research has focused on extending the performance capability of electric robot actuators by expanding the torque and speed range of the servomotors with a variable gear reduction strategy. With the variable loading and inertia conditions inherent to robot manipulator dynamics, the performance of variable speed-ratio robot actuators is difficult to predict on even an order-of-magnitude level. The governing equations for such actuators can become quite complex—even at the joint level. As a design tool, we would like to predict how various shifting strategies will affect joint-level performance for a manipulator.

This chapter demonstrates a method of solving the governing equation for an electric robot actuator that incorporates a continuously variable transmission. The shifting strategy is left open for various schemes in that this formulation will allow

a fundamental prediction of how the shifting strategy will affect the joint level performance. In particular, the results of this analysis will quantitatively determine the severity of variable dynamic loading (i.e. variable static torque in this case) on the overall response of the system.

A weighted residual scheme is chosen for the numerical solution for both accuracy and speed of convergence. The temporal variable will be treated in an elliptic fashion such that the inherent initial value problem is "transformed" or "converted" into a boundary value problem. In essence, the temporal variable is mapped from $t \in [0, t_{max}]$ to $\xi \in [-1, 1]$. This is of great interest and advantage in several types of problems including fracture mechanics, inverse solidification design problems, and heat transfer, because it introduces stability into otherwise ill-posed and unstable problems [43, 44, 45].

B.2 Problem Statement

A simple schematic of an electric actuator system is shown in Figure B.1. For a continuously variable transmission, the gear reduction, N, is a continuous function of time, $N(t)$. The effective inertia about the *joint* axis is given by:

$$I_{eff}(t) = I_{motor}N^2(t) + I_e, \quad t \geq 0, \tag{B.1}$$

where I_{motor} and I_e are the motor and external mass moments of inertia, respectively. For this analysis, we assume that the external inertia remains constant (i.e. constant downstream configuration). For a direct current (DC) motor under constant voltage

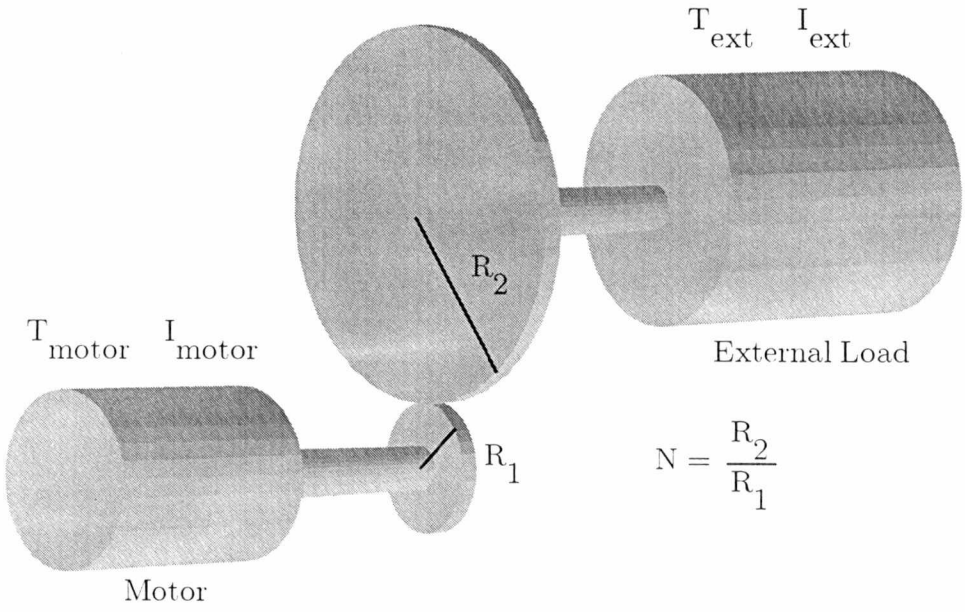

Figure B.1: Schematic of an electric actuator (repeated).

conditions, the effective driving torque about the motor axis is given by:

$$T_{eff}(t) = T_o N(t) \left[1 - \frac{N(t)\dot{\theta}(t)}{\omega_o} \right], \quad t \geq 0, \tag{B.2}$$

where T_o, and ω_o are the stall torque and no-load speed of the motor, respectively, and the dot denotes a derivative with respect to time. Here, $\theta(t)$ is the joint position. Assuming the load is being accelerated, a torque summation about the joint axis and some rearranging gives

$$\ddot{\theta}(t) + \left[\frac{T_o N^2(t)}{\omega_o I_{eff}(t)} \right] \dot{\theta}(t) + \frac{T_e}{I_{eff}(t)} \cos\left(\theta(t)\right) = \frac{T_o N(t)}{I_{eff}(t)}, \quad t \geq 0, \tag{B.3}$$

where T_e is the maximum external gravity torque associated with a fully horizontal arm. This nonlinear second order ordinary differential equation is subject to the initial conditions:

$$\theta(0) = \theta_i \tag{B.4}$$

$$\dot{\theta}(0) = \omega_i. \tag{B.5}$$

B.3 Problem Formulation

For numerical solution of (B.3), we will use a series method based on the collocation method using Chebyshev polynomials of the first kind as basis functions. Chebyshev polynomials have been shown to have the fastest convergence rate of all polynomial bases [46, 47, 48]. These polynomials are defined by the relation:

$$T_n(\xi) \equiv \cos(n \cos^{-1}(\xi)) \quad n = 0, 1, 2, \ldots \quad \xi \in [-1, 1]. \tag{B.6}$$

Since these polynomials are only defined over the range $[-1, 1]$, our first step is to map the temporal variable onto this domain. A maximum time is specified over which the response is to be evaluated, just as is done with a marching scheme such as Runge-Kutta. Denoting this maximum time by t_{max}, we introduce the mapping:

$$t = \lambda(1 + \xi), \quad t \in [0, t_{max}], \quad \xi \in [-1, 1], \tag{B.7}$$

where

$$\lambda \equiv \frac{t_{max}}{2}. \tag{B.8}$$

Note that this will map the temporal variable as if it were a *spatial* variable; the resulting transformed differential equation will look like a boundary value problem formulation. For clarity between the domains, we define:

$$\phi(\xi) \equiv \theta(t) = \theta(\lambda(1 + \xi)), \tag{B.9}$$

$$\hat{N}(\xi) \equiv N(t) = N(\lambda(1 + \xi)), \tag{B.10}$$

$$\hat{I}(\xi) \equiv I_{eff}(t) = I_{eff}(\lambda(1 + \xi)). \tag{B.11}$$

It follows that (B.3) becomes:

$$\frac{1}{\lambda^2}\frac{d^2\phi}{d\xi^2}(\xi)+\frac{1}{\lambda}\frac{T_o\hat{N}^2(\xi)}{\omega_o\hat{I}(\xi)}\frac{d\phi}{d\xi}(\xi)+\frac{T_e}{\hat{I}(\xi)}\cos\left(\phi(\xi)\right)=\frac{T_o\hat{N}(\xi)}{\hat{I}(\xi)},\quad \xi\in[-1,1]. \tag{B.12}$$

which simplifies to

$$\frac{d^2\phi}{d\xi^2}(\xi)+\beta(\xi)\frac{d\phi}{d\xi}(\xi)+\gamma(\xi)\cos\left(\phi(\xi)\right)=\delta(\xi),\quad \xi\in[-1,1], \tag{B.13}$$

where we have defined

$$\beta(\xi)\equiv\frac{\lambda T_o\hat{N}^2(\xi)}{\omega_o\hat{I}(\xi)} \tag{B.14}$$

$$\gamma(\xi)\equiv\frac{\lambda^2 T_e}{\hat{I}(\xi)} \tag{B.15}$$

$$\delta(\xi)\equiv\frac{\lambda^2 T_o\hat{N}(\xi)}{\hat{I}(\xi)}. \tag{B.16}$$

Equation (B.13) is subject to the initial conditions

$$\phi(-1)=\theta_i \tag{B.17}$$

$$\frac{d\phi}{d\xi}(-1)=\omega_i. \tag{B.18}$$

B.4 Method of Solution

We assume the solution of (B.13) is of the form:

$$\phi(\xi)=\sum_{m=0}^{\infty}a_m T_m(\xi),\quad \xi\in[-1,1], \tag{B.19}$$

where $T_m(\xi)$ are Chebyshev Polynomials of the first kind and the $\{a_m\}_{m=0}^{\infty}$ are the unknown coefficients. In practice we must truncate the series to a finite number of

terms, say $m = 0, 1, 2, \ldots, N$ such that we retain $N + 1$ terms. This *approximate* series becomes

$$\phi(\xi) \approx \phi^{N+1}(\xi) = \sum_{m=0}^{N+1} a_m^{N+1} T_m(\xi), \quad \xi \in [-1, 1]. \tag{B.20}$$

Here, the superscript denotes the number of terms retained in the truncated series. Clearly, the $\{a_m^{N+1}\}_{m=0}^{N+1}$ coefficients closely resemble the $\{a_m\}_{m=0}^{\infty}$ coefficients as N becomes large.

B.4.1 Elimination of Boundary Error

Here, we will release terms from the series and introduce the boundary conditions. We do this such that NO ERROR is introduced into the approximate solution at the boundary. Releasing the first term ($m = 0$) from (B.20) and applying boundary condition (B.17) gives

$$a_0 = \theta_i + \sum_{m=1}^{N+1} (-1)^{m+1} a_m. \tag{B.21}$$

Similarly, we release the second term and apply boundary condition (B.18) to get

$$a_1 = \omega_i + \sum_{m=2}^{N+1} (-1)^m m^2 a_m. \tag{B.22}$$

Using (B.21) and (B.22), the approximate solution can be represented as

$$\phi^N(\xi) = \theta_i + (1+\xi)\omega_i + \sum_{k=1}^{N} a_{k+1}^N \left[(-1)^k + (k+1)^2 (-1)^{k+1} (1+\xi) + T_{k+1}(\xi) \right], \tag{B.23}$$

where we have re-indexed such that the summation starts at one by letting $k = m - 1$. Finally, this can be written more compactly as

$$\phi^N(\xi) = \theta_i + (1+\xi)\omega_i + \sum_{k=1}^{N} C_k^N \Psi_k(\xi), \quad \xi \in [-1, 1], \tag{B.24}$$

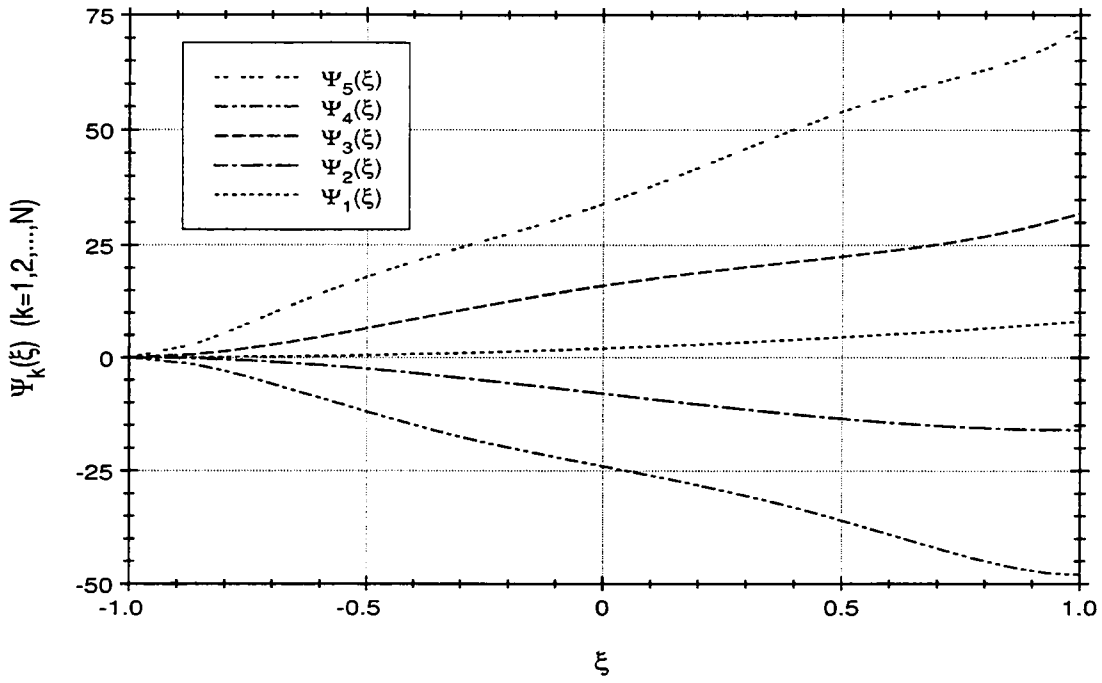

Figure B.2: Plot of the first 5 trial functions, $\Psi_k(\xi), \quad k = 1, 2, \ldots, 5$.

where we have defined

$$C_k^N \equiv a_{k+1}^N \tag{B.25}$$

$$\Psi_k(\xi) \equiv (-1)^k + (k+1)^2(-1)^{k+1}(1+\xi) + T_{k+1}(\xi), \quad \xi \in [-1, 1]. \tag{B.26}$$

The functions $\{\Psi_k(\xi)\}_{k=1}^N$ are the *trial functions* for this problem. Note that these functions satisfy the homogeneous version of the boundary conditions. As a consequence of this, the approximation solution has *zero error* at the boundary for all possible values of the expansion coefficients $\{C_k^N\}_{k=1}^N$ as desired. Figure B.2 shows a plot of the trial functions corresponding to $k = 1, 2, \ldots, 5$.

B.4.2 Explicit Expression for the Residual Function

The differential equation (B.13) can be written as:

$$\frac{d^2\phi}{d\xi^2}(\xi) + \beta(\xi)\frac{d\phi}{d\xi}(\xi) + \gamma(\xi)\cos\left(\phi(\xi)\right) - \delta(\xi) = 0, \quad \xi \in [-1,1]. \tag{B.27}$$

When the approximate solution (and its derivatives) are used, this becomes:

$$\frac{d^2\phi^N}{d\xi^2}(\xi) + \beta(\xi)\frac{d\phi^N}{d\xi}(\xi) + \gamma(\xi)\cos\left(\phi^N(\xi)\right) - \delta(\xi) \approx 0, \quad \xi \in [-1,1]. \tag{B.28}$$

Since equation (B.28) is in terms of the approximate solution $\phi^N(\xi)$, the equality therein emphatically *must* be approximate as indicated. Introduction of a *residual function*, $R_N\left(\phi^N(\xi)\right)$, allows use of a true equality sign....

$$\frac{d^2\phi^N}{d\xi^2}(\xi)+\beta(\xi)\frac{d\phi^N}{d\xi}(\xi)+\gamma(\xi)\cos\left(\phi^N(\xi)\right)-\delta(\xi) = R_N\left(\phi^N(\xi)\right), \quad \xi \in [-1,1]. \tag{B.29}$$

Expressions for the derivative terms in (B.29) are obtained from the approximate solution, (B.28). The first derivative is given by

$$\frac{d\phi^N}{d\xi}(\xi) = \omega_i + \sum_{k=1}^{N} C_k^N \Delta_k(\xi), \quad \xi \in [-1,1], \tag{B.30}$$

where

$$\Delta_k(\xi) \equiv (k+1)^2(-1)^{k+1} + (k+1)\left[\frac{\xi T_{k+1}(\xi) - T_{k+2}(\xi)}{1-\xi^2}\right], \quad \xi \in [-1,1]. \tag{B.31}$$

Similarly, the expression for the second derivative is

$$\frac{d^2\phi^N}{d\xi^2}(\xi) = \sum_{k=1}^{N} C_k^N \Omega_k(\xi), \quad \xi \in [-1,1], \tag{B.32}$$

where

$$\Omega_k(\xi) \equiv \frac{k+1}{(1-\xi^2)^2}\left[\left(\xi^2(k+2)+1\right)T_{k+1}(\xi) - \xi(2k+5)T_{k+2}(\xi) + (k+2)T_{k+3}(\xi)\right]. \tag{B.33}$$

Using (B.23), (B.30), and (B.32) in (B.29) gives

$$\sum_{k=1}^{N} C_k^N \Omega_k(\xi) + \beta(\xi)\left[\omega_i + \sum_{k=1}^{N} C_k^N \Delta_k(\xi)\right] + \gamma(\xi)\cos\left[\theta_i + (1+\xi)\omega_i + \sum_{k=1}^{N} C_k^N \Psi_k(\xi)\right] - \delta(\xi) = R_N\left(\phi^N(\xi)\right) \quad \text{(B.34)}$$

In order to make (B.34) more compact, define the following terms:

$$\sigma\left(\xi, \left\{C_k^N\right\}_{k=1}^{N}\right) \equiv \omega_i\beta(\xi) + \gamma(\xi)\cos\left[\theta_i + (1+\xi)\omega_i + \sum_{r=1}^{N} C_r^N \Psi_r(\xi)\right] - \delta(\xi), \quad \text{(B.35)}$$

$$\mu_k(\xi) \equiv \Omega(\xi) + \beta(\xi)\Delta_k(\xi), \quad \xi \in [-1,1]. \quad \text{(B.36)}$$

Please note that r in (B.35) is simply a dummy counter. Using both (B.35) and (B.36), (B.34) can be written in the following concise form:

$$R_N\left(\phi^N(\xi)\right) = \sum_{k=1}^{N} C_k^N \mu_k(\xi) + \sigma\left(\xi, \left\{C_k^N\right\}_{k=1}^{N}\right), \quad \xi \in [-1,1]. \quad \text{(B.37)}$$

Equation (B.37) is the desired explicit expression for the residual function.

B.4.3 Collocation Statement

Equation (B.37) represents the residual function that allows the use of an equality sign in the approximate form of the differential equation, (B.29). Since our desired end result is to have the solution to (B.37) closely approximate the analytically unknown solution to (B.27), we must require that the residual function $R_N\left(\phi^N(\xi)\right)$ be minimized in some sense. That is, we wish to determine the coefficients $\{C_k^N\}_{k=1}^{N}$ in such a manner that some measure of the residual is small. A systematic way of expressing this is to require that the following orthogonality condition holds [46, 47]:

$$\left\langle R_N\left(\phi^N(\xi)\right), \psi_j(\xi)\right\rangle_{w(\xi)} = 0, \quad j = 1, 2, \ldots, N. \quad \text{(B.38)}$$

Equation (B.38) demands that the residual function $R_N\left(\phi^N(\xi)\right)$ and a *test function* $\psi_j(\xi)$ be orthogonal with respect to the *weight function*, $w(\xi)$ on the given interval. The particular choice of the test and weight functions indicate the particular weighted residual method. Here, we will use the *Method of Collocation.*

In the Collocation Method, the residual function is required to be identically zero at pre-defined locations called *collocation points.* For this method, the test function is chosen to be the Dirac delta function (i.e. $\psi(\xi) \equiv \delta(\xi - \xi_j)$, $j = 1, 2, \ldots, N.$), with a corresponding weight function of unity (i.e. $w(\xi) \equiv 1$). Using these choices for $\psi(\xi)$ and $w(\xi)$, (B.38) becomes:

$$\left\langle R_N\left(\phi^N(\xi)\right), \delta(\xi - \xi_j)\right\rangle_1 = 0, \quad j = 1, 2, \ldots, N. \tag{B.39}$$

Equation (B.39) is the general form of the *collocation statement.* We now make use of this statement for our problem at hand by first defining our collocation points using the open rule:

$$\xi_j = \cos\left(\frac{(2j-1)\pi}{2N}\right), \quad j = 1, 2, \ldots, N. \tag{B.40}$$

Substituting (B.37) into (B.39) we find

$$\left\langle \sum_{k=1}^{N} C_k^N \mu_k(\xi) + \sigma\left(\xi, \left\{C_k^N\right\}_{k=1}^{N}\right), \delta\left(\xi - \xi_j\right)\right\rangle_1 = 0, \quad j = 1, 2, \ldots, N. \tag{B.41}$$

It follows that

$$\left\langle \sum_{k=1}^{N} C_k^N \mu_k(\xi), \delta\left(\xi - \xi_j\right)\right\rangle_1 = -\left\langle \sigma\left(\xi, \left\{C_k^N\right\}_{k=1}^{N}\right), \delta\left(\xi - \xi_j\right)\right\rangle_1, \quad j = 1, 2, \ldots, N. \tag{B.42}$$

Recalling the "sifting" nature of the Dirac delta function within an inner product, this gives

$$\sum_{k=1}^{N} C_k^N \mu_k\left(\xi_j\right) = -\sigma\left(\xi_j, \left\{C_k^N\right\}_{k=1}^{N}\right), \quad j = 1, 2, \ldots, N. \tag{B.43}$$

This can be written is matrix form as:

$$\begin{bmatrix} \mu_1(\xi_1) & \mu_2(\xi_1) & \cdots & \mu_N(\xi_1) \\ \mu_1(\xi_2) & \mu_2(\xi_2) & \cdots & \mu_N(\xi_2) \\ \vdots & \vdots & \vdots & \vdots \\ \mu_1(\xi_N) & \mu_2(\xi_N) & \cdots & \mu_N(\xi_N) \end{bmatrix} \begin{Bmatrix} C_1^N \\ C_2^N \\ \vdots \\ C_N^N \end{Bmatrix} = \begin{Bmatrix} -\sigma\left(\xi_1, \left\{C_k^N\right\}_{k=1}^N\right) \\ -\sigma\left(\xi_2, \left\{C_k^N\right\}_{k=1}^N\right) \\ \vdots \\ -\sigma\left(\xi_N, \left\{C_k^N\right\}_{k=1}^N\right) \end{Bmatrix} \tag{B.44}$$

Equation (B.44) is of the form

$$[A]\left\{C_k^N\right\}_{k=1}^N = \{f\}, \tag{B.45}$$

where $[A]$ is an $N \times N$ invertible square matrix. Once the matrix $[A]$ is formed, its inverse yields the expansion coefficients by use of the relation

$$\left\{C_k^N\right\}_{k=1}^N = [A]^{-1}\{f\}. \tag{B.46}$$

Note that $\{f\}$ is *dependent* upon (i.e. $\{f\}$ is a *function of*) the expansion coefficients $\{C_k^N\}_{k=1}^N$. This is how the nonlinearity of the original differential equation shows up in the solution formulation. If the equation were a *linear* ordinary differential equation, then "$\{f\}$" would be independent of the expansion coefficients and the problem could be solved in one fatal swoop by inverting the matrix $[A]$ and using (B.46). However, with the nonlinearity present, we must form some initial guess and solve the problem iteratively. There are generally ways of conjuring intelligent initial guesses such that the solution converges quickly. In any case, we solve (B.46) iteratively until the maximum change in any of the N expansion coeffiecients falls below some set convergence criteria. Once the expansion coefficients are found, the approximate solution for $\phi^N(\xi)$ is directly built using (B.23). Finally, the solution for $\theta^N(t)$ is obtained via the transform

$$\theta^N(t) = \theta^N(\lambda(1+\xi)) = \phi^N(\xi) \quad \xi \in [-1,1], \quad t \in [0, t_{max}]. \tag{B.47}$$

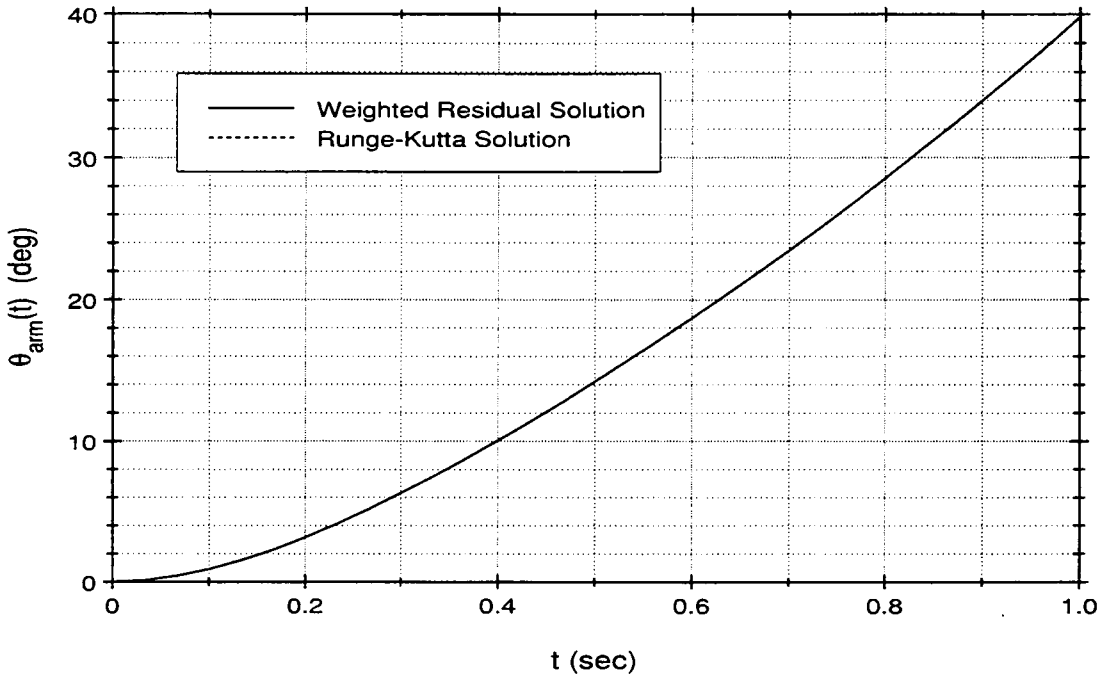

Figure B.3: Weighted residual and R-K solutions for $\theta^N(t)$. $t_{max} = 1$ second.

B.5 Results

The solutions for $\theta^N(t)$ are shown in Figures B.3–B.5. Each plot also shows a numerical solution obtained with a 4th-order Runge-Kutta method. The solutions are virtually identical on the plots. Plots of the corresponding residual functions, $R_N\left(\phi^N(\xi)\right)$, for the intermediate variable $\phi^N(\xi)$ are shown in Figures B.6–B.8. Each plot shows the number of terms, N, that were retained in the series solution. These numbers were chosen such that the resulting residual functions were small. Note that in all cases, the number of "zeroes" (corresponding to the collocation points) in the residual plot corresponds directly to the number of terms retained in the series. It is clear that, conceptually, in the limit as the number of retained terms increases, the residual is eventually forced to be zero everywhere. Physically, however, the number of terms

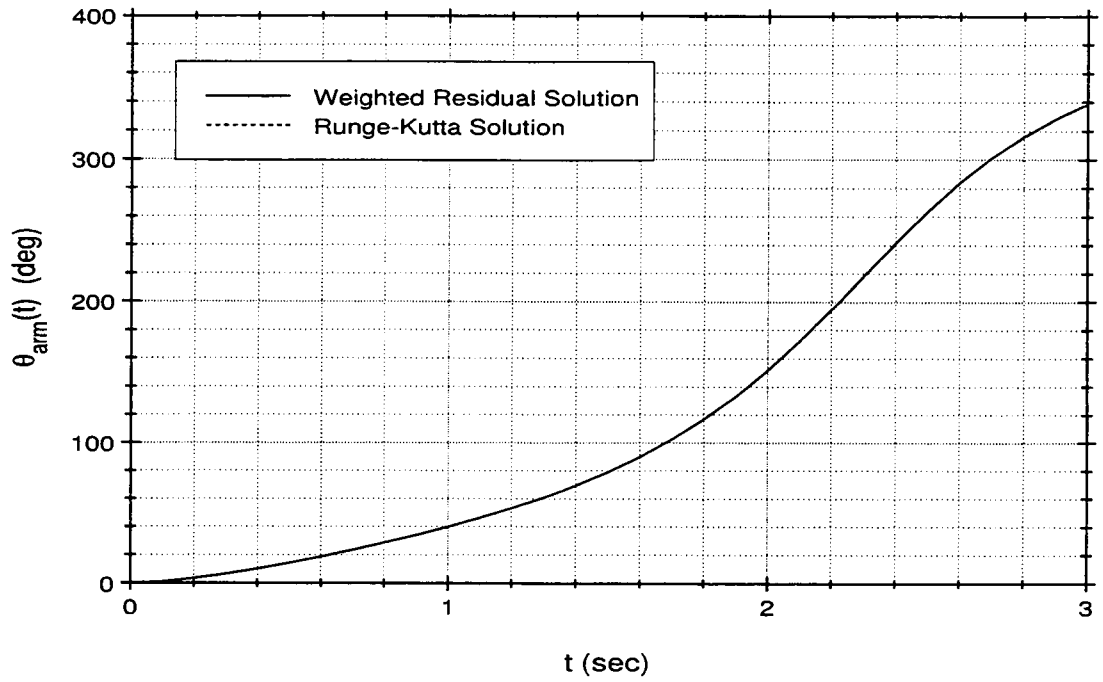

Figure B.4: Weighted residual and R-K solutions for $\theta^N(t)$. $t_{max} = 3$ seconds.

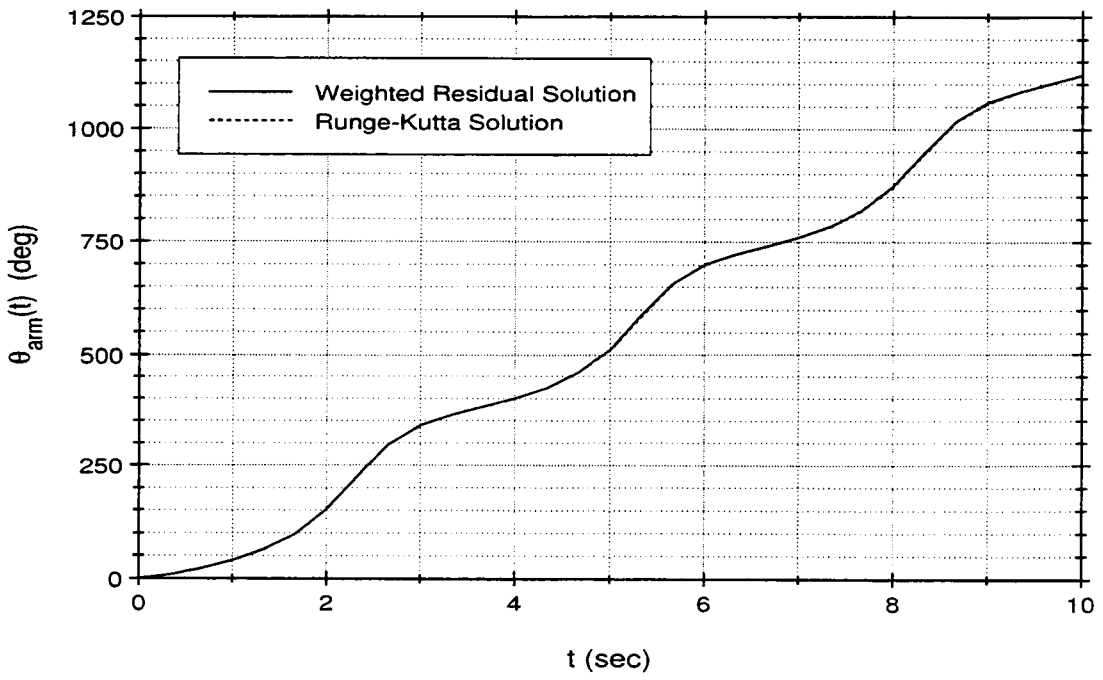

Figure B.5: Weighted residual and R-K solutions for $\theta^N(t)$. $t_{max} = 10$ seconds.

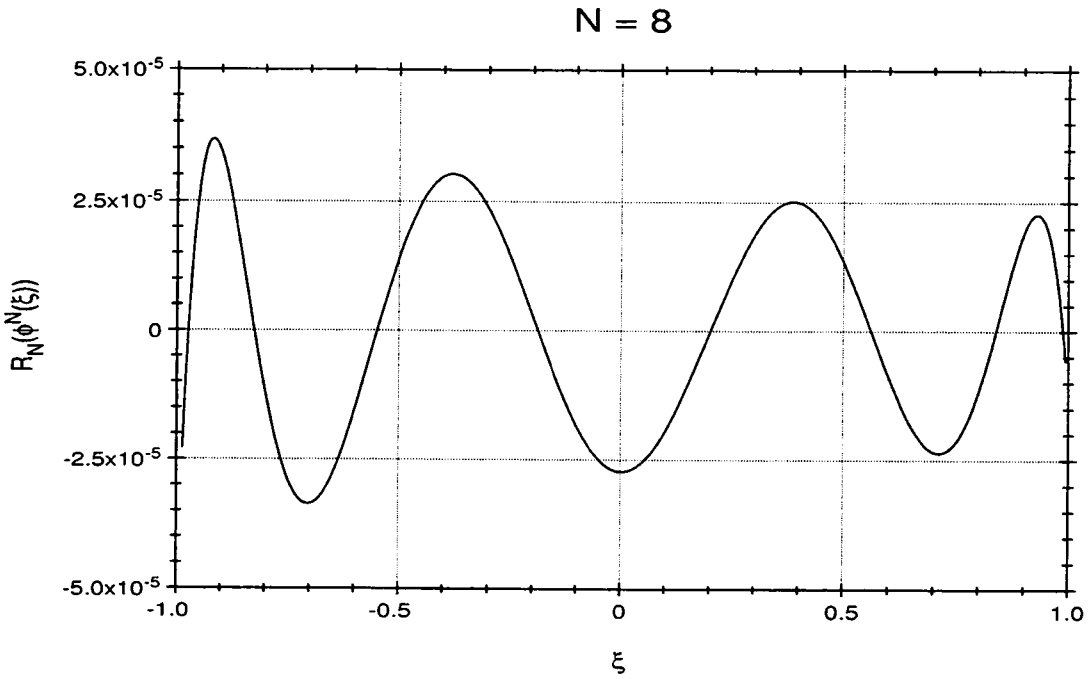

Figure B.6: Plot of residual function, $R_N\left(\phi^N(\xi)\right)$, for $t_{max} = 1$ second.

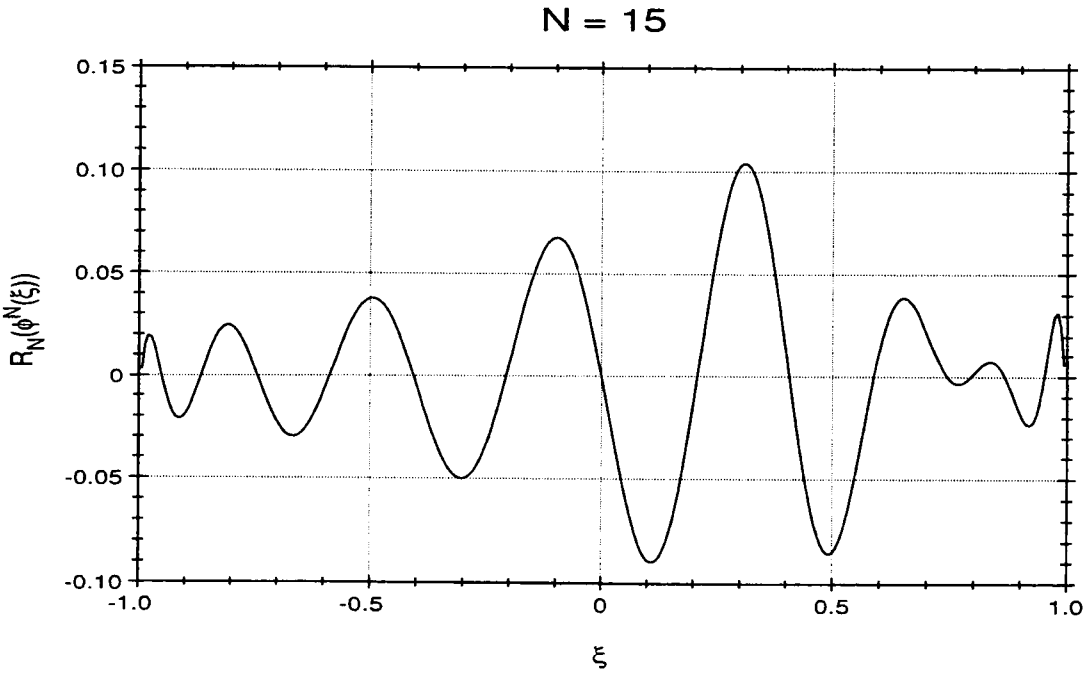

Figure B.7: Plot of residual function, $R_N\left(\phi^N(\xi)\right)$, for $t_{max} = 3$ seconds.

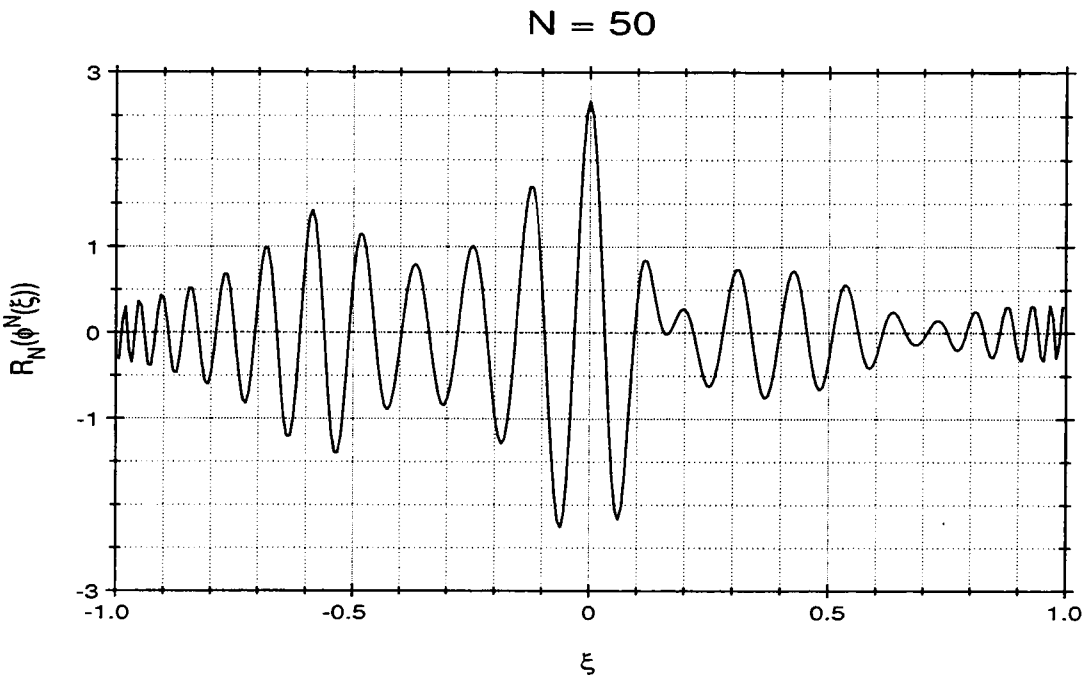

Figure B.8: Plot of residual function, $R_N\left(\phi^N(\xi)\right)$, for $t_{max} = 10$ seconds.

is limited due to round-off error. For example, if we attempt to retain, say, 500 terms, when only, say, 100 are needed, then the coeffiecient calculations are compromised in trying to establish non-zero coefficients for the 400 "redundant" terms. Any non-zero, no matter how small, coefficients—if they are not required in reality— will inherently lead to round-off error in the end. Hence, the analyst should be content and retain no more terms when the residual plot is "sufficiently" small throughout the domain.

The overall result of this analysis has shown us that the nonlinearity associated with a shoulder pitchup maneuver having a variable gravitational torque does not have severe effects on the response times of the arm—especially for reasonable pitch angles, say $\theta_{arm} \in [0, 90°]$. However, for general arm configurations with several joints moving at once (hence variable loading *and* inertia), this method could be of use in investigating the arm dynamics and their effect on the overall joint trajectories.

Appendix C

CVT Shifting Strategy for a Desired Trajectory

C.1 Matching the *ASM* Baseline Performance

In Section 3.1, we outlined the analysis of a fixed-reduction actuator (*FRA*). An expression for the motor speed vs. time was derived. For a *FRA*, the joint speed is related to the motor speed by the (fixed) gear reduction ratio, N. In this section, we wish to calculate a *variable* gear reduction (as a function of maneuver time) that will achieve the same joint speed (and, hence, position) response as the baseline case. In essence, this result will show how a *CVT* could be used in conjunction with a smaller motor to allow a distributed actuator manipulator to achieve identical performance to the baseline model.

C.1.1 Calculation of the Gear Reduction as a Function of Time

For the *FRA*, we saw that the differential equation (3.5) could be solved by elementary methods to give an expression for the motor speed as a function of time (see equation

(3.7)). For a *FRA*, the *joint* speed is of the exact same form, differing only by a factor of the (fixed) gear reduction, N (See (3.26) with $n = 1$). For a summation of torques about the *joint* axis, the governing differential equation is quite similar and given by

$$\frac{d\omega(t)}{dt} + \left(\frac{T_o}{I_{eff}\omega_o}\right)\omega(t) = \frac{T_o - T_{eff}}{I_{eff}N} \tag{C.1}$$

The ASM joint speed can be written as:

$$\omega_{asm}(t) = \left(\frac{\omega_i - \Omega}{N_{ASM}}\right)\exp\left(\frac{-t}{\tau_{ASM}}\right) + \frac{\Omega}{N_{ASM}} \tag{C.2}$$

A time derivative gives the joint acceleration of the *ASM* vs. time:

$$\frac{d\omega_{ASM}(t)}{dt} = \left(\frac{\Omega - \omega_i}{N_{ASM}\tau_{ASM}}\right)\exp\left(\frac{-t}{\tau_{ASM}}\right) \tag{C.3}$$

Making use of (C.1) through (C.3), we obtain an algebraic (quadratic) equation for the gear reduction as a function of time that is needed such that the transmission-based system matches the baseline *ASM* performance:

$$\left[I_{motor}\frac{d\omega_{ASM}(t)}{dt} + T_o\left(\frac{\omega_{ASM}(t)}{\omega_o}\right)\right]N^2(t) - T_oN(t) + I_{ext}\frac{d\omega_{ASM}(t)}{dt} + T_{ext} = 0. \tag{C.4}$$

This equation can be solved numerically at each time step for the gear reduction $N(t)$. Recall that *all* parameters to be used in (C.1) other than those shown in (C.2–C.3) are associated with the smaller *TBA* servomotor. The resulting curve shows the gear reduction vs. time that, when used in conjunction with the smaller motor and a distributed actuator layout, will yield an equivalent response to the current *ASM*.

C.1.2 Sample Result for Calculation of Gear Reduction

Figure C.1 shows the gear reduction vs. time that allows the distributed actuator layout to match the *ASM* performance shown earlier. Again, the curve only represents

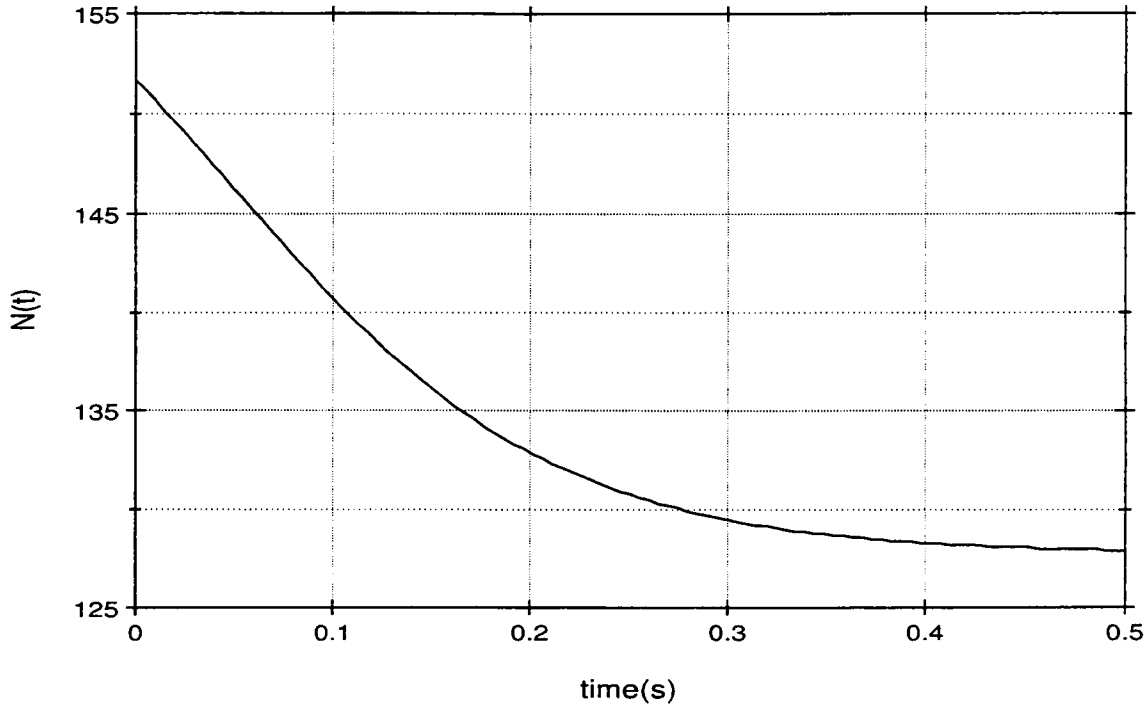

Figure C.1: *CVT* gear reduction vs. time needed for equivalent joint motion.

the time period associated with the acceleration portion of the motion. In essence, if a *CVT* is to be used with the actuator, this curve represents how the transmission must alter the gear reduction over the maneuver. If a discretely geared transmission is to be used, then it should, within the bounds of the gear span, approximate this curve as closely as possible. Even if a discretely geared transmission is to be used, this curve offers some valuable information towards shifting strategy.

C.2 The Transmission's Job: A Closer Look

Some physical insight as to the transmission's job can be obtained via equation (C.4). After some studying, equation (C.4) has an inherent small parameter as the coefficient

of the square term; below, we denote the small parameter as ϵ:

$$\underbrace{\left[I_{motor}\frac{d\omega_{ASM}(t)}{dt}+T_o\left(\frac{\omega_{ASM}(t)}{\omega_o}\right)\right]}_{\epsilon}N^2(t)-T_oN(t)+I_{ext}\frac{d\omega_{ASM}(t)}{dt}+T_{ext}=0. \quad \text{(C.5)}$$

To see that the coefficient is "small", first note that the second term in ϵ is *very* small for all time t, since it is essentially a ratio of the *joint* speed to to the (*theoretical*) free motor speed. Hence, this term is essentially always close to zero. The first term represents the dynamic torque contribution from the motor inertia I_{motor} reflected through the gear train; even for high accelerations, due to the low amount of inertia in the rotor, this term is also "small". Hence, we conclude that the entire leading coefficient is a relatively small term.

As $\epsilon \rightarrow 0$, we find:

$$N(t) \rightarrow \frac{I_{ext}\frac{d\omega_{ASM}(t)}{dt}+T_{ext}}{T_o} \quad \text{(C.6)}$$

Examination of this equation shows that the CVT alters the gear reduction N in such a way that the following balance occurs: (First Order: $\epsilon \rightarrow 0$)

$$\underbrace{N(t)T_o}_{\text{Reflected Maximum Motor Torque}} \rightarrow \underbrace{I_{ext}\frac{d\omega_{ASM}(t)}{dt}+T_{ext}}_{\text{Total Dynamic Torque}} \quad \text{(C.7)}$$

Hence, to first order, the transmission essentially performs a dynamic torque balance at the joint. And, as mentioned earlier, the rest of the transmission's work essentially continues this torque balance with the effects of the rotor inertia thrown into the mix.

Appendix D

Selecting a Motor: A Power Constraint

D.1 Derivation of the Constraint

Consider the following effective system: A motor with a fixed gear reduction between itself and its external loading has the following equivalent external torque and inertia about the *motor* axis:

$$T_{eff} = \frac{T_{ext}}{N} \tag{D.1}$$

$$I_{eff} = \frac{I_{ext}}{N^2} + I_{motor} \tag{D.2}$$

As we have seen, the for a constant voltage control situation, the motor has the following linear torque-speed relationship:

$$T_m(\omega) = T_o \left(1 - \frac{\omega}{\omega_o}\right). \tag{D.3}$$

We wish to find an expression that assists motor selection for use with a system of this type.

When selecting a motor, the *bottom line* (and "64 dollar") question is whether or not the motor is capable of driving the load while meeting some sort of performance

criteria. This criteria, in most cases, asks that the load be driven at some specified speed. We seek a constraint on the motor characteristics as a function of the loading and speed requirements that can be used as an aid during motor selection.

Specifications: Let the specified (i.e. demanded by design requirements) maximum joint speed and maximum external loading be denoted by ω_{joint} and T_{ext}, respectively. That is, here:

$$\omega_{joint} \equiv \text{required maximum joint speed}$$

$$T_{ext} \equiv \text{specified maximum external loading at the joint.}$$

Further, denote the maximum attainable motor speed (for the given external loading by Ω:

$$\Omega \equiv \text{maximum motor speed for a given loading.}$$

The speed response of a motor using a fixed amount of reduction is given by the following equation assuming zero initial conditions for position and speed:

$$\omega_{motor}(t) = \underbrace{(1-\beta)\,\omega_o}_{\Omega}\left[1 - \exp\frac{-t}{\tau}\right], \tag{D.4}$$

where we have defined:

$$\beta \equiv \text{effective torque ratio} = \frac{T_{ext}}{NT_o},$$

$$\tau \equiv \text{motor speed time constant} = \frac{I_{eff}\omega_o}{T_o}.$$

We see that the maximum attainable motor speed is given by:

$$\Omega = \left(1 - \frac{T_{ext}}{NT_o}\right)\omega_o. \tag{D.5}$$

Since we wish that this maximum motor speed correspond (at least) to our specified joint speed, we must require that

$$\omega_{joint} \stackrel{set}{=} \frac{\Omega}{N} = \left(1 - \frac{T_{ext}}{NT_o}\right)\frac{\omega_o}{N}. \tag{D.6}$$

Rearranging gives us the following:

$$N^2 - \left(\frac{\omega_o}{\omega_{joint}}\right)N + \left(\frac{T_{ext}\omega_o}{T_o\omega_{joint}}\right) = 0, \tag{D.7}$$

which is a quadratic equation for the transmission ratio, N. Define:

$$\omega^* \equiv \frac{\omega_o}{\omega_{joint}} = \text{“motor to joint speed ratio”}$$
$$T^* \equiv \frac{T_o}{T_{ext}} = \text{“motor to joint torque ratio”}.$$

Using these definitions, the equation (D.7) becomes:

$$N^2 - \omega^* N + \frac{\omega^*}{T^*} = 0. \tag{D.8}$$

The roots of (D.8) are real if and only if:

$$\omega^{*2} - \frac{4\omega^*}{T^*} \geq 0, \tag{D.9}$$

or,

$$\omega^* T^* \geq 4,$$
$$\frac{T_o\omega_o}{T_{ext}\omega_{joint}} \geq 4. \tag{D.10}$$

Note that this result is an absolute constraint on the motor parameters ω_o and T_o. If (D.10) does not hold, then the motor must be eliminated from consideration for the application. Furthermore, if no available motor can meet this constraint, then an

alternative actuation scheme such as hydraulics must be used. It must be stressed that *no gear reduction strategy can overcome this constraint.*

We now seek to show, from a physical standpoint, the origin of the peculiar "factor of 4" on the right hand side of (D.10). We have seen that the joint speed is defined by the relation:

$$\omega_{joint} = \left[1 - \frac{T_{ext}}{NT_o}\right] \frac{\omega_o}{N}. \tag{D.11}$$

Clearly, the joint speed is a function of the gear reduction. We wish to *eliminate* (from consideration) motors that cannot, for *any* amount of gear reduction, drive the load at a specified joint speed. The limiting case occurs when the maximum motor speed corresponds to the speed which, when transmitted through the gear reduction, gives the desired joint speed. In other words, motors on the threshold of being incapable of meeting the design requirements correspond to those whose maximum speed yields the required joint speed.

Hence, here we ask for the (single-valued) gear reduction, N that maximizes the joint speed. We find this by differentiating (D.11) with respect to N and setting the result to zero:

$$\begin{aligned} \omega_{joint} &= \frac{\omega_o}{N} - \frac{T_{ext}\omega_o}{T_o N^2} = \omega_{joint}(N) \\ \frac{d\omega_{joint}(N)}{dN} &= \frac{-\omega_o}{N^2} + \frac{2T_{ext}\omega_o}{T_o N^3} \stackrel{set}{=} 0. \end{aligned} \tag{D.12}$$

Since N is strictly non-zero here, this can be reduced to

$$N^* = \frac{2T_{ext}}{T_o}. \tag{D.13}$$

This is the gear reduction value that maximizes the joint speed. If this maximum speed corresponds to the required joint speed, then clearly the motor just barely meets the design criteria.

Now, we show that this case corresponds to the equality in (D.10). In other words, we wish to show that the above value of N renders

$$\frac{T_o\omega_o}{T_{ext}\omega_{joint}} = 4, \tag{D.14}$$

...which furthermore offers evidence that this ratio corresponds to a constraint on the motor specifications.

In general, the following is true:

$$\omega_{joint} = \frac{\omega_{motor}}{N}.$$

Replacing N by the value in (D.13) gives

$$\omega_{joint} = \frac{T_o\omega_{motor}}{2T_{ext}}. \tag{D.15}$$

In the derivation for the gear reduction, we were maximizing the joint speed. We also know, however, that joint speed is maximized when the motor is at maximum speed, Ω. Thus, we use the expression for N to back out an expression for the motor speed as follows.

$$\begin{aligned}\omega_m \stackrel{set}{=} \Omega &= \left(1 - \frac{T_{ext}}{NT_o}\right)\omega_o \\ &= \frac{\omega_o}{2}.\end{aligned} \tag{D.16}$$

So, the motor reaches precisely half of its no-load speed. It is easily shown that use of (D.13) and (D.16) in (D.11) verifies (D.10) for the equality.

D.2 Interpretation of the Result

If the motor is barely capable of metting the design requirements, then the only possibility for success occurs if we run the motor with the optimum gear reduction.

If this gear reduction is used, we have seen that the equality in (D.10) holds. This corresponds to a double root of the quadratic for N, equation (D.7), since the radical is zero.

On the other hand, if the motor can easily meet the specifications, we may not be forced to run the motor at the optimum gear reduction. If this is the case, the motor has the capability of surpassing the required joint speed, if desired. In any case, this corresponds to a situation where the (D.7) has two distinct, real roots; the lower is the only one that we are interested in, since it corresponds to the minimum gear reduction that can be used for the system[1]. Consequences of this result are twofold: First, equation (D.10) represents an absolute constraint on motor selection. Specifically, any motor not satisfying the constraint has no possible chance (theoretically or physically) of meeting the joint torque/speed design requirements. Also, the equality in (D.10) is really only academic and of no use. A motor satisfying the equality in (D.10) only reaches the desired joint speed "when" the motor reaches its maximum speed. The motor speed response, (D.4), shows that mathematically this "never" occurs. Thus, in real world problems we not only omit the equality but stay sufficiently far away from it such that our actuator can easily meet the specifications.

The second consequence applies after the motor selection process has taken place and is to be used with a multi-speed transmission. Once the motor is chosen, the *minimum* usable gear reduction can be calculated by taking the smaller root of (D.7). This root corresponds to the minimum gear ratio value that can be used in the multi-speed transmission and still meet the design requirements. As with motor selection, the value should be selected with some form of a factor of safety (for lack of a better

[1]The larger root yields the case where the motor spins at high speed and the large gear reduction gives the desired joint speed.

term) which accounts for the fact that the constraint derivations were based on an ideal model.

The constraint (D.10) can be rewritten to physically show why the gear reduction value is optimum[2]:

$$\frac{T_o}{2}\frac{\omega_o}{2} > T_{ext}\omega_{joint}. \tag{D.17}$$

In words, (D.17) reveals a fundamental power statement: *the motor torque-speed product at maximum power must exceed the joint torque-speed product.* In other words, if the motor cannot satisfy the joint torque-speed requirement while itself sitting at maximum power, there is *NO* gear reduction strategy that will achieve the desired joint response. This result reaffirms that the motor output itself is simply a torque-speed product, and a multi-speed transmission simply allows a trade-off of speed capacity for torque-capacity within the available motor power. Understanding this is paramount to the *TBA* idea: transmissions allow us to *manipulate* the torque-speed product to our advantage. Selecting a motor that meets the design requirements as outlined in this chapter is a fundamental first step to implementing the idea.

[2]Here the equality is omitted

VITA

Chris Widner was born on December 8, 1969 in Fayetteville, Tennessee. The youngest (by quite a stretch) of four children, Chris was somewhat like an only child in that his older siblings were already off to college during his childhood. Perhaps his parents had finally solved the mystery of exactly how to efficiently raise a child and wanted one last shot at proving their conjectures. Being raised alone had many particular advantages. Chris's siblings felt that by the time he came into the world that the parents had softened; to this day, they claim that he had it easier than they did. Chris claims that he simply caused his parents the fewest headaches. Opinions vary, but he grew up very happily.

As a child, pretty much anything Chris could get his hands on would set his little brain into motion. His brain developed at a much faster rate than the rest of him. He came into the world at a whopping 3 *lbs* and 14 *ounces*. He could talk—even lecture—way before he could walk. He spent so much time talking to everyone—and everything—that he actually postponed walking until the ripe old age of 2. He learned to read by age 3 and is still amazed that he can't remember how he learned.

The diversity of Chris's parents exposed him to so many aspects of learning that he pretty much just had to learn everything he got his hands on. His dad was a lover of math and science and his mother was a lover of the arts. Because of this, each

subject in school had an appropriate tutor in the household. Because of his mother, literature and music—especially music—were central to Chris while at home. And his father would ignite just as much interest in math, science, and sports.

Growing up in such an environment made school a rather straightforward affair, and sometimes it was just more interesting for Chris if he shook up the system on occasion. For some teachers he was the ideal student; for others he was an absolute nightmare. Chris was the student that *always* questioned the reasoning of the teachers and could ask "WHY?" relentlessly—to the point of getting himself into trouble. Strangely, he never got himself into trouble asking questions unless the teachers didn't seem to have the answers. Overall, though, his education through high school was enjoyable and, if not perfect, close enough to inspire him to further his education.

After graduating from Lincoln County High School in May, 1988, he enrolled at the University of Tennessee as a prospective engineering student. He chose engineering—perhaps because of his father—but more likely because math and science had become his favorite subjects. He had developed quite a passion for each of them and these feelings came about from two wonderful teachers. Sarah Raby, his math teacher for three years, instilled a great respect for the power of mathematics. John Jeffries, his chemistry and physics teacher in high school, showed Chris (for the first time in his life) the intricate relationship between mathematics and the real world. These two teachers made such an impact on Chris's life that he learned more than just the material; he learned that there is nothing more special than an effective teacher. Although he didn't know it at the time, teaching would perhaps become Chris's foremost passion.

Entering the university in August of 1988, Chris trudged forward for four years

and graduated right on schedule (much to the relief of his parents) with a Bachelor of Science degree in Mechanical Engineering in May, 1992. During the final semester of his Senior year, he was amazed to discover that opportunities existed where a student could not only continue on (for only *two* years!) and receive a Master's degree, but also be *paid* to do so. After all, he had made it through four years, so how hard could another couple of years be? And to get of all this without financially burdening his parents any further—it seemed too good to be true. When it was confirmed that he could receive the degree while teaching classes to pay the bills, the job search process was over. He immediately entered graduate school in June 1992.

The tables had turned. Chris, the often troublesome student in high school, had become the teacher. Often, when one of his students would ask (repeatedly) questions as to his reasoning, he would be reminded of himself doing the same to his teachers in high school. Perhaps several of his high school faculty would consider this as a fitting fate, but it was quite enjoyable for Chris, and he wondered what all the fuss was really about. Teaching, to this day, is so much fun that it is hardly like a job, and he looks forward to someday being a professor on a regular basis. Chris taught various classes throughout his tenure as a Master's student, and graduated in December 1993 with a M.S. degree, also in Mechanical Engineering.

Faced again with the threat of having to get a "real" job, Chris said "why stop now?" and, much to the disbelief of his father, decided to *keep* continuing his education and pursue a doctorate. All had gone smoothly to this point, and a Ph.D. would open the door to teach forever, and that, over anything else, was the deciding factor. He entered the Ph.D. program, still at the University of Tennessee, in January, 1994. Some would say that another university would have been a better idea, but a few

factors kept him in Knoxville. Her name was Josie.

Chris met the girl of his dreams on April 2, 1992, just before graduating with his BSME. She was also an M.E. student and he couldn't believe that it took three years for her to cross his path. He was smitten from the start and still is. In January 1994 Josie was a mechanical engineer in Knoxville, and leaving her side was out of the question. Chris and Josie were married on August 24, 1996.

Going through the motions to get a Ph.D. is a far cry from getting a MS. It can be painful. In fact, it can downright smart. Sure, on paper the MS degree is basically halfway concerning classes, but other than that, nothing is the same. The classes are not only tougher, they are *much* tougher to find—perhaps because the doctoral student body is so small. The comprehensive examinations struck fear into Chris's heart—perhaps for the first time in his life. School had always come easily to Chris, and failure had never really been a consideration. But Chris had seen several sharp (*really sharp*) colleagues come up just short of passing those exams, and he didn't want to lose his dream of teaching because, of all things, he couldn't defeat a few *tests*. Getting past those examinations was a pinnacle in his life, and he can only thank God, Josie, and his Ph.D. committee chairman, Dr. Bill Hamel, for giving him the strength to pass them.

So, around five years after starting his Ph.D., Chris finally gets to change his job specification from "Professional Student" to "Dr. Chris". The journey has been a challenging one to say the least, but, as someone (who looks a lot like Tom Hanks) once said, "*...it's the hard that makes it great...*". Chris cherishes all the moments, good and bad, that happened during those years and remembers the experience quite fondly. And there is no way in Hell he would go through it all again.

Chris and Josie are a small but incredibly happy family with no children (yet) except for their two gorgeous and gloriously jolly Labrador Retrievers—Alex and Wiley. They are looking forward to opening a new chapter in their lives and starting a (bigger) family together. Chris was delighted (almost as much as Josie) to be awarded the Ph.D. degree in Mechanical Engineering in May, 1999. Ten years of higher education, and Chris still can't remember how he learned to read. He supposes that some things are just gifts from God. Looking back at all of this has made him realize that all good things in life really are.

